NUMERICAL METHODS IN TURBULENCE

by

Carolina Cardoso Manica

B.S. Mathematics, Universidade Federal do Rio Grande do Sul, Brazil, 1999

M.S. Mathematics, Universidade Federal do Rio Grande do Sul, Brazil, 2001

Submitted to the Graduate Faculty of

the Department of Mathematics in partial fulfillment

of the requirements for the degree of

Doctor of Philosophy

University of Pittsburgh

2006

UNIVERSITY OF PITTSBURGH

MATHEMATICS DEPARTMENT

This dissertation was presented

by

Carolina Cardoso Manica

It was defended on

July 7th 2006

and approved by

Prof. William Layton, Mathematics Department, University of Pittsburgh

Prof. Vincent Ervin, Mathematics Department, Clemson University

Prof. Beatrice Riviere, Mathematics Department, University of Pittsburgh

Prof. Ivan Yotov, Mathematics Department, University of Pittsburgh

Dissertation Director: Prof. William Layton, Mathematics Department, University of

Pittsburgh

NUMERICAL METHODS IN TURBULENCE

Carolina Cardoso Manica , PhD

University of Pittsburgh, 2006

Fluid motion and its richness of detail are described by the Navier-Stokes equations. Most of the numerical analysis existent to date is applicable for strong solutions (typically small body force and initial data). We prove that statistics of weak solutions are optimally computable in the simple but important case of small body force and large initial data. These estimates are used to predict drag and lift statistics, quantities of great interest in engineering. In the case of arbitrarily large body force and initial data, for shear flows, statistics of the computed solution are shown to behave according to the Kolmogorov theory.

Many times, in turbulent fluid flow, a direct numerical simulation becomes expensive. One alternative is Large Eddy Simulation (LES). It exploits the decoupling of scales, achieved via introduction of a filter, thus reducing the number of degrees of freedom in a simulation. A relatively new family of LES models is the Approximate Deconvolution Models (ADM). They have remarkable mathematical properties and perform well in computations. However, some reports claim that they are unstable for simulations with walls and require the addition of explicit stabilization.

We show that, given the right formulation, variational discretizations of the Zeroth Order Model, a member of the ADM family, are indeed stable. We present evidence that stability of one formulation is sensitive to the exact way in which filtering is performed and show some numerical results. An alternative formulation, which does not depend on the way filtering is performed, is also presented. In both cases we perform convergence studies. This is a first step in determining stable and robust discretizations for the whole family of ADM, as well as guidance for dealing with arbitrary geometries/domains that arise in practical applications.

Getting a prediction of a turbulent flow right also means getting the energy balance and the rotational structures correct, which means (in the large) matching the energy and helicity statistics. We apply similarity theory to the ADM and show that the model has a helicity cascade, linked to its energy cascade, which predicts the correct helicity statistics up to the cut-off frequency.

Acknowledgements

I would like to thank everyone who has helped me to write this thesis. Not only those who contributed with mathematical feedback and technical detail, but especially those who went beyond that and helped me personally to go through these beautiful (and at the same time hard) years as a graduate student (and the years before that, which served as a well paved path for this achievement).

I am forever indebted to my advisor, Prof. William Layton, for leading the way, and instigating me to work on beautiful problems with practical applications. His passion and enthusiasm for the combination of fluids and mathematics is contagious!

It is also my pleasure to thank Professors Vincent Ervin, Beatrice Riviere and Ivan Yotov, for teaching me many of the tools I needed in my research and for constructive discussions along the way. Most of all, for their careful observations in the process of writing this thesis.

I would also like to thank the *FreeFem++* team, for making their software available and especially Prof. Frederich Hecht, for some suggestions regarding the examples in Chapter 7.

A major part of this work was influenced by Professors William Layton and Volker John, as well as my friends Songul K. Merdan, Monika Neda and Leo Rebholz. I would like to thank them for countless hours of mutual effort that led to the joint work presented in Chapters 4, 6, 8, and 9 and in [46, 63, 64, 55].

I cannot forget my professors and my friends in Brazil, who showed me the possibilities and believed I was capable of pursuing them. I will always remember their lessons and their friendship.

A warm and special thanks goes to my parents and my family, who are constantly present in my life, and with whom I have learned invaluable lessons and shared precious moments.

Lastly, but perhaps the most important, I would like to thank my husband, Evandro, who has always managed to be patient and good humored even in the hardest moments, always trying to lift my spirits. His enthusiasm, love and support (both morally and technically, since he is also a mathematician!) mean a lot to me, much more than words can possibly express.

To my husband, Evandro, and my parents, Odilon and Maria Helena

TABLE OF CONTENTS

LIST OF TABLES

LIST OF FIGURES

1.0   INTRODUCTION

"Considering the diversity and complexity of fluid flows, it is quite remarkable that the relatively simple Navier-Stokes equations describe them accurately and in complete detail. However, in the context of turbulent flows, their power is also their weakness: the equations describe every detail of the turbulent velocity field from the largest to the smallest length and time scales. The amount of information contained in the velocity field is vast, and as a consequence (in general) the direct approach of solving the Navier-Stokes equations is impossible."
(S. Pope, Turbulent Flows, 2000)

Physically important and mathematically challenging. That characterizes the study of turbulence and its connection to the Navier-Stokes equations, described accurately in the words of Pope [72]. Every contribution in this field is important. One of the aspects that deserves attention is the numerical analysis of turbulent flows. Experiments may impose high costs or many times they can even be unattainable. The increase in computing power, allied with powerful algorithms and new ideas embodies a very attractive alternative. Understanding how this power should be used is very important. In my research, I consider two ways of looking at this problem:

1. Assuming that it is possible to resolve computationally all the information obtained from the Navier-Stokes equations and bearing in mind that turbulent flows are often irregular: What is meaningful to compute? Further, can approximations be optimally computable?

2. Assuming that truncation of scales is needed and one chooses a specific Large Eddy Simulation (LES) model:

    a. What is the best finite element discretization for this model?

b. How does the model predict helicity statistics?

These ideas are addressed in more detail in the main body of this thesis, which is outlined as follows.

In Chapter 2, notation and preliminaries are presented. Chapter 3 gives a brief discussion about turbulence and explains why it deserves to be better understood. Then, the equations of fluid motion, the Navier-Stokes equations, are presented. A brief review of the theory is in order, to set the path to the next chapter.

Chapter 4 addresses item 1 above. We study the problem of whether statistics of turbulent flows are optimally computable. We show that for arbitrarily large initial data, and provided the equilibrium problem has a unique solution, time averaged errors can be estimated under no extra regularity assumptions. For shear flows we prove that the time averaged energy dissipation rate of the approximate solution scales according to Kolmogorov's theory, provided that the first mesh line is chosen within $\mathcal{O}(1/Re)$ of the moving wall. This result indicates that the computed solution is faithful to the true solution, although it does not verify its accuracy.

Chapter 5 gives a brief description of Large Eddy Simulation (LES) models, focusing on the properties of the Approximate Deconvolution Models (ADM). In Chapters 6, 7 and 8 we concentrate on one of these ADM in an effort to address item 2 above. Our contribution is to investigate possible discretizations for these models. We start with the simplest and lowest order model of the family, the Zeroth Order Model.

In Chapter 6, we explore the usual finite element techniques when applied to the Zeroth Order LES model. When discretizing the model equations, one also has to decided how to perform the filtering operation, i.e. the corresponding differential equation must also be discretized. Filtering can be done on the same mesh on which the actual problem is being computed, or it can be done on a finer mesh. In the latter case, we can only show that the scheme is stable for finite time, whereas the former is stable for all time. The analysis, though, is much more involving and full of technical details.

Some numerical experiments are presented in Chapter 7. We compare the exact and discrete filters for a simple problem and then test the discrete filter on some more interesting problems.

An alternative formulation for the Zeroth Order Model is introduced in Chapter 8. We write it in mixed form and then use the finite element method to approximate the solution. This formulation is based on the idea of developing a discretization that has the right energy balance, but does not require the use of more sophisticated finite element spaces. The analysis shows that the scheme is stable and convergent under reasonable assumptions.

In Chapter 9, we investigate the existence of a joint energy-helicity cascade for the ADM, showing that they predict the correct helicity statistics up to the cut-off wave number $O(1/\delta)$.

Lastly, in Chapter 10, we present some conclusions and possibilities for future research.

2.0   MATHEMATICAL PRELIMINARIES AND NOTATION

We use standard notation for Lebesgue and Sobolev spaces, as in Adams [2]. The $L^2(\Omega)$ norm and inner product are denoted by $|| \cdot ||$ and $(\cdot, \cdot)$, respectively. For the Hilbert space $H^k(\Omega)$, the norm is denoted by $|| \cdot ||_k$.

For $\mathbf{Y}$ being a function space of functions $\mathbf{v} : [0, \infty) \to \mathbf{Y}$, we use the notation

$$L^p(0, T; \mathbf{Y}) = \left\{ \mathbf{v} : \mathbf{v}(t) : (0, T) \to \mathbf{Y}, \text{strongly measurable and } \int_0^T || \mathbf{v}(t) ||_{\mathbf{Y}}^p \, dt < \infty \right\},$$

with $1 \le p < \infty$, and the usual modification is made if $p = \infty$.

The velocity at a given time t is sought in the space

$$\mathbf{X} = H_0^1(\Omega)^d = \{ \mathbf{v} \in L^2(\Omega)(d = 2, 3) : \nabla \mathbf{v} \in L^2(\Omega)^{d \times d} \quad \text{and} \quad \mathbf{v} = 0 \text{ on } \partial\Omega \}$$

equipped with the norm $\|\mathbf{v}\|_{\mathbf{X}} = \|\nabla \mathbf{v}\|$. The dual space of $\mathbf{X}$ is denoted by $\mathbf{X}'$, and its norm, by $|| \cdot ||_{-1}$. For any ϕ in $\mathbf{X}'$, we define

$$\|\phi\|_{-1} = \sup_{\mathbf{v} \in \mathbf{X}} \frac{|(\phi, \mathbf{v})|}{\|\nabla \mathbf{v}\|},$$

The pressure at time t is sought in

$$Q = L_0^2(\Omega) = \left\{ q : q \in L^2(\Omega), \int_\Omega q \, d\mathbf{x} = 0 \right\}.$$

In addition, the space of weakly divergence free functions is denoted by

$$\mathbf{V} = \{ \mathbf{v} \in \mathbf{X} : (\nabla \cdot \mathbf{v}, q) = 0 \text{ for all } q \in Q \}.$$

We often use the following inequalities:

Young's Inequality:

$$ab \leq \frac{\epsilon}{p}a^p + \frac{\epsilon^{-q/p}}{q}b^q, \quad 1 < q,\, p < \infty, \quad \frac{1}{q} + \frac{1}{p} = 1, \quad a, b \in \mathbb{R}.$$

Poincaré-Friedrich's Inequality:

$$\|\mathbf{v}\| \leq C_{PF}\|\nabla\mathbf{v}\| \quad \forall \mathbf{v} \in \mathbf{X},$$

where C_{PF} is a constant depending on Ω.

2.1 THE TRILINEAR FORM

In the theory and numerical analysis of the Navier-Stokes equations, stated precisely in Chapter 3, the nonlinear term will be associated with the trilinear form defined below.

Definition 2.1.1. *On* $\mathbf{X} \times \mathbf{X} \times \mathbf{X}$*, let*

$$b(\mathbf{u}, \mathbf{v}, \mathbf{w}) = (\mathbf{u} \cdot \nabla\mathbf{v}, \mathbf{w}). \tag{2.1.1}$$

Lemma 2.1.1. *For* $\mathbf{u} \in \mathbf{V}$ *and* $\mathbf{v}, \mathbf{w} \in \mathbf{X}$,

$$b(\mathbf{u}, \mathbf{v}, \mathbf{w}) = -b(\mathbf{u}, \mathbf{w}, \mathbf{v}) \qquad and \qquad b(\mathbf{u}, \mathbf{v}, \mathbf{v}) = 0.$$

Proof. The results follow from integration by parts. $\qquad\qquad\square$

These properties rely on the fact that $\mathbf{u} \in \mathbf{V}$, something which is not true when $\mathbf{u}$ is discrete. This motivates the definition of a explicitly skew-symmetrized trilinear form.

Definition 2.1.2. *On* $\mathbf{X} \times \mathbf{X} \times \mathbf{X}$*, let*

$$b^*(\mathbf{u}, \mathbf{v}, \mathbf{w}) = \frac{1}{2}(\mathbf{u} \cdot \nabla\mathbf{v}, \mathbf{w}) - \frac{1}{2}(\mathbf{u} \cdot \nabla\mathbf{w}, \mathbf{v}). \tag{2.1.2}$$

Remark 2.1.1. *It can be easily checked that when* $\mathbf{u} \in \mathbf{V}$*, (2.1.1) and (2.1.2) are equivalent and have the same properties. Thus, for the sake of simple notation, we will always use* $b(\mathbf{u}, \mathbf{v}, \mathbf{w})$*, rather than* $b^*(\mathbf{u}, \mathbf{v}, \mathbf{w})$*.*

Lemma 2.1.2. *Let $\Omega \subset \mathbb{R}^d, d = 2$ or 3. Then there exists a constant $M = M(\Omega) < \infty$ such that*

$$b(\mathbf{u}, \mathbf{v}, \mathbf{w}) \leq M || \nabla \mathbf{u} \, || \, || \nabla \mathbf{v} \, || \, || \nabla \mathbf{w} \, ||, \qquad \forall \, \mathbf{u}, \mathbf{v}, \mathbf{w} \in \mathbf{X}. \tag{2.1.3}$$

When $d = 3$, this can be improved to

$$b(\mathbf{u}, \mathbf{v}, \mathbf{w}) \leq M \sqrt{|| \, \mathbf{u} \, || \, || \nabla \mathbf{u} \, ||} \, || \nabla \mathbf{v} \, || \, || \nabla \mathbf{w} \, ||, \qquad \forall \, \mathbf{u}, \mathbf{v}, \mathbf{w} \in \mathbf{X}. \tag{2.1.4}$$

or, equivalently, to

$$b(\mathbf{u}, \mathbf{v}, \mathbf{w}) \leq M || \nabla \mathbf{u} \, || \, || \nabla \mathbf{v} \, || \sqrt{|| \, \mathbf{w} \, || \, || \nabla \mathbf{w} \, ||}, \qquad \forall \, \mathbf{u}, \mathbf{v}, \mathbf{w} \in \mathbf{X}. \tag{2.1.5}$$

Proof. We refer to Girault and Raviart [30] for the proof of inequality (2.1.3). To prove (2.1.4), we first use Lemma 2.1 p.12 of Temam [84]:

$$b(\mathbf{u}, \mathbf{v}, \mathbf{w}) \leq C(\Omega) \|\mathbf{u}\|_{1/2} \|\mathbf{v}\|_1 \|\mathbf{w}\|_1.$$

Then, using Poincaré-Friedrich's inequality,

$$\|\mathbf{v}\|_1 \leq C \|\nabla \mathbf{v}\|, \ \|\mathbf{w}\|_1 \leq C \|\nabla \mathbf{w}\|.$$

Lastly, an interpolation inequality between $L^2(\Omega)$ and $H^1(\Omega)$ (see Adams [2]) gives

$$\|\mathbf{u}\|_{1/2} \leq C(\Omega) \|\mathbf{u}\|^{1/2} \|\mathbf{u}\|_1^{1/2} \leq C(\Omega) \|\mathbf{u}\|^{1/2} \|\nabla \mathbf{u}\|^{1/2}.$$

Similarly, (2.1.5) follows from

$$b(\mathbf{u}, \mathbf{v}, \mathbf{w}) \leq C(\Omega) \|\mathbf{u}\|_1 \|\mathbf{v}\|_1 \|\mathbf{w}\|_{1/2}.$$

$\square$

The best possible constant in Lemma 2.1.2 is

$$M := \sup_{\mathbf{u}, \mathbf{v}, \mathbf{w} \in \mathbf{X}} \frac{b(\mathbf{u}, \mathbf{v}, \mathbf{w})}{|| \nabla \mathbf{u} \, || \, || \nabla \mathbf{v} \, || \, || \nabla \mathbf{w} \, ||} < \infty \tag{2.1.6}$$

and if $\mathbf{u}, \mathbf{v}, \mathbf{w} \in \mathbf{V}$, then it can be replaced by

$$N := \sup_{\mathbf{u}, \mathbf{v}, \mathbf{w} \in \mathbf{V}} \frac{b(\mathbf{u}, \mathbf{v}, \mathbf{w})}{|| \nabla \mathbf{u} \, || \, || \nabla \mathbf{v} \, || \, || \nabla \mathbf{w} \, ||} < \infty. \tag{2.1.7}$$

Since $\mathbf{V} \subset \mathbf{X}$, we have $0 < N \leq M < \infty$.

2.2   A WORD ON THE FINITE ELEMENT SPACES

We shall assume throughout this thesis that the velocity-pressure finite element spaces $\mathbf{X}^h \subset \mathbf{X}$ and $Q^h \subset Q$ are conforming (where h denotes the mesh size), have approximation properties typical of finite element spaces commonly in use and satisfy the discrete inf-sup condition,

$$\inf_{q^h \in Q^h} \sup_{\mathbf{v}^h \in \mathbf{X}^h} \frac{(q^h, \nabla \cdot \mathbf{v}^h)}{\|\nabla \mathbf{v}^h\| \|q^h\|} \geq \beta^h > \beta > 0. \tag{2.2.1}$$

The space of discretely divergence free functions is defined as

$$\mathbf{V}^h = \{\mathbf{v}^h \in \mathbf{X}^h : (q^h, \nabla \cdot \mathbf{v}^h) = 0, \, \forall\, q^h \in Q^h\}.$$

For examples of such spaces see, e.g., Gunzburger [33], Brezzi and Fortin [9] and Girault and Raviart [30].

We assume that the following approximation properties, typical of piecewise polynomial velocity-pressure finite element spaces of degree $(k, k-1)$, hold: there is $k \geq 1$ such that for any $\mathbf{u} \in (H^{k+1}(\Omega))^d \cap \mathbf{X}$ and $p \in (H^k(\Omega) \cap Q)$:

$$\inf_{\mathbf{v}^h \in \mathbf{X}^h} \left\{ \|\mathbf{u} - \mathbf{v}^h\| + h\|\nabla(\mathbf{u} - \mathbf{v}^h)\| \right\} \leq Ch^{k+1} \|\mathbf{u}\|_{k+1}, \tag{2.2.2}$$

$$\inf_{q^h \in Q^h} \|p - q^h\| \leq Ch^k \|p\|_k. \tag{2.2.3}$$

Furthermore, we assume that $\mathbf{X}^h$ is such that an inverse inequality holds:

$$\|\nabla \mathbf{v}^h\| \leq C\, h^{-1} \|\mathbf{v}^h\|, \qquad \forall\, \mathbf{v}^h \in \mathbf{X}^h.$$

Throughout this thesis, C is a generic constant that does not depend on the mesh size h or the filter width δ (to be defined in more detail in Chapter 5).

We also introduce the discrete Laplace operator, as described by Thomée [86].

Definition 2.2.1. *For $\boldsymbol{\zeta}^h \in \mathbf{X}^h$, $\Delta^h : \mathbf{X}^h \to \mathbf{X}^h$, the discrete Laplacian, is defined as*

$$(\Delta^h \boldsymbol{\zeta}^h, \mathbf{v}^h) = -(\nabla \boldsymbol{\zeta}^h, \nabla \mathbf{v}^h), \qquad \forall \mathbf{v}^h \in \mathbf{X}^h. \tag{2.2.4}$$

Lemma 2.2.1. *The discrete Laplacian is well defined. Moreover, $-\Delta^h$ is self-adjoint and positive definite.*

Proof. Existence and uniqueness follow directly from the Riesz Representation Theorem. Alternatively, since $\mathbf{X}^h$ is finite dimensional, we can take $\{\boldsymbol{\varphi}_j\}_{j=1}^N$ (where N is the dimension of $\mathbf{X}^h$) and write $\Delta^h \boldsymbol{\zeta}^h = \sum_{j=1}^N c_j \boldsymbol{\varphi}_j$. Consequently, (2.2.4) gives the system

$$\sum_{j=1}^N c_j (\boldsymbol{\varphi}_j, \boldsymbol{\varphi}_i) = -(\nabla \boldsymbol{\zeta}^h, \nabla \boldsymbol{\varphi}_i), \quad \forall i = 1, \cdots, N,$$

which has a unique solution, since the mass matrix is positive definite. Self-adjointness and positive definiteness of $-\Delta^h$ are easy to check. $\qquad \square$

2.3   PROPERTIES OF THE TIME AVERAGING OPERATOR

The time averaging operator is defined in terms of the limit superior (*limsup*) of a function. Thus, we will use many properties of *limsup*, especially in Chapter 4. Next, we list some of them and prove others. Let $\{a_n\}$ and $\{b_n\}$ be sequences in $\mathbb{R}$. Then

1. $\limsup_{n\to\infty} (a_n + b_n) \le \limsup_{n\to\infty} a_n + \limsup_{n\to\infty} b_n$;
2. $|\limsup_{n\to\infty} a_n| \le \limsup_{n\to\infty} |a_n|$;
3. $\limsup_{n\to\infty} (a_n b_n) \le \limsup_{n\to\infty} a_n \limsup_{n\to\infty} b_n$, if $a_n, b_n \ge 0 \,\forall\, n$;
4. $\limsup_{n\to\infty} (c\, a_n) = c \limsup_{n\to\infty} a_n$, for $c \ge 0$;
5. if $a_n \le b_n$ for each n, then $\limsup_{n\to\infty} a_n \le \limsup_{n\to\infty} b_n$.

Lemma 2.3.1. *If $a_n \ge 0$ for all n, then $\limsup_{n\to\infty} \sqrt{a_n} \le \sqrt{\limsup_{n\to\infty} a_n}$.*

Proof. Since $\limsup_{n\to\infty} \sqrt{a_n}$ is an accumulation point of $\{\sqrt{a_n}\}$ (the largest), there exists a subsequence $\{\sqrt{a_{n_j}}\}$ such that

$$\limsup_{n\to\infty} \sqrt{a_n} = \lim_{n_j\to\infty} \sqrt{a_{n_j}} = \sqrt{\limsup_{n\to\infty} a_{n_j}},$$

by continuity of the square root function. Moreover, since $\{a_{n_j}\}$ is non-negative and convergent, $\lim_{n\to\infty} a_n = \limsup_{n_j\to\infty} a_{n_j}$, and $\limsup_{n_j\to\infty} a_{n_j} \le \limsup_{n\to\infty} a_n$. $\qquad \square$

Lemma 2.3.2. *If $a_n \ge 0$ for all n, then*

1. $\limsup_{n\to\infty} (a_n)^p \le (\limsup_{n\to\infty} a_n)^p$, *where p is a non-negative real number.*

2. $|\limsup_{n\to\infty}(a_n)| = \limsup_{n\to\infty}|a_n|$.

Proof. Work with subsequences, as in the proof of Lemma 2.3.1. The first claim follows from the continuity of the power function and the second, from the continuity of the absolute value function. $\qquad\square$

We are almost ready to introduce the time averaging operator. For a function $q = q(t)$, let

$$< q >_T = \frac{1}{T} \int_0^T q(t)\, dt.$$

Important properties are that

$$|< q >_T| \;\leq\; < |q| >_T, \tag{2.3.1}$$

and, similarly, for any function $q(t, \mathbf{x})$, where $||\cdot||$ is a spacial norm of $q(t, \mathbf{x})$,

$$|| < q >_T || \;\leq\; < ||q|| >_T. \tag{2.3.2}$$

Let $\mathbf{u} \in L^p(\Omega)$, $\mathbf{v} \in L^q(\Omega)$ with $p^{-1} + q^{-1} = 1$, $p, q \in [1, \infty]$. Using the Hölder inequality for Lebesgue spaces, one can show a Hölder inequality of the form

$$
\begin{aligned}
|< (\mathbf{u}, \mathbf{v}) >_T| \;&\leq\; \frac{1}{T}\int_0^T |(\mathbf{u}, \mathbf{v})|\, dt \leq \frac{1}{T}\int_0^T ||\mathbf{u}||_{L^p}||\mathbf{v}||_{L^q}\, dt \\
&\leq\; \left(\frac{1}{T}\int_0^T ||\mathbf{u}||_{L^p}^p\, dt\right)^{1/p}\left(\frac{1}{T}\int_0^T ||\mathbf{v}||_{L^q}^q\, dt\right)^{1/q} \\
&=\; < ||\mathbf{u}||_{L^p}^p >_T^{1/p}< ||\mathbf{v}||_{L^q}^q >_T^{1/q}.
\end{aligned}
\tag{2.3.3}
$$

With the same arguments, one obtains for $\mathbf{u} \in H_0^1(\Omega)$ and $\mathbf{v} \in H^{-1}(\Omega)$,

$$|< (\mathbf{u}, \mathbf{v}) >_T| \;\leq\; < ||\nabla \mathbf{u}||_{L^2}^2 >_T^{1/2}< ||\mathbf{v}||_{H^{-1}}^2 >_T^{1/2}. \tag{2.3.4}$$

We now define the time averaging operator as

$$< q > = \limsup_{T\to\infty} < q >_T = \limsup_{T\to\infty} \frac{1}{T}\int_0^T q(t)\, dt.$$

9

Using the properties of *limsup* described in the beginning of this section, it is easy to show that

$$| <q> | \quad \leq \quad <|q|> \tag{2.3.5}$$

$$|| <q> || \quad \leq \quad <||q||> \tag{2.3.6}$$

$$| <(\mathbf{u}, \mathbf{v})> | \quad \leq \quad <||\mathbf{u}||_{L^p}^p >^{1/p} < ||\mathbf{v}||_{L^q}^q >^{1/q} \tag{2.3.7}$$

$$| <(\mathbf{u}, \mathbf{v})> | \quad \leq \quad <||\nabla\mathbf{u}||_{L^2}^2 >^{1/2} < ||\mathbf{v}||_{H^{-1}}^2 >^{1/2} \tag{2.3.8}$$

if the right hand sides of these inequalities are well defined.

2.4   A CONTINUATION LEMMA

We next prove a *Continuation Lemma*, useful in the proof of Theorem 6.3.2. It allows us to conclude that the solution to a certain nonlinear ordinary differential equation is bounded for a finite interval of time in terms of the problem data. We present it here because it is a very general result and many existence theorems use this type of argument.

Lemma 2.4.1 (Continuation Lemma)**.** *Let $y(t) \in C^1[0,1]$ be a non negative function satisfying*

$$\begin{aligned} y' + \alpha y &\leq \beta y^3 + \gamma \\ y(0) &\leq \gamma, \end{aligned} \tag{2.4.1}$$

where $\alpha \in L^1(0,1)$, $\beta > 0$ and $\gamma > 0$ are constants.

Then, there exists $\gamma_0 > 0$ and a constant $M \geq 1$ such that for $\gamma < \gamma_0$, y satisfies $y \leq M\gamma$, for $0 \leq t \leq 1$.

Proof. Let $I = \{t \in [0,1] : y \leq M\gamma\}$. We show that $I = [0,1]$ by showing that I is both closed and open in $[0,1]$ for γ_0 small enough and M large enough.

First, observe that I is nonempty, since $M \geq 1$ implies that $0 \in I$. Also, I is closed because it is the pre-image of a closed set under a continuous mapping. Next, we still need to show that I is open.

Let $[0, t^*] \subset I$. We show that for ϵ small enough, $t^* + \epsilon \in I$, i.e. $y(t^*) < M\gamma$.

Using an integrating factor and integrating (2.4.1) from 0 to t^* gives

$$y(t^*) \leq \int_0^{t^*} e^{\int_{t^*}^t \alpha(t')\,dt'} (\beta y^3 + \gamma)dt.$$

Let $K = e^{||\alpha||_{L^1(0,1)}}$. Since $[0, t^*] \subset I$ and $t^* < 1$,

$$y(t^*) < K\left(\gamma + \beta M^3 \gamma^3\right).$$

Let $M > 2K$ so that $K\gamma < M\frac{\gamma}{2}$ and let $K\beta M^2 \gamma^2 < \frac{1}{2}$. Under these conditions, $y(t^*) < M\gamma$ and, by continuity, $y(t) \leq M\gamma$ for $t^* \leq t \leq t^* + \epsilon$, showing that I is open. $\square$

Remark 2.4.1. *Lemma 2.4.1 can be extended for the interval $0 \leq t \leq T$, for fixed T and the result is valid for exponents other than 3 on the right-hand side of (2.4.1).*

3.0 TURBULENCE AND THE NAVIER-STOKES EQUATIONS

Who has not, at least once, wondered about turbulence? Most people often associate turbulence with nothing beyond bumpy planes and tornadoes. However, it is much more than that. Most flows in nature and in engineering applications are turbulent, so much that turbulence is considered to be the rule, and not the exception. Some applications in which turbulence plays an important role include reducing aerodynamic drag on vehicles and aircrafts, improving fuel efficiency of engines and simulating blood flow in artificial hearts. The classical example is the golf ball. Take two of them, one with a smooth surface and the other with small indentations. When they are hit, the latter will reach at least twice as far as the former. This simple example illustrates that for some applications, turbulence improves performance: the mixing of fuel and oxidizers produces cleaner and more efficient combustion; fuel efficiency is determined by drag, which depends a lot on turbulence.

In a time of great concern about natural resources and global warming, there is no doubt that understanding, predicting, quantifying, simulating and controlling turbulence has become one of the most important goals in science and engineering. Turbulent flows have many characteristics, some of which are listed by Tennekes and Lumley [85] and summarized here:

- irregularity: main reason why we resort to statistical methods;
- diffusivity: causes rapid mixing and increased rates of momentum, heat and mass transfer; it is the single most important feature as far as applications are concerned;
- large Reynolds number: turbulent flows often originate as an instability of laminar flows if the Reynolds number, Re (ratio between the inertial and viscous forces), becomes too large;

- three dimensional vorticity fluctuations: turbulence is rotational and three dimensional, thus being characterized by high levels of fluctuating vorticity;

- dissipation: turbulent flows are always dissipative; viscous shear stresses perform deformation work that increases the internal energy of the fluid at the expense of kinetic energy. If no energy is supplied, turbulence decays rapidly;

- continuum: even the smallest scales are far larger than any molecular length scale.

Important as it may be, turbulence still encompasses many secrets. In the words of H. Lamb: "I am an old man now, and when I die and go to heaven there are two matters on which I hope for enlightenment. One is quantum electrodynamics and the other is the turbulence motion of fluids. About the former I am rather optimistic."

The possibility of using only computers to simulate fluid motion, without having to construct and rely on expensive (and sometimes unattainable) experiments is very promising. Unfortunately, as it should be expected, this approach has its drawbacks too. There are many unresolved issues in the mathematical and physical fronts, but perhaps the major obstacle is the estimate that to resolve a flow completely, the number of mesh points (in three dimensions) must be proportional to $Re^{9/4}$. Considering that in most applications the Reynolds number can vary from thousands to thousands of millions, this estimate poses quite a challenge.

Nevertheless, much insight has been achieved by simulating simple turbulent flows, with simple geometries (e.g. channel flow) at moderate Reynolds number. For high Reynolds number, the natural alternative is to pursue a statistical approach, i.e. to describe turbulent flow in terms of some statistics (averaged values) of the velocity field, rather than pointwise values (which may not even be available). The idea is that statistics are more tractable. When turbulence is spatially homogeneous (invariant under translations), statistical and time averages are regarded as equivalent, Dubois, Jauberteau and Temam [21].

Let us now take a closer look at the equations of fluid motion and some of their mathematical properties, which are also nicely summarized in Berselli [5] and John [42].

3.1 MATHEMATICAL PROPERTIES OF THE NAVIER-STOKES EQUATIONS

One of the many reasons why the Navier-Stokes equations attract so much attention is the fact that they describe accurately conservation of mass and momentum in turbulent flows. They are the commonly accepted physical model for compressible and incompressible fluid flow. The mathematical theory is more advanced in the incompressible case, in which the equations (with initial and boundary conditions) are given by

$$\mathbf{u}_t + \mathbf{u} \cdot \nabla \mathbf{u} - \nu \nabla \mathbf{u} + \nabla p = \mathbf{f}(\mathbf{x}, t), \quad \mathbf{x} \in \Omega, \quad 0 < t < \infty \qquad (3.1.1)$$

$$\nabla \cdot \mathbf{u} = 0, \quad \mathbf{x} \in \Omega, \quad 0 < t < \infty$$

$$\mathbf{u}(\mathbf{x}, 0) = \mathbf{u}_0(\mathbf{x}), \quad \mathbf{x} \in \Omega$$

$$\mathbf{u} = 0 \quad \text{on} \quad \partial \Omega, \quad t \geq 0.$$

Here, Ω denotes a bounded and regular flow domain in $\mathbb{R}^d$ (d=2 or 3), $\mathbf{u}(\mathbf{x}, t)$, $p(\mathbf{x}, t)$ denotes the fluid velocity and pressure, ν is the viscosity, $\mathbf{f}(\mathbf{x}, t) \in L^\infty(0, \infty; L^2(\Omega))$ are the body forces and $\mathbf{u}_0 \in L^2(\Omega)$ is a weakly divergence free initial condition. The Reynolds number Re is the inverse of the viscosity. The derivation of these equations can be found in many books, such as Chorin and Marsden [15].

Historically, Euler formulated the first mathematical model (based on Newton's laws) in the simplified case of an ideal fluid, which means that his model did not account for the internal friction of the fluid, i.e. $\nu = 0$. This was incorporated by Navier, in 1822, when he derived the equations at a molecular level, from a purely theoretical point of view. However, he gave no particular physical meaning to the parameter ν. Later, Stokes (1845) rederived the same equations, making it clear that ν is the viscosity (friction) of the fluid.

Engineers, mathematicians and other scientists have devoted much of their time and energy to understand the mysteries of fluid flow. From a physical point of view, many problems are very simple in their formulation, but are still a challenge to solve, such as the determination of the forces exerted by a turbulent flow on its boundary. Mathematically, much more is known at this time than it was a century ago, but nevertheless, it is not satisfactory.

This is such a central problem in mathematical physics that it figures as one of the Clay Prize Problems. The question is whether (in three spatial dimensions), the velocity field of a fluid, initially smooth, remains smooth for all time. Regular solutions exist and are unique for finite time, but it is not known whether after the instant of time for which they lose regularity, they can become non unique. Leray [58, 59, 60] introduced the concept of weak solutions to prove the existence of solutions in a larger class, which may not be unique, based on energy estimates. His results were improved and the proofs, simplified, by Hopf [36]. Fundamental contributions in this area were also provided by Kiselev and Ladyzhenskaya [48] and Ladyzhenskaya [51].

The key term in the theory is (not surprisingly) the nonlinear term. It could be responsible for blow up (development of a singularity) in finite time, since it is intimately related to vorticity (and therefore, to the vortex stretching mechanism). By taking the curl of the momentum equation, and setting $\boldsymbol{\omega} = \nabla \times \mathbf{u}$ ($\boldsymbol{\omega}$ represents vorticity), that equation becomes

$$\boldsymbol{\omega}_t + \mathbf{u} \cdot \nabla \boldsymbol{\omega} - \boldsymbol{\omega} \cdot \nabla \mathbf{u} - \nu \Delta \boldsymbol{\omega} = \nabla \times \mathbf{f}(\mathbf{x}, t), \quad \mathbf{x} \in \Omega, \quad 0 < t < \infty.$$

In two dimensions, since $\boldsymbol{\omega}$ is a vector perpendicular to the two dimensional vector field, the vortex stretching term, $\boldsymbol{\omega} \cdot \nabla \mathbf{u}$, vanishes and does not contribute to the evolution of the vorticity field. In three dimensions, this term may give rise to the vortex stretching mechanism, since it does not necessarily vanish. This mechanism can amplify the vorticity magnitude and cause the production of smaller structures in the flow, thus implying a transfer of energy from large scale to small scale structures, creating the so called energy cascade. Therefore, although the nonlinear term does not participate in the global kinetic energy balance, since $(\mathbf{u} \cdot \nabla \mathbf{u}, \mathbf{u}) = 0$, it is responsible for redistributing energy from the large scales (created by the body force and boundary conditions) to the small scales (when viscosity becomes dominant).

3.1.1 Weak vs. Strong Solutions of the Navier-Stokes Equations

The problem of turbulence is perhaps intimately connected with questions about weak solutions vs. strong solutions of the Navier Stokes equations. It is well-known that weak solutions

exist but it is not known if they are unique. (Thus, different methods of proving existence might possibly lead to different solutions.) A strong solution is generally defined as a weak solution which has enough extra regularity to ensure global uniqueness, i.e., which fulfills Serrin's condition, e.g Serrin [77]. In $\mathbb{R}^3$, it is also unknown if strong solutions exist, see Galdi [28] and Sohr [79]. But if a strong solution exists, it is unique. Strong solutions might conceivably describe all fluid motion. However, in at least one conjecture about turbulence the case of strong solutions is associated with laminar flow.

For clarity of notation, we will give the definition of a weak and a strong solution, following Galdi [28]:

Definition 3.1.1. *Let*

1. $\mathbf{D}_T = \{\mathbf{v} \in C^\infty(\Omega \times [0,T]) : \mathbf{v}(t) \in C_0^\infty(\Omega) \text{ for each } t\}^d$,

2. $\mathcal{D} = \{\boldsymbol{\psi} \in C^\infty(\Omega)^d : \boldsymbol{\psi} \text{ has compact support in } \Omega \text{ and } \nabla \cdot \boldsymbol{\psi} = 0 \text{ in } \Omega\}$,

3. $H(\Omega) \equiv \{\mathbf{v} \in L^2(\Omega) : \nabla \cdot \mathbf{v} = 0 \text{ and } \mathbf{v} \cdot \hat{\mathbf{n}} \text{ on } \partial\Omega\}$, where $\hat{\mathbf{n}}$ is the outward unit normal.

4. $\mathcal{D}_T = \{ \boldsymbol{\phi}(\mathbf{x},t) \in C^\infty(\Omega \times [0,T]) : \boldsymbol{\phi}(\mathbf{x},t) \in \mathcal{D} \text{ for each } t, \; 0 \le t \le T\}$.

Let $\mathbf{u}_0 \in H(\Omega)$, $\mathbf{f} \in L^2(0,T;L^2(\Omega))$. *A measurable function* $\mathbf{u}(\mathbf{x},t) : \Omega \times [0,T] \to \mathbb{R}^d$ *is a weak solution of the Navier-Stokes equations if, for all* $T > 0$

1. $\mathbf{u} \in L^2(0,T;\mathbf{V}) \cap L^\infty(0,T;H(\Omega))$,

2. $\mathbf{u}$ *satisfies the integral relation*

$$(\mathbf{u}(T), \boldsymbol{\phi}(T)) - \int_0^T \left[\left(\mathbf{u}, \frac{\partial \boldsymbol{\phi}}{\partial t}\right) - \nu \left(\nabla \mathbf{u}, \nabla \boldsymbol{\phi}\right) - (\mathbf{u} \cdot \nabla \mathbf{u}, \boldsymbol{\phi}) \right] dt$$
$$= (\mathbf{u}(0), \boldsymbol{\phi}(0)) + \int_0^T (\mathbf{f}, \boldsymbol{\phi}) \, dt \qquad (3.1.2)$$

for all $\boldsymbol{\phi} \in \mathcal{D}_T$, *which is equivalent to*

$$\frac{d}{dt}(\mathbf{u}, \mathbf{v}) + \nu(\nabla \mathbf{u}, \nabla \mathbf{v}) + (\mathbf{u} \cdot \nabla \mathbf{u}, \mathbf{v}) - (\mathbf{f}, \mathbf{v}) = 0 \qquad (3.1.3)$$

for all $\mathbf{v} \in \mathbf{V}$.

3. $\mathbf{u}$ *is a strong solution if* $\mathbf{u}$ *is a weak solution and* $\mathbf{u} \in L^\infty(0,T;\mathbf{V})$ *for any* $T > 0$.

It is also known, [28], that weak solutions satisfy the energy inequality: for any $t \in [0, T]$,

$$\frac{1}{2} || \mathbf{u}(T) ||^2 + \nu \int_0^T || \nabla \mathbf{u}(t) ||^2 \, dt \leq \frac{1}{2} || \mathbf{u}_0 ||^2 + \int_0^T (\mathbf{u}(t), \mathbf{f}(t)) \, dt. \qquad (3.1.4)$$

Strong solutions satisfy even an energy equality, i.e., (3.1.4) with "$\leq$" replaced by "$=$".

We note that if Ω is a bounded domain with $\partial\Omega$ satisfying a cone condition, then it is known that, given a weak solution $\mathbf{u}$, there exists a pressure $p(\mathbf{x}, t) \in L^\infty(0, T; L_0^2(\Omega))$ (see, e.g. Galdi [28], Remark 2.5) satisfying

$$(\mathbf{u}(T), \boldsymbol{\phi}(T)) - \int_0^T \left(\mathbf{u}, \frac{\partial \boldsymbol{\phi}}{\partial t} \right) - \nu \, (\nabla \mathbf{u}, \nabla \boldsymbol{\phi}) - (\mathbf{u} \cdot \nabla \mathbf{u}, \boldsymbol{\phi}) - (p, \nabla \cdot \boldsymbol{\phi}) \, dt$$
$$= (\mathbf{u}(0), \boldsymbol{\phi}(0)) + \int_0^T (\mathbf{f}, \boldsymbol{\phi}) \, dt \quad \forall \, \boldsymbol{\phi} \in \mathbf{D}_T. \qquad (3.1.5)$$

This is equivalent to

$$\frac{d}{dt}(\mathbf{u}, \mathbf{v}) + \nu \, (\nabla \mathbf{u}, \nabla \mathbf{v}) + (\mathbf{u} \cdot \nabla \mathbf{u}, \nabla \mathbf{v}) - (p, \nabla \cdot \mathbf{v}) = (\mathbf{f}, \mathbf{v}) \qquad \forall \, \mathbf{v} \in \mathbf{X}. \qquad (3.1.6)$$

The proof of existence of weak solutions is based on the construction of a Leray-Hopf sequence of Galerkin approximations with eigenfunctions of the Stokes operator, say $\mathbf{u}_N$, in order to get an energy estimate (by multiplying (3.1.1) by $\mathbf{u}_N$). Then use it to get bounds on the approximations in the appropriate norms. The last steps are the extraction of subsequences and the use of additional compactness results.

The existence of strong solutions is also based on Galerkin approximations and energy estimates, but we multiply (3.1.1) by $A\mathbf{u}_N$, instead, where A is the Stokes operator (see Constantin and Foias [17]). In the two dimensional case, see Kiselev and Ladyzhenskaya [48] strong solutions exist for all time $T > 0$. However, in three dimensions, they only exist for arbitrary T if the initial data and body force are small. The condition on the data can be relaxed, but then existence is restricted to finite T.

Weak solutions are unique in two dimensions, since $\mathbf{u} \in L^4(0, T, \mathbf{V})$ (a condition also satisfied by strong solutions). Thus, a weak solution is actually a strong solution. However, in three dimensions, this is still an open question.

3.2   THE FINITE ELEMENT DISCRETIZATION

Consider the standard finite element discretization of the Navier-Stokes equations (3.1.1). The semi-discrete (continuous in time) finite element approximations $\mathbf{u}^h = \mathbf{u}^h(\cdot, t)$ and $p^h = p^h(\cdot, t)$ are functions $\mathbf{u}^h : [0, \infty) \to \mathbf{X}^h$, $p^h : [0, \infty) \to Q^h$ satisfying

$$(\mathbf{u}_t^h, \mathbf{v}^h) + \nu(\nabla \mathbf{u}^h, \nabla \mathbf{v}^h) + b(\mathbf{u}^h, \mathbf{u}^h, \mathbf{v}^h) - (p^h, \nabla \cdot \mathbf{v}^h) = (\mathbf{f}, \mathbf{v}^h) \quad \forall \mathbf{v}^h \in \mathbf{X}^h \quad (3.2.1)$$

$$(\nabla \cdot \mathbf{u}^h, q^h) = 0 \quad \forall q^h \in Q^h \qquad (3.2.2)$$

$$(\mathbf{u}^h(\cdot, 0) - \mathbf{u}_0, \mathbf{v}^h) = 0 \quad \forall \mathbf{v}^h \in \mathbf{X}^h.$$

Under the inf-sup condition (2.2.1), this is equivalent to: find $\mathbf{u}^h : [0, \infty) \to \mathbf{V}^h$ satisfying

$$(\mathbf{u}_t^h, \mathbf{v}^h) + \nu(\nabla \mathbf{u}^h, \nabla \mathbf{v}^h) + b(\mathbf{u}^h, \mathbf{u}^h, \mathbf{v}^h) = (\mathbf{f}, \mathbf{v}^h), \qquad \forall \mathbf{v}^h \in \mathbf{V}^h, \qquad (3.2.3)$$

$$(\mathbf{u}^h(\cdot, 0) - \mathbf{u}_0, \mathbf{v}^h) = 0 \quad \forall \mathbf{v}^h \in \mathbf{V}^h.$$

3.3   THE ASSOCIATED EQUILIBRIUM PROBLEM

Consider the Navier-Stokes (3.1.1). When $\mathbf{f}(\mathbf{x}, t) \to \mathbf{f}^*(\mathbf{x})$ as $t \to \infty$, we can associate with (3.1.1) the following equilibrium problem: find $\mathbf{u}^*(\mathbf{x})$, $p^*(\mathbf{x})$ satisfying

$$
\begin{aligned}
-\nu \Delta \mathbf{u}^* + \mathbf{u}^* \cdot \nabla \mathbf{u}^* + \nabla p^* &= \mathbf{f}^* & \text{in } \Omega \\
\nabla \cdot \mathbf{u}^* &= 0 & \text{in } \Omega \\
\mathbf{u}^* &= 0, \quad \text{on } \partial\Omega, \quad \text{and} \quad \int_\Omega p^* d\mathbf{x} = 0.
\end{aligned}
\qquad (3.3.1)
$$

The variational formulation of the equilibrium problem is: Find $\mathbf{u}^* \in \mathbf{X}$ and $p^* \in Q$ such that

$$\nu(\nabla \mathbf{u}^*, \nabla \mathbf{v}) + b(\mathbf{u}^*, \mathbf{u}^*, \mathbf{v}) - (p^*, \nabla \cdot \mathbf{v}) = (\mathbf{f}^*, \mathbf{v}) \quad \forall \mathbf{v} \in \mathbf{X} \qquad (3.3.2)$$

$$(\nabla \cdot \mathbf{u}^*, q) = 0 \quad \forall q \in Q \qquad (3.3.3)$$

or, equivalently: Find $\mathbf{u}^* \in \mathbf{V}$ such that

$$\nu(\nabla \mathbf{u}^*, \nabla \mathbf{v}) + b(\mathbf{u}^*, \mathbf{u}^*, \mathbf{v}) = (\mathbf{f}^*, \mathbf{v}) \qquad \forall \mathbf{v} \in \mathbf{V}. \tag{3.3.4}$$

The finite element approximations $\mathbf{u}^{*h}$ and p^{*h} satisfy the equations

$$\nu(\nabla \mathbf{u}^{*h}, \nabla \mathbf{v}^h) + b(\mathbf{u}^{*h}, \mathbf{u}^{*h}, \mathbf{v}^h) - (p^{*h}, \nabla \cdot \mathbf{v}^h) = (\mathbf{f}^*, \mathbf{v}^h) \qquad \forall \mathbf{v}^h \in \mathbf{X}^h \tag{3.3.5}$$
$$(\nabla \cdot \mathbf{u}^{*h}, q^h) = 0 \qquad \forall q^h \in Q^h.$$

This becomes in $\mathbf{V}^h$: Find $\mathbf{u}^{*h} \in \mathbf{V}^h$ such that

$$\nu(\nabla \mathbf{u}^{*h}, \nabla \mathbf{v}^h) + b(\mathbf{u}^{*h}, \mathbf{u}^{*h}, \mathbf{v}^h) = (\mathbf{f}^*, \mathbf{v}^h) \qquad \forall \mathbf{v}^h \in \mathbf{V}^h. \tag{3.3.6}$$

It is known that solutions of the equilibrium problem are nonsingular for small data, generically nonsingular for large data and optimally approximated by $\mathbf{u}^{*h}$ when nonsingular, e.g. Girault and Raviart [31]. Setting $\mathbf{v} = \mathbf{u}^*$ in (3.3.2) and $\mathbf{v}^h = \mathbf{u}^{*h}$ in (3.3.5), it is easy to check the a priori bounds

$$\| \nabla \mathbf{u}^* \| \leq \nu^{-1} \| \mathbf{f}^* \|_{-1}, \qquad \| \nabla \mathbf{u}^{*h} \| \leq \nu^{-1} \| \mathbf{f}^* \|_{-1}. \tag{3.3.7}$$

Both bounds can be sharpened slightly. In the continuous case, $\| \mathbf{f}^* \|_{-1}$ can be replaced by the dual norm of $\mathbf{V}$,

$$\| \mathbf{f}^* \|_* := \sup_{\mathbf{v} \in \mathbf{V}} \frac{(\mathbf{f}^*, \mathbf{v})}{\| \nabla \mathbf{v} \|},$$

and in the discrete case by the dual norm of $\mathbf{V}^h$,

$$\| \mathbf{f}^* \|_{*h} := \sup_{\mathbf{v}^h \in \mathbf{V}^h} \frac{(\mathbf{f}^*, \mathbf{v}^h)}{\| \nabla \mathbf{v}^h \|}.$$

It is known that if the problem data is small enough, concretely if

$$M \nu^{-2} \| \mathbf{f}^* \|_{-1} < 1, \tag{3.3.8}$$

then $\mathbf{u}^*$ is unique. If additionally $\mathbf{f}(\mathbf{x}, t) \equiv \mathbf{f}^*(\mathbf{x})$, $\mathbf{u}(\mathbf{x}, t) \to \mathbf{u}^*(\mathbf{x})$ in $L^2(\Omega)$ exponentially fast as $t \to \infty$ and $(\mathbf{u}^h, p^h)$ approximates $(\mathbf{u}, p)$ optimally, e.g. Girault and Raviart [30], Layton [52] and Gunzburger [33].

4.0 CONVERGENCE OF TIME AVERAGED STATISTICS OF FINITE ELEMENT APPROXIMATIONS OF THE NAVIER-STOKES EQUATIONS

The motion of an incompressible fluid is governed by the incompressible Navier-Stokes equations. A fundamental problem of fluid motion is turbulence and a fundamental problem in the Navier-Stokes equations is that of uniqueness of weak solutions in the general case of no assumed extra regularity or small data. The Leray conjecture [60] is that these two problems are connected: the lack of uniqueness of weak solutions (which he called "turbulent solutions") is not an artifact of imperfect mathematical techniques but it reflects fundamental physical mechanisms of turbulence.

The numerical analysis of turbulent flows is caught between the gaps in the physical understanding of turbulence and those in the mathematical foundations of the Navier-Stokes equations. For example, smooth strong solutions are not expected while, if the uniqueness of the weak solution is unknown, bounding the error in a numerical simulation is currently not possible without assuming extra regularity on the solution, or without assuming both the initial data $\mathbf{u}_0$ and the body force $\mathbf{f}(\mathbf{x}, t)$ are very small.

On the other hand, computational simulations are carried out and statistics of computed fluid velocities and pressures often reflect rather accurately statistics of physical flows even in the absence of mathematical justification for this accuracy. Further, statistics (by which we shall mean long time averages) are often smooth, behave deterministically (often in accord with the Kolmogorov theory, e.g. Kolmogorov [49]) in both numerical simulations and in physical experiments. From this situation, a challenge for the numerical analysis of fluid motion arises: develop a rigorous understanding of how statistics computed from numerical simulations reflect those for the unknown solution of the Navier-Stokes equations.

We will study statistics of the energy dissipation rate and the total kinetic energy of the

flow. The energy dissipation rate of the flow at time t is given by

$$\varepsilon(\mathbf{u}) := \frac{\nu}{|\Omega|} \| \nabla \mathbf{u}(\cdot, t) \|^2,$$

where $|\Omega|$ is the measure of Ω and $\|\cdot\|$ denotes the $L^2(\Omega)$-norm, and its total kinetic energy is

$$k(\mathbf{u}) := \frac{1}{2} \| \mathbf{u}(\cdot, t) \|^2.$$

The time average of the energy dissipation rate is

$$< \varepsilon(\mathbf{u}) > = \limsup_{T \to \infty} \frac{1}{T} \int_0^T \varepsilon(\mathbf{u}) \, dt = \limsup_{T \to \infty} \frac{1}{T} \int_0^T \frac{\nu}{|\Omega|} \| \nabla \mathbf{u} \|^2 \, dt,$$

and the time average of the kinetic energy is

$$< k(\mathbf{u}) > = \limsup_{T \to \infty} \frac{1}{T} \int_0^T k(\mathbf{u}) \, dt.$$

In practical simulations of turbulent flows, it is typical to output time averaged flow statistics (which are then matched against benchmark averages, e.g. Berselli, Iliescu and Layton [6], John and Kaya [43], Hughes, Oberai and Mazzei [37], Iliescu and Fischer [38], Moser, Kim and Mansour [68] and Deardorff [18]). However, there is very little numerical analysis in support of these calculations. Of course, if the error in certain norms of the velocity and the pressure is provably optimal over $0 \le t < \infty$ then time averages involving these norms are convergent as well. But, the practical case is complementary: time averages seem to be predictable even when dynamic flow behavior over bounded time intervals is irregular. This is the case we aim to study. However, a complete analysis seems to be still beyond the present mathematical tools.

We consider herein as a first step the case of arbitrary initial data $\mathbf{u}_0$ and asymptotically small body forces which converge to a stationary limit $\mathbf{f}^*(\mathbf{x}) = \lim_{t \to \infty} \mathbf{f}(\mathbf{x}, t)$. Let $(\mathbf{u}^h, p^h)$ be a finite element approximation of the velocity field and the pressure and assume that a small data condition is satisfied. Let $\mathbf{u}^*$ be the solution of the stationary Navier-Stokes equations with body force $\mathbf{f}^*$. In Section 4.1, we show that

$$< \varepsilon(\mathbf{u} - \mathbf{u}^*) > = 0, \quad < \varepsilon(\mathbf{u}^h - \mathbf{u}^{*h}) > = 0,$$

and we prove, see Theorem 4.1.2, an error estimate which shows that the problem of estimating $< \varepsilon(\mathbf{u} - \mathbf{u}^h) >$ reduces to the one of estimating $||\nabla(\mathbf{u}^* - \mathbf{u}^{*h})||^2$. So the error goes to zero optimally as the mesh width $h \to 0$. This result is plausible because the possible irregularities caused by large initial data are washed out by the time averaging.

Section 4.2 studies the flow around a body. The results of Section 4.1 are used to give estimates for the time averaged drag and the lift coefficients at the body.

In Section 4.3, we consider the complementary situation of a flow driven by a large and persistent boundary condition. We are not (yet) able to perform a complete error analysis in this case. However, following the important work of Constantin and Doering [16] in the continuous case, we show that provided the first mesh line in the finite element mesh is within $O(1/Re)$ of the moving wall which drives the flow, then the computed time averaged energy dissipation rate for the shear flow scales as predicted for the continuous flow by the Kolmogorov theory:

$$< \varepsilon(\mathbf{u}^h) > \quad \leq \quad C\frac{U^3}{L}.$$

This restriction on the mesh size arises from mathematical analysis of constructible background flows in finite element spaces and their subsequent analysis. However, it is consistent with entirely different observation of the thickness of time averaged turbulent boundary layers, see e.g. Schlichting [76].

4.1   ANALYSIS OF TIME AVERAGED ERRORS

We present some results involving the time averaged energy dissipation rate, aiming at establishing an error estimate for this quantity. For a force $\mathbf{f}$ independent of time, we first show that the time averaged energy dissipation rate $< \varepsilon(\mathbf{u}) >$ is bounded by the time averaged power input to the flow through body force-flow interaction. It is significant that this upper bound is independent of the initial condition (then it is reasonable that errors in its approximation could be insensitive to the size of $\mathbf{u}_0$). We establish time averaged errors for the pressure.

Lemma 4.1.1. *Let* $\mathbf{u}$ *be a weak solution to the Navier Stokes equations (obtained by the Leray-Hopf construction). If* $\mathbf{f} \in L^\infty(0, \infty; H^{-1}(\Omega))$, *then* $|| \mathbf{u} ||$ *is uniformly bounded*

$$\frac{1}{2}|| \mathbf{u} ||^2(T) \leq e^{-\nu C_{PF}^{-2} T}|| \mathbf{u}(0) ||^2 + \frac{C_{PF}^2}{\nu^2}|| \mathbf{f} ||^2_{L^\infty(0,\infty;H^{-1})}, \qquad (4.1.1)$$

where C_{PF} *is the Poincaré-Friedrich's constant of* Ω, *and consequently*

$$\lim_{T \to \infty} \frac{1}{T}|| \mathbf{u} ||^2(T) = 0.$$

Proof. Let V_N be a span of eigenfunctions of the Stokes operator. The Leray-Hopf construction of weak solutions gives a sequence $\mathbf{u}_N$ in $\mathbf{V}_N$ satisfying

$$(\mathbf{u}_{N,t}, \mathbf{v}) + \nu(\nabla \mathbf{u}_N, \nabla \mathbf{v}) + b(\mathbf{u}_N, \mathbf{u}_N, \mathbf{v}) = (\mathbf{f}, \mathbf{v}), \qquad \forall \mathbf{v} \in \mathbf{V}_N, \qquad (4.1.2)$$

with a subsequence $\mathbf{u}_{N_j} \to \mathbf{u}$, the weak solution, in $L^2(0, T; H(\Omega))$ strongly and $L^2(0, T; \mathbf{V})$ weakly.

This is a system of ordinary differential equations; setting $\mathbf{v} = \mathbf{u}_N$ and using Cauchy-Schwarz and Young inequalities, followed by Poincaré-Friedrich's inequality, we have

$$\frac{d}{dt}|| \mathbf{u}_N(t) ||^2 + \nu C_{PF}^{-2}|| \mathbf{u}_N(t) ||^2 \leq \frac{1}{\nu}|| \mathbf{f} ||^2_{-1}.$$

Using an integrating factor, we obtain a differential inequality which can be integrated on $(0, T)$, yielding

$$|| \mathbf{u}_N(T) ||^2 \leq e^{-\nu C_{PF}^{-2} T}|| \mathbf{u}_N(0) ||^2 + \frac{1}{\nu^2 C_{PF}^{-2}}|| \mathbf{f} ||^2_{L^\infty(0,\infty;H^{-1})}.$$

This shows the uniform boundedness of $|| \mathbf{u}_N(T) ||$. Passing to subsequences, taking the limit inferior of both sides and using a weak convergence argument (which is standard for the Navier-Stokes equations and which we show in detail in the proof of Proposition 4.1.3), letting $N_j \to \infty$, we recover (4.1.1) for $\mathbf{u}$. The second claim now follows from the first. $\square$

Lemma 4.1.2. *Let* $\mathbf{f} \in L^\infty(0, \infty; H^{-1}(\Omega))$ *and let* $\mathbf{u}^h$ *satisfy* (3.2.3). *Then* $|| \mathbf{u}^h ||$ *is uniformly bounded and consequently*

$$\lim_{T \to \infty} \frac{1}{T}|| \mathbf{u}^h ||^2 = 0, \qquad and \qquad \lim_{T \to \infty} \frac{1}{T}|| \mathbf{u} - \mathbf{u}^h ||^2 = 0.$$

Proof. Take $\mathbf{v}^h = \mathbf{u}^h$ in (3.2.3) (a step not possible in the continuous case of Lemma 4.1.1) and proceeding as in the proof of Lemma 4.1.1, we prove a similar uniform bound for $|| \, \mathbf{u}^h \, ||$. This proves the first equation and the bound on $|| \, \mathbf{u} - \mathbf{u}^h \, ||$ follows by the triangle inequality and Lemma 4.1.1. $\qquad \square$

We next consider time averages.

Proposition 4.1.1. *Let $\mathbf{u}$ be a weak solution of the Navier-Stokes equations satisfying the energy inequality (3.1.4). Then*

$$< \varepsilon(\mathbf{u}) > \; \leq \; \limsup_{T \to \infty} \frac{1}{|\, \Omega \,|\, T} \int_0^T (\, \mathbf{f}, \mathbf{u} \,) \, dt = \frac{1}{|\, \Omega \,|} < (\mathbf{f}, \mathbf{u}) > . \qquad (4.1.3)$$

If $\mathbf{u}$ satisfies the energy equality then the above inequality can be replaced by equality. Further, if $\mathbf{f} \in L^\infty(0, \infty; H^{-1}(\Omega)) \cap L^2(0, T; L^2(\Omega))$ for every $0 < T < \infty$ then

$$< \varepsilon(\mathbf{u}) > \; \leq \; \nu^{-1} \left\langle \frac{1}{|\, \Omega \,|} || \, \mathbf{f} \, ||_{-1}^2 \right\rangle \; \leq \; \frac{\nu^{-1}}{|\, \Omega \,|} || \, \mathbf{f} \, ||_{L^\infty(0, \infty; H^{-1}(\Omega))}^2. \qquad (4.1.4)$$

The semidiscrete finite element approximation $\mathbf{u}^h$ of $\mathbf{u}$ also satisfies inequalities of form (4.1.3) and (4.1.4), where in (4.1.3) even equality holds.

Proof. Since $\mathbf{u}$ satisfies the energy inequality (3.1.4), we have

$$\frac{1}{2T} \frac{1}{|\, \Omega \,|} || \, \mathbf{u}(T) \, ||^2 + \frac{1}{T} \int_0^T \frac{\nu}{|\, \Omega \,|} || \, \nabla \mathbf{u}(t) \, ||^2 \, dt \leq \frac{1}{2T} \frac{1}{|\, \Omega \,|} || \, \mathbf{u}_0 \, ||^2 + \frac{1}{T} \int_0^T \frac{1}{|\, \Omega \,|} (\mathbf{f}, \mathbf{u}) \, dt.$$

Since $\frac{1}{2T} || \, \mathbf{u}(T) \, ||^2 \to 0$ by Lemma 4.1.1 and $\frac{1}{2T} || \, \mathbf{u}_0 \, ||^2 \to 0$ as $T \to \infty$, we obtain (4.1.3). If we use as starting point the energy equality, the equal sign will be preserved.

For proving the last claim, we apply inequality (2.3.8) to (4.1.3)

$$\begin{aligned}
< \varepsilon(\mathbf{u}) > \; &\leq \; \frac{\nu}{2|\, \Omega \,|} < || \, \nabla \mathbf{u}(t) \, ||^2 > + \frac{1}{2\nu|\, \Omega \,|} < || \, \mathbf{f} \, ||_{-1}^2 > \\
&\leq \; \frac{1}{2} < \varepsilon(\mathbf{u}) > + \frac{1}{2\nu|\, \Omega \,|} || \mathbf{f} ||_{L^\infty(0, \infty; H^{-1})}^2.
\end{aligned}$$

In the semidiscrete case take $\mathbf{u}^h$ as test function in (3.2.3). This gives

$$\frac{1}{2} \frac{d}{dt} || \, \mathbf{u}^h(t) \, ||^2 + \nu || \, \nabla \mathbf{u}^h(t) \, ||^2 = (\mathbf{u}^h(t), \mathbf{f}(t)).$$

Integration in $(0, T)$ shows that $\mathbf{u}^h$ fulfills an energy equality. Now, the arguments to derive the estimates of form (4.1.3) and (4.1.4) for $\mathbf{u}^h$ are the same as in the continuous case. $\qquad \square$

24

Lemma 4.1.3. *Let* $(\mathbf{u}, p)$ *be a weak solution of the Navier-Stokes equations and* $(\mathbf{u}^h, p^h)$ *its finite element approximation in finite dimensional subspaces* $\mathbf{X}^h \subset \mathbf{X}$ *and* $Q^h \subset Q$. *Let* $\mathbf{e} = \mathbf{u} - \mathbf{u}^h$. *Then, for any* C^1 *functions* $\mathbf{v}^h : [0, T] \to \mathbf{X}^h$, $q^h : (0, T] \to Q^h$ *(for each* T, $0 < T < \infty$*),*

$$(\mathbf{e}(T), \mathbf{v}^h(T)) - \int_0^T \left[\left(\mathbf{e}, \frac{\partial \mathbf{v}^h}{\partial t}\right) - \nu(\nabla \mathbf{e}, \nabla \mathbf{v}^h) - b(\mathbf{u}, \mathbf{u}, \mathbf{v}^h) + b(\mathbf{u}^h, \mathbf{u}^h, \mathbf{v}^h) \right.$$
$$\left. + (p - p^h, \nabla \cdot \mathbf{v}^h) + (\nabla \cdot (\mathbf{u} - \mathbf{u}^h), q^h) \right] dt = (\mathbf{e}(0), \mathbf{v}^h(0)) \qquad (4.1.5)$$

which is equivalent to

$$\frac{d}{dt}(\mathbf{e}, \mathbf{v}^h) - \left(\mathbf{e}, \frac{\partial \mathbf{v}^h}{\partial t}\right) + \nu(\nabla \mathbf{e}, \nabla \mathbf{v}^h) + b(\mathbf{u}, \mathbf{u}, \mathbf{v}^h)$$
$$- b(\mathbf{u}^h, \mathbf{u}^h, \mathbf{v}^h) - (p - p^h, \nabla \cdot \mathbf{v}^h) = 0 \qquad (4.1.6)$$
$$(\nabla \cdot (\mathbf{u} - \mathbf{u}^h), q^h) = 0$$

Proof. We shall prove (4.1.6). The connection between (4.1.6) and (4.1.5) is the same as (3.1.5) and (3.1.6).

First, note that both follow by subtraction provided (3.1.5) can be shown to hold for $\phi \in C^1(0, T; \mathbf{X}^h)$ or (3.1.6) can be shown for $\mathbf{v} \in C^1(0, T; \mathbf{X}^h)$ (since $\mathbf{X}^h \subset \mathbf{X}$). We show the latter.

Since $\mathbf{X}^h \subset \mathbf{X}$ (3.1.6) holds for all $\mathbf{v}^h(\mathbf{x}) \in \mathbf{X}^h$. Next, let $A(t)$ be a $C^1(0, T)$ function. Multiplication of (3.1.6) by $A(t)$ and using

$$A(t)\frac{d}{dt}(\mathbf{u}, \mathbf{v}^h) = \frac{d}{dt}(\mathbf{u}, A(t)\mathbf{v}^h) - (\mathbf{u}, A'(t)\mathbf{v}^h)$$

gives that $\mathbf{u}$ and p satisfy

$$\frac{d}{dt}(\mathbf{u}, \mathbf{v}^h) - \left(\mathbf{u}, \frac{\partial \mathbf{v}^h}{\partial t}\right) + \nu(\nabla \mathbf{u}, \nabla \mathbf{v}^h) + (\mathbf{u} \cdot \nabla \mathbf{u}, \mathbf{v}^h) + (p, \nabla \cdot \mathbf{v}^h) = (\mathbf{f}, \mathbf{v}^h)$$

with $\mathbf{v}^h = A(t)\mathbf{v}^h(\mathbf{x})$. The same equation holds for $\mathbf{u}^h$ and p^h. Subtracting gives (4.1.6) for any $\mathbf{v}^h$ of the form $\mathbf{v}^h = A(t)\mathbf{v}^h(\mathbf{x})$.

Since (4.1.6) is linear in $\mathbf{v}^h$, it also follows for any $\mathbf{v}^h$ which is a finite linear combination of such function,

$$\mathbf{v}^h(\mathbf{x}, t) = \sum_{i=1}^{N} A_i(t) \mathbf{v}_i^h(\mathbf{x}).$$

Picking $\mathbf{v}_i^h(\mathbf{x})$ to be a basis for $\mathbf{X}^h$ completes the proof. $\qquad\qquad\square$

Next, we consider the time averaged errors. It is important to note that there is a difference between $|| < \nabla(\mathbf{u} - \mathbf{u}^h) > ||$ and $< ||\nabla(\mathbf{u} - \mathbf{u}^h)|| >$. By Minkowski's inequality, the second is an upper bound for the first. Experience with turbulent flows suggests that $< \nabla \mathbf{u} >$ might be smooth (and thus approximable). Thus, ideally we would like estimates for the first $|| < \nabla(\mathbf{u} - \mathbf{u}^h) > ||$. In the case of the error in the pressure, we are able to prove such a bound.

Theorem 4.1.1. *Let $\mathbf{f} \in L^\infty(0, \infty; H^{-1}(\Omega))$ and let $(\mathbf{X}^h, Q^h)$ satisfy the discrete inf-sup condition (2.2.1). Then,*

$$
\limsup_{T \to \infty} || < p - p^h >_T || \;\leq\; \frac{\nu}{\beta}(1 + 2M\nu^{-2}||\mathbf{f}||_{L^\infty(0,\infty;H^{-1}(\Omega))}) \left\langle ||\nabla(\mathbf{u} - \mathbf{u}^h)||^2 \right\rangle^{1/2}
$$
$$
+ \left(1 + \frac{C}{\beta}\right) \inf_{q^h \in Q^h} \limsup_{T \to \infty} || < p - q^h >_T ||.
$$

Proof. A straightforward calculation shows that (4.1.5) is equivalent to

$$
-\int_0^T (p^h - q^h, \nabla \cdot \mathbf{v}^h)\, dt = (\mathbf{e}(T), \mathbf{v}^h(T)) - (\mathbf{e}(0), \mathbf{v}^h(0))
$$
$$
- \int_0^T \left[\left(\mathbf{e}, \frac{\partial \mathbf{v}^h}{\partial t}\right) - \nu(\nabla \mathbf{e}, \nabla \mathbf{v}^h) - b(\mathbf{u}, \mathbf{e}, \mathbf{v}^h) - b(\mathbf{e}, \mathbf{u}^h, \mathbf{v}^h) + (p - q^h, \nabla \cdot \mathbf{v}^h)\right] dt
$$

for all $(\mathbf{v}^h, q^h) \in X^h \times Q^h$. Since the velocity finite element functions are continuous in $\overline{\Omega}$, all terms are well defined. Let $\mathbf{v}^h = \mathbf{v}^h(\mathbf{x})$. Division by T gives

$$
(< q^h - p^h >_T, \nabla \cdot \mathbf{v}^h) \;\leq\; \frac{1}{T}(\mathbf{e}(T), \mathbf{v}^h) - \frac{1}{T}(\mathbf{e}(0), \mathbf{v}^h) + \nu(< \nabla \mathbf{e} >_T, \nabla \mathbf{v}^h) + < b(\mathbf{u}, \mathbf{e}, \mathbf{v}^h) >_T
$$
$$
+ < b(\mathbf{e}, \mathbf{u}^h, \mathbf{v}^h) >_T - (< p - q^h >_T, \nabla \cdot \mathbf{v}^h). \tag{4.1.7}
$$

For estimating (4.1.7), one uses again that $\mathbf{v}^h$ does not depend on time, (2.1.3) and $||\nabla\cdot\mathbf{v}^h|| \le C\,||\nabla\mathbf{v}^h||$ to obtain

$$
\begin{aligned}
\left|(< q^h - p^h >_T, \nabla \cdot \mathbf{v}^h)\right| \ \le\ & \frac{C_{PF}}{T}||\,\mathbf{e}(T)\,||\,||\,\nabla\mathbf{v}^h\,|| + \frac{C_{PF}}{T}||\,\mathbf{e}(0)\,||\,||\,\nabla\mathbf{v}^h\,|| \\
& + \nu\,||< \nabla\,\mathbf{e} >_T\,||\,||\,\nabla\,\mathbf{v}^h\,|| + M <||\,\nabla\,\mathbf{u}\,||\,||\,\nabla\,\mathbf{e}\,|| >_T ||\,\nabla\,\mathbf{v}^h\,|| \\
& + M <||\,\nabla\,\mathbf{e}\,||\,||\,\nabla\,\mathbf{u}^h\,|| >_T ||\,\nabla\,\mathbf{v}^h\,|| + C\,||< p - q^h >_T\,||\,||\,\nabla\,\mathbf{v}^h\,||.
\end{aligned}
$$

Dividing by $||\,\nabla\,\mathbf{v}^h\,||$ and applying the discrete inf-sup condition (2.2.1) on the left hand side of this inequality leads to

$$
\begin{aligned}
\beta||< q^h - p^h >_T\,|| \ \le\ & \frac{C_{PF}}{T}||\,\mathbf{e}(T)\,|| + \frac{C_{PF}}{T}||\,\mathbf{e}(0)\,|| + \nu\,||< \nabla\,\mathbf{e} >_T\,|| \\
& + M <||\,\nabla\,\mathbf{u}\,||\,||\,\nabla\,\mathbf{e}\,|| >_T + M <||\,\nabla\,\mathbf{e}\,||\,||\,\nabla\,\mathbf{u}^h\,|| >_T \\
& + C\,||< p - q^h >_T\,||.
\end{aligned}
$$

The first term on the right hand side can be estimated first with (2.3.2) and then with (2.3.3). The other terms can be bounded directly with (2.3.3), resulting in

$$
\begin{aligned}
\beta||< q^h - p^h >_T\,|| \ \le\ & \frac{C}{T}||\,\mathbf{e}(T)\,|| + \frac{C}{T}||\,\mathbf{e}(0)\,|| + \nu <||\,\nabla\,\mathbf{e}\,||^2 >_T^{1/2} \\
& + M <||\,\nabla\,\mathbf{u}\,||^2 >_T^{1/2} <||\,\nabla\,\mathbf{e}\,||^2 >_T^{1/2} \\
& + M <||\,\nabla\,\mathbf{e}\,||^2 >_T^{1/2} <||\,\nabla\,\mathbf{u}^h\,||^2 >_T^{1/2} + C\,||< p - q^h >_T\,||.
\end{aligned}
$$

The triangle inequality then implies that

$$
\begin{aligned}
||< p - p^h >_T\,|| \ \le\ & \frac{C}{T}||\,\mathbf{e}(T)\,|| + \frac{C}{T}||\,\mathbf{e}(0)\,|| + \frac{\nu}{\beta} <||\,\nabla\,\mathbf{e}\,||^2 >_T^{1/2} \\
& + \frac{M}{\beta} <||\,\nabla\,\mathbf{u}\,||^2 >_T^{1/2} <||\,\nabla\,\mathbf{e}\,||^2 >_T^{1/2} \\
& + \frac{M}{\beta} <||\,\nabla\,\mathbf{e}\,||^2 >_T^{1/2} <||\,\nabla\,\mathbf{u}^h\,||^2 >_T^{1/2} + \left(1 + \frac{C}{\beta}\right)||< p - q^h >_T\,||.
\end{aligned}
$$

Taking *limsup* as $T \to \infty$ on both sides of the inequality and using Lemmas 4.1.1 and 4.1.2, together with properties of *limsup*, give

$$
\begin{aligned}
\limsup_{T\to\infty} ||< p - p^h >_T\,|| \ \le\ & \frac{\nu}{\beta} <||\,\nabla\,\mathbf{e}\,||^2 >^{1/2} + \frac{M}{\beta} <||\,\nabla\,\mathbf{u}\,||^2 >^{1/2} <||\,\nabla\,\mathbf{e}\,||^2 >^{1/2} \\
& + \frac{M}{\beta} <||\,\nabla\,\mathbf{e}\,||^2 >^{1/2} <||\,\nabla\,\mathbf{u}^h\,||^2 >^{1/2} \\
& + \left(1 + \frac{C}{\beta}\right) \limsup_{T\to\infty} ||< p - q^h >_T\,||.
\end{aligned}
$$

The norms of the weak and the discrete solution can be estimated with the results of Proposition 4.1.1. The proof concludes by taking the infimum over $q^h \in Q^h$. □

Corollary 4.1.1. *If the assumptions of Theorem 4.1.1 hold true, then*

$$
\begin{aligned}
|| < p - p^h > || \;\; \leq \;\; & \frac{\nu}{\beta}(1 + 2M\nu^{-2}||\,\mathbf{f}\,||_{L^\infty(0,\infty;H^{-1}(\Omega))})\left\langle\,|| \nabla(\mathbf{u} - \mathbf{u}^h)||^2\,\right\rangle^{1/2} \\
& + \left(1 + \frac{C}{\beta}\right) \inf_{q^h \in Q^h} \limsup_{T \to \infty} || < p - q^h >_{_T} ||.
\end{aligned}
$$

Proof. The lower bound on the left hand side is a consequence of properties of *limsup*. □

The key idea in the above proofs was to restrict $\mathbf{v}^h \in \mathbf{V}^h$ to be time independent. Then, (finite) time averaging can be applied and brought inside upon the pressure error directly. It is interesting that the equations of motion give a different realization of time averaged error for the velocity and pressure ($< ||\nabla(\mathbf{u} - \mathbf{u}^h)|| >$ versus $|| < p - p^h > ||$). This appears also in the time averaged lift and drag error estimates in Theorem 4.2.1. At this point, we do not know if this distinction has other, deeper causes or implications.

We next turn to the error inequalities for the time averaged velocity error $< \varepsilon(\mathbf{u} - \mathbf{u}^h) >$.

Proposition 4.1.2. *Let $Y = L^2(0,T;H^1(\Omega)) \cap L^\infty(0,T;V^h)$ and assume $\mathbf{u}_t \in L^1(0,T;\mathbf{X}')$ for every $0 < T < \infty$. Then the time averaged velocity error satisfies the following inequalities*

$$
\begin{aligned}
< \varepsilon(\mathbf{u} - \mathbf{u}^h) > \;\; \leq \;\; & C \inf_{q^h \in Q^h} \nu^{-1} < || p - q^h ||^2 > + 2 < |\, b(\mathbf{u} - \mathbf{u}^h, \mathbf{u}, \mathbf{u} - \mathbf{u}^h)\,| > \\
& + C \inf_{\tilde{\mathbf{u}} \in Y} \big[< \varepsilon(\mathbf{u} - \tilde{\mathbf{u}}) > + \nu^{-1} < || (\mathbf{u} - \tilde{\mathbf{u}})_t ||^2_{-1} > \\
& \quad + 2\left\langle\, |\, b(\mathbf{u}, \mathbf{u} - \mathbf{u}^h, \mathbf{u} - \tilde{\mathbf{u}})\,| + |\, b(\mathbf{u} - \mathbf{u}^h, \mathbf{u}, \mathbf{u} - \tilde{\mathbf{u}})\,| \right. \\
& \quad\quad \left. + |\, b(\mathbf{u} - \mathbf{u}^h, \mathbf{u} - \mathbf{u}^h, \mathbf{u} - \tilde{\mathbf{u}})\,|\,\right\rangle \big],
\end{aligned}
$$

and

$$
\begin{aligned}
< \varepsilon(\mathbf{u} - \mathbf{u}^h) > \;\; \leq \;\; & C \inf_{q^h \in Q^h} \nu^{-1} < || p - q^h ||^2 > \\
& + \; C \inf_{\tilde{\mathbf{u}} \in Y} \big[< \varepsilon(\mathbf{u} - \tilde{\mathbf{u}}) > + \nu^{-1} < || (\mathbf{u} - \tilde{\mathbf{u}})_t ||^2_{-1} > \\
& \quad + \nu^{-3} \left\langle\, || \mathbf{u} - \mathbf{u}^h ||^{2/3} || \nabla\mathbf{u} ||^{4/3} || \nabla(\mathbf{u} - \tilde{\mathbf{u}}) ||^{4/3} \right\rangle \\
& \quad + \; \nu^{-3} \left\langle\, || \mathbf{u} - \mathbf{u}^h ||^2 || \nabla(\mathbf{u} - \tilde{\mathbf{u}}) ||^4 \right\rangle + C \left\langle\, \nu^{-1} || \nabla\mathbf{u} ||^2 || \mathbf{u} - \tilde{\mathbf{u}} || \,|| \nabla(\mathbf{u} - \tilde{\mathbf{u}}) || \right\rangle \big] \\
& \quad + \; \nu^{-3} \left\langle\, || \nabla\mathbf{u} ||^4 || \mathbf{u} - \mathbf{u}^h ||^2 \right\rangle.
\end{aligned}
$$

Remark 4.1.1. *If $||\nabla\mathbf{u}||$ is uniformly bounded in time, then these equations can be closed provided $<||\mathbf{e}||^2>\le Ch^\alpha<||\nabla\mathbf{e}||^2>$ for some $\alpha>0$ and provided h is small enough. However, this is again the case when pointwise accuracy in time is reasonable to expect rather than accuracy in time averaged statistics. Thus, the problem of closing the circle in the velocity error equation for the time averaged statistics seems to catch at the same point as in the standard error analysis.*

We shall see that in at least one case the circle of analysis is closable. In more general cases, we believe the problem is due to the fact that we are estimating $<||\nabla(\mathbf{u}-\mathbf{u}^h)||^2>$ rather than $||<\nabla(\mathbf{u}-\mathbf{u}^h)>||^2$.

Proof. Since $\mathbf{u}_t\in L^1(0,T;\mathbf{X}')$, the weak solution satisfies the variational formulation

$$(\mathbf{u}_t,\mathbf{v}^h)+\nu(\nabla\mathbf{u},\nabla\mathbf{v}^h)+b(\mathbf{u},\mathbf{u},\mathbf{v}^h)-(p,\nabla\cdot\mathbf{v}^h)=(\mathbf{f},\mathbf{v}^h)\qquad\forall\mathbf{v}^h\in L^\infty(0,T;\mathbf{X}^h).\quad(4.1.8)$$

A similar equation holds for $\mathbf{u}^h$, so subtraction and the fact that, for $q^h\in Q^h$, $(q^h,\nabla\cdot\mathbf{v}^h)=0$, give an equation for the error $\mathbf{e}=\mathbf{u}-\mathbf{u}^h$:

$$(\mathbf{e}_t,\mathbf{v}^h)+\nu(\nabla\mathbf{e},\nabla\mathbf{v}^h)\quad+\quad b(\mathbf{u},\mathbf{u},\mathbf{v}^h)-b(\mathbf{u}^h,\mathbf{u}^h,\mathbf{v}^h)$$
$$-(p-q^h,\nabla\cdot\mathbf{v}^h)=0\quad\forall\mathbf{v}^h\in L^\infty(0,T;\mathbf{V}^h).\quad(4.1.9)$$

Let $\tilde{\mathbf{u}}$ be an interpolant of $\mathbf{u}$ with $\tilde{\mathbf{u}}\in L^2(0,\infty;H^1(\Omega))\cap L^\infty(0,\infty;\mathbf{V}^h)$ and write $\mathbf{e}=\boldsymbol{\eta}-\boldsymbol{\phi}^h$, where $\boldsymbol{\eta}=\mathbf{u}-\tilde{\mathbf{u}}$ and $\boldsymbol{\phi}^h=\mathbf{u}^h-\tilde{\mathbf{u}}$. Adding

$$-b(\mathbf{e},\mathbf{e},\mathbf{e})+b(\mathbf{u},\mathbf{u}^h,\boldsymbol{\phi}^h)-b(\mathbf{u},\mathbf{u}^h,\boldsymbol{\phi}^h),$$

where the first term vanishes, we get with $\mathbf{v}^h=\boldsymbol{\phi}^h$

$$\frac{1}{2}\frac{d}{dt}||\boldsymbol{\phi}^h||^2+\nu||\nabla\boldsymbol{\phi}^h||^2\quad=\quad(\boldsymbol{\eta}_t,\boldsymbol{\phi}^h)+\nu(\nabla\boldsymbol{\eta},\nabla\boldsymbol{\phi}^h)-(p-q^h,\nabla\cdot\boldsymbol{\phi}^h)$$
$$+b(\mathbf{e},\mathbf{u},\boldsymbol{\eta})-b(\mathbf{e},\mathbf{e},\boldsymbol{\eta})-b(\mathbf{e},\mathbf{u},\mathbf{e})+b(\mathbf{u},\mathbf{e},\boldsymbol{\eta}).$$

Time averaging the equation above and observing that $||\boldsymbol{\phi}^h||$ is uniformly bounded in time (since $||\mathbf{u}^h||$ is bounded and $\tilde{\mathbf{u}}\in L^\infty(0,\infty;L^2(\Omega)))$, we have

$$<\varepsilon(\boldsymbol{\phi}^h)>\quad\le\quad\frac{1}{|\Omega|}\Big[<|(\boldsymbol{\eta}_t,\boldsymbol{\phi}^h)|>+<\nu|(\nabla\boldsymbol{\eta},\nabla\boldsymbol{\phi}^h)|>+<|(p-q^h,\nabla\cdot\boldsymbol{\phi}^h)|>$$
$$+<|b(\mathbf{e},\mathbf{u},\boldsymbol{\eta})|>+<|b(\mathbf{e},\mathbf{e},\boldsymbol{\eta})|>+<|b(\mathbf{e},\mathbf{u},\mathbf{e})|>+<|b(\mathbf{u},\mathbf{e},\boldsymbol{\eta})|>\Big].$$

The time-averaged Cauchy-Schwarz-Young inequality (2.3.7) now gives

$$
\frac{1}{2} < \varepsilon(\boldsymbol{\phi}^h) > \ \leq \ C\nu^{-1} < \|\boldsymbol{\eta}_t\|^2_{-1} > + < \varepsilon(\boldsymbol{\eta}) > + C\,\nu^{-1} < \|\,p - q^h\,\|^2 >
$$
$$
+ < |\,b(\mathbf{e},\mathbf{u},\boldsymbol{\eta})\,| > + < |\,b(\mathbf{e},\mathbf{e},\boldsymbol{\eta})\,| > + < |\,b(\mathbf{e},\mathbf{u},\mathbf{e})\,| > + < |\,b(\mathbf{u},\mathbf{e},\boldsymbol{\eta})\,| > .
$$

The triangle inequality then gives the first claimed time-averaged error inequality.

For the second inequality we use the following bounds on the trilinear form, see Lemma 2.1.2, together with Young's inequality

$$
< |\,b(\mathbf{e},\mathbf{u},\mathbf{e})\,| > \ \leq \ C < \|\nabla\mathbf{u}\|\,\|\,\mathbf{e}\,\|^{1/2}\,\|\nabla\mathbf{e}\,\|^{3/2} >
$$
$$
\leq \ \frac{\nu}{8} < \|\nabla\mathbf{e}\,\|^2 > + C\,\nu^{-3} < \|\nabla\mathbf{u}\,\|^4\,\|\,\mathbf{e}\,\|^2 >,
$$

$$
< |\,b(\mathbf{e},\mathbf{e},\eta)\,| > \ \leq \ C < \|\,\mathbf{e}\,\|^{1/2}\,\|\nabla\mathbf{e}\,\|^{3/2}\,\|\nabla\boldsymbol{\eta}\,\| >
$$
$$
\leq \ \frac{\nu}{8} < \|\nabla\mathbf{e}\,\|^2 > + C\,\nu^{-3} < \|\,\mathbf{e}\,\|^2\,\|\nabla\boldsymbol{\eta}\,\|^4 >,
$$

$$
< |\,b(\mathbf{e},\mathbf{u},\eta)\,| > \ \leq \ C < \|\,\mathbf{e}\,\|^{1/2}\,\|\nabla\mathbf{e}\,\|^{1/2}\,\|\nabla\mathbf{u}\,\|\,\|\nabla\boldsymbol{\eta}\,\| >
$$
$$
\leq \ \frac{\nu}{8} < \|\nabla\mathbf{e}\,\|^2 > + C\,\nu^{-3} < \|\,\mathbf{e}\,\|^{2/3}\,\|\nabla\mathbf{u}\,\|^{4/3}\,\|\nabla\boldsymbol{\eta}\,\|^{4/3} >,
$$

$$
< |\,b(\mathbf{u},\mathbf{e},\eta)\,| > \ \leq \ C < \|\nabla\mathbf{u}\,\|\,\|\nabla\mathbf{e}\,\|\,\|\,\boldsymbol{\eta}\,\|^{1/2}\,\|\nabla\boldsymbol{\eta}\,\|^{1/2} >
$$
$$
\leq \ \frac{\nu}{8} < \|\nabla\mathbf{e}\,\|^2 > + C < \nu^{-1}\|\nabla\mathbf{u}\,\|^2\,\|\,\boldsymbol{\eta}\,\|\,\|\nabla\boldsymbol{\eta}\,\| > .
$$

Thus

$$
< \varepsilon(\mathbf{u} - \mathbf{u}^h) > \ \leq \ C < \varepsilon(\mathbf{u} - \tilde{\mathbf{u}}) > + C\,\nu^{-1} < \|\,p - q^h\,\|^2 >
$$
$$
+ C\left[\,\nu^{-1} < \|\boldsymbol{\eta}_t\|^2_{-1} > + \nu^{-3} < \|\,\mathbf{e}\,\|^{2/3}\,\|\nabla\mathbf{u}\,\|^{4/3}\,\|\nabla\boldsymbol{\eta}\,\|^{4/3} >\right.
$$
$$
+ \nu^{-3} < \|\,\mathbf{e}\,\|^2\,\|\nabla\boldsymbol{\eta}\,\|^4 > + < \nu^{-1}\|\nabla\mathbf{u}\,\|^2\,\|\,\boldsymbol{\eta}\,\|\,\|\nabla\boldsymbol{\eta}\,\| >
$$
$$
\left.+ \nu^{-3} < \|\nabla\mathbf{u}\,\|^4\,\|\,\mathbf{e}\,\|^2 >\right],
$$

which is the second error inequality, completing the proof. □

4.1.1 The Case of Large $\mathbf{u}_0$ and Small $\mathbf{f}^*(\mathbf{x})$

There is at least one interesting case in which the error equations for the time-averaged velocity error, $< \varepsilon(\mathbf{u} - \mathbf{u}^h) >$, can be closed: the case of large initial condition $\mathbf{u}_0$ and asymptotically small body force $\mathbf{f}(\mathbf{x}, t)$. In this subsection we assume

$$\mathbf{f}(\mathbf{x}, t) \in L^\infty(0, \infty; H^{-1}(\Omega)), \qquad \mathbf{f}(\mathbf{x}, t) \to \mathbf{f}^*(\mathbf{x}) \text{ as } t \to \infty$$

and

$$\nu^{-2} M \, ||\, \mathbf{f}^* \,||_{-1} =: \alpha < 1.$$

In this case, it is possible time averaging will eventually wash out the irregularities caused by the large initial condition. We show that this is indeed the case. To shorten the presentation, we shall simplify the condition on $\mathbf{f}$ to

$$\mathbf{f}(\mathbf{x}, t) \equiv \mathbf{f}^*(\mathbf{x}) \qquad \text{and} \qquad \nu^{-2} M \, ||\, \mathbf{f}^* \,||_{-1} = \alpha < 1. \tag{4.1.10}$$

Proposition 4.1.3. *Suppose (4.1.10) holds. Then*

$$< \varepsilon(\mathbf{u} - \mathbf{u}^*) >= 0, \tag{4.1.11}$$

where $\mathbf{u}^*$ is the solution of the equilibrium Navier-Stokes equations (3.3.2)-(3.3.3).

Proof. Let V_N be a span of eigenfunctions of the Stokes operator. The Leray-Hopf Galerkin construction gives a sequence $\mathbf{u}_N$ in V_N that satisfies

$$(\mathbf{u}_{N,t}, \mathbf{v}) + \nu(\nabla \mathbf{u}_N, \nabla \mathbf{v}) + (\mathbf{u}_N \cdot \nabla \mathbf{u}_N, \mathbf{v}) = (\mathbf{f}, \mathbf{v}) \quad \forall \mathbf{v} \in V_N, \tag{4.1.12}$$

with a subsequence $\mathbf{u}_{N_j}$ in V_N converging to a weak solution $\mathbf{u}$, as $N_j \to \infty$, strongly in $L^2(0, T; H(\Omega))$, and weakly in $L^2(0, T; \mathbf{V})$.

Let $\mathbf{u}_N^* \in V_N$ be the Galerkin projection of $\mathbf{u}^*$ in V_N. Then $\mathbf{u}_N^*$ satisfies

$$\nu(\nabla \mathbf{u}_N^*, \nabla \mathbf{v}) + (\mathbf{u}_N^* \cdot \nabla \mathbf{u}_N^*, \mathbf{v}) = (\mathbf{f}, \mathbf{v}) \quad \forall \mathbf{v} \in V_N, \tag{4.1.13}$$

and $\mathbf{u}_N^* \to \mathbf{u}^*$ in $\mathbf{X}$ and $\mathbf{V}$ as $N \to \infty$.

Set $\phi_N = \mathbf{u}_N(\mathbf{x}, t) - \mathbf{u}_N^*(\mathbf{x})$ and subtract (4.1.13) from (4.1.12) to get

$$(\phi_{N,t}, \mathbf{v}) + \nu(\nabla\phi_N, \nabla\mathbf{v}) + (\mathbf{u}_N \cdot \nabla\mathbf{u}_N, \mathbf{v}) - (\mathbf{u}_N^* \cdot \nabla\mathbf{u}_N^*, \mathbf{v}) = 0 \qquad \forall\, \mathbf{v} \in V_N. \quad (4.1.14)$$

Let $\mathbf{v} = \phi_N$, add and subtract $(\mathbf{u}_N \cdot \nabla\mathbf{u}_N^*, \mathbf{v})$ and integrate from 0 to T to get

$$\frac{1}{2}||\phi_N(T)||^2 + \int_0^T \nu||\nabla\phi_N||^2\, dt = \frac{1}{2}||\phi_N(0)||^2 + \int_0^T -b(\phi_N, \mathbf{u}_N^*, \phi_N)\, dt$$

Next, using the bound on the trilinear form, the á priori bound (3.3.7) and the small data assumption (4.1.10) gives

$$\frac{1}{2}||\phi_N(T)||^2 + (1-\alpha)\nu\int_0^T ||\nabla\phi_N||^2\, dt \ \leq\ \frac{1}{2}||\phi_N(0)||^2.$$

Thus, dropping the first term,

$$\int_0^T \nu||\nabla\phi_N||^2\, dt \leq (1-\alpha)^{-1}\frac{1}{2}||\phi_N(0)||^2. \qquad (4.1.15)$$

Passing to subsequences, and using classical properties of weak limits, we have

$$\lim_{N\to\infty} \inf \left(\int_0^T ||\nabla\phi_N||^2\, dt \right) \geq \int_0^T ||\nabla\phi||^2\, dt.$$

Therefore, taking limit inferior on both sides of (4.1.15), gives

$$\int_0^T \nu||\nabla\phi||^2\, dt \leq (1-\alpha)^{-1}\frac{1}{2}||\phi(0)||^2.$$

Dividing by T and taking the limit superior as $T \to \infty$ proves the result. $\qquad\square$

The next proposition is needed in order to prove the desired error estimate on $< \varepsilon(\mathbf{u} - \mathbf{u}^h) >$, given below, in Theorem 4.1.2.

Proposition 4.1.4. *Assume that (4.1.10) holds. Then*

$$< \varepsilon(\mathbf{u}^h - \mathbf{u}^{*h}) >= 0, \qquad (4.1.16)$$

Proof. The proof works in the same way as that of Proposition 4.1.3. It is based on subtracting (3.2.3) and (3.3.6). $\qquad\square$

Remark 4.1.2. *The statements of Propositions 4.1.3 and 4.1.4 also hold for the kinetic energy.*

Theorem 4.1.2. *Suppose that (4.1.10) holds. Then*

$$< \varepsilon(\mathbf{u} - \mathbf{u}^h) > \ \leq \ C\,\nu\,||\nabla(\mathbf{u}^* - \mathbf{u}^{*h})||^2, \tag{4.1.17}$$

where the constant C depends on the domain.

Proof. We can start by writing

$$||\nabla(\mathbf{u} - \mathbf{u}^h)||^2 = ||\nabla(\mathbf{u} - \mathbf{u}^* + \mathbf{u}^* - \mathbf{u}^{*h} + \mathbf{u}^{*h} - \mathbf{u}^h)||^2.$$

Next, we use the triangle inequality, together with Proposition 4.1.3 and Proposition 4.1.4 to get

$$\limsup_{T \to \infty} \frac{1}{T} \int_0^T \nu\,||\nabla(\mathbf{u} - \mathbf{u}^h)||^2\,dt \leq C\,\nu\,||\nabla(\mathbf{u}^* - \mathbf{u}^{*h})||^2.$$

$\square$

Remark 4.1.3. *The statement of Theorem 4.1.2 says that the problem of estimating $< \varepsilon(\mathbf{u} - \mathbf{u}^h) >$ reduces to the one of estimating $||\nabla(\mathbf{u}^* - \mathbf{u}^{*h})||^2$. Standard finite element error estimates thus immediately imply $< \varepsilon(\mathbf{u} - \mathbf{u}^h) >$ is optimal.*

Corollary 4.1.2. *Suppose the small data assumption (4.1.10) holds, $(\mathbf{X}^h, Q^h)$ satisfies the inf-sup condition. Then*

$$< \varepsilon(\mathbf{u} - \mathbf{u}^h) > \leq C \left[\inf_{\mathbf{v}^h \in \mathbf{X}^h} \nu||\nabla(\mathbf{u}^* - \mathbf{v}^h)||^2 + \inf_{q^h \in Q^h} \nu^{-1}||p^* - q^h||^2 \right]$$

Proof. This follows by inserting the error estimates for $||\nabla(\mathbf{u}^* - \mathbf{u}^{*h})||$ from Girault and Raviart [30] into the right hand side of (4.1.17). $\square$

Concerning the time averaged error in the pressure, we have the following corollary. It is a direct consequence of Theorem 4.1.1.

Corollary 4.1.3. *Let the assumptions of Corollary 4.1.1 be fulfilled. Suppose additionally that assumptions (4.1.10) hold. Then*

$$||<p - p^h>|| \leq \frac{3\nu}{\beta} \left\langle ||\nabla(\mathbf{u} - \mathbf{u}^h)||^2 \right\rangle^{1/2} + \left(1 + \frac{C}{\beta} \right) \inf_{q^h \in Q^h} \limsup_{T \to \infty} || <p - q^h>_T ||.$$

4.2 TIME AVERAGED ERRORS IN DRAG AND LIFT

Consider the flow around a body in a channel with flow region Ω and boundary Γ, which consists of Γ_b (boundary of the body) and $\Gamma_c = \Gamma_i \cup \Gamma_o \cup \Gamma_w$ (where Γ_i, Γ_o correspond to the inflow and outflow and Γ_w, to the walls).

Define

$$\boldsymbol{\sigma} = -p\,\mathbb{I} + 2\,\nu\,\nabla^s \mathbf{u},$$

where ∇^s indicates the symmetric part of the operator ∇.

Let ρ be the density of the fluid. Then consider the Navier-Stokes equations written in the form:

$$\rho(\mathbf{u}_t + \mathbf{u} \cdot \nabla\mathbf{u}) = \nabla \cdot \boldsymbol{\sigma} + \mathbf{f} \qquad \text{in } \Omega \qquad\qquad (4.2.1)$$

$$\nabla \cdot \mathbf{u} = 0 \qquad \text{in } \Omega$$

$$\mathbf{u} = \mathbf{g} \qquad \text{on } \Gamma$$

$$\mathbf{u}(\mathbf{x}, 0) = \mathbf{u}_0(\mathbf{x}) \qquad \text{in } \Omega$$

satisfying the compatibility condition $\int_\Gamma \mathbf{g} \cdot \hat{\mathbf{n}} dS = 0$. We assume $\mathbf{g} = \mathbf{0}$ on Γ_w and Γ_b.

We introduce the spaces

$$\mathbf{X}_g = \left\{ \mathbf{v} \in H^1(\Omega)^d : \mathbf{v}|_\Gamma = \mathbf{g} \right\}, \quad \mathbf{X}_0 = H^1_0(\Omega)^d.$$

A weak formulation of (4.2.1) reads: Find $\mathbf{u} : [0, T] \to \mathbf{X}_g$ and $p : (0, T] \to Q$ such that

$$\rho\,(\mathbf{u}_t, \mathbf{v}) \;\; + \;\; 2\,\nu(\nabla^s \mathbf{u}, \nabla^s \mathbf{v}) + \rho\,b(\mathbf{u}, \mathbf{u}, \mathbf{v})$$

$$+ \;\; (p, \nabla \cdot \mathbf{v}) + (\nabla \cdot \mathbf{u}, q) = (\mathbf{f}, \mathbf{v}) \qquad \forall(\mathbf{v}, q) \in \mathbf{X}_0 \times Q. \qquad (4.2.2)$$

Drag and lift are defined as

$$D = - \int_{\Gamma_b} \hat{\mathbf{e}}_1 \cdot \boldsymbol{\sigma} \cdot \hat{\mathbf{n}}\,d\gamma \qquad \text{and} \qquad L = - \int_{\Gamma_b} \hat{\mathbf{e}}_2 \cdot \boldsymbol{\sigma} \cdot \hat{\mathbf{n}}\,d\gamma,$$

respectively, where $\hat{\mathbf{e}}_\mathbf{i}$ is the unit vector in the ith direction and $\hat{\mathbf{n}}$ is the outward pointing unit normal to Γ_b. (We assume that $+\hat{\mathbf{e}}_1$ is the direction of motion and $-\hat{\mathbf{e}}_2$ is the direction of gravity.)

Remark 4.2.1. *Deriving mathematical estimates of drag and lift involves some technical points necessary to ensure that the trace of $\boldsymbol{\sigma} \cdot \mathbf{n}$ on Γ is well defined in an appropriate space. Requiring $\boldsymbol{\sigma} \cdot \mathbf{n}$ to be well defined at each t requires regularity. On the other hand, time averages of $\boldsymbol{\sigma} \cdot \mathbf{n}$ seem to require less regularity. In this section, we assume that $(\mathbf{u}, p)$ is slightly more regular than a general weak solution to ensure $\boldsymbol{\sigma} \cdot \mathbf{n} \in L^1(0, T; H^{-1/2}(\Gamma_b))$. In particular, we assume that, for some $s > 1/2$, for a.e. $T > 0$, $\mathbf{u} \in L^1(0, T; H^{1+s}(\Omega))$ and $p \in L^1(0, T; H^s(\Omega))$. This implies, by the Trace Theorem, that $\boldsymbol{\sigma} \cdot \mathbf{n} \in L^1(0, T; H^{s-1/2}(\Gamma_b))$.*

Lemma 4.2.1. *Let $\mathbf{u} \in L^1(0, T; H^{s+1}(\Omega)) \cap \mathbf{X}_g$, $\mathbf{u}_t \in L^1(0, T; H^{-1}(\Omega))$ and $p \in L^1(0, T; H^s(\Omega))$, for some $s > 1/2$ be solutions of (4.2.2). Then $\boldsymbol{\sigma} \cdot \mathbf{n} \in L^1(0, T; H^{s-1/2}(\Gamma_b))$ and*

$$\int_0^T \int_{\Gamma_b} \mathbf{v} \cdot \boldsymbol{\sigma} \cdot \hat{\mathbf{n}} \, d\gamma \, dt \tag{4.2.3}$$

$$= \int_0^T \left\{ \rho \, (\mathbf{u}_t, \mathbf{v}) + 2 \, \nu (\nabla^s \mathbf{u}, \nabla^s \mathbf{v}) + \rho \, b(\mathbf{u}, \mathbf{u}, \mathbf{v}) - (p, \nabla \cdot \mathbf{v}) - (\mathbf{f}, \mathbf{v}) \right\} dt$$

for any $\mathbf{v} \in L^\infty(0, T; H^1(\Omega))$ with $\mathbf{v} = 0$ on Γ_c.

Remark 4.2.2. *In particular, in (4.2.3), one choice of $\mathbf{v}$ satisfying $\mathbf{v} = \hat{\mathbf{e}}_1$ on Γ_b gives a formula for the drag and $\mathbf{v} = \hat{\mathbf{e}}_2$, one for the lift.*

Proof. The proof uses a density argument. First, let $\{\mathbf{v}_j\}_{j=1}^\infty$ be a sequence in $C^\infty([0, T] \times \Omega)$ with $\mathbf{v}_j|_{\Gamma_c} = 0$ for all j, $\mathbf{v}_j \to \mathbf{v}$ in $L^\infty(0, T; H^1(\Omega))$. Then, by the definition of distributional derivatives, equation (4.2.3) holds true with $\mathbf{v}$ replaced by $\mathbf{v}_j$. For $\mathbf{u}, p$ with the assumed regularity, each term in (4.2.3) is a bounded linear functional of $\mathbf{v}$ in $L^\infty(0, T; H^1(\Omega))$. Thus it is continuous on $L^\infty(0, T; H^1(\Omega))$. Therefore we may let $j \to \infty$ and (4.2.3) holds for $\mathbf{v} \in L^\infty(0, T; H^1(\Omega))$, since $C^\infty([0, T] \times \Omega)$ is dense in $L^\infty(0, T; H^1(\Omega))$. $\qquad\square$

Theorem 4.2.1. *Let the assumptions of Lemmas 4.2.1 and 4.1.1 and Proposition 4.1.1 be fulfilled. The time averaged drag and lift can be estimated as*

$$| < D - D_h > |, | < L - L_h > | \leq C(\nu + \nu^{-1}\|\mathbf{f}\|_{L^\infty(0,\infty;H^{-1}(\Omega))}) < \|\nabla (\mathbf{u} - \mathbf{u}^h)\|^2 >^{1/2}$$

$$+ C \limsup_{T \to \infty} \| < p - p^h >_T \|.$$

35

Proof. We present here a proof for the drag estimate, since the same argument follows for the lift estimate, according to an appropriate choice of $\mathbf{w}$.

Let $\mathbf{w}$ be a smooth time-independent vector field satisfying $\mathbf{w} = \hat{\mathbf{e}}_1$ on Γ_b and $\mathbf{w} = 0$ on Γ_c. If we take $\mathbf{v} = \mathbf{w}$ in (4.2.3), then we get a formula for the drag as follows

$$\int_0^T D\,dt = \int_0^T \{\rho\,(\mathbf{u}_t, \mathbf{w}) + 2\,\nu(\nabla^s\,\mathbf{u}, \nabla^s\,\mathbf{w}) + \rho\,b(\mathbf{u}, \mathbf{u}, \mathbf{w}) - (p, \nabla\cdot\mathbf{w}) - (\mathbf{f}, \mathbf{w})\}\,dt.$$

Now let $i_h\mathbf{w}$ be a finite element interpolant to $\mathbf{w}$. Then

$$
\begin{aligned}
\int_0^T D - D_h\,dt \;=\; & \int_0^T \{\rho\,(\mathbf{u}_t, \mathbf{w}) + 2\,\nu(\nabla^s\,\mathbf{u}, \nabla^s\,\mathbf{w}) + \rho\,b(\mathbf{u}, \mathbf{u}, \mathbf{w}) \\
& - (p, \nabla\cdot\mathbf{w}) - (\mathbf{f}, \mathbf{w}) - \rho\,(\mathbf{u}_t^h, i_h\mathbf{w}) - 2\,\nu(\nabla^s\,\mathbf{u}^h, \nabla^s\,i_h\mathbf{w}) \\
& - \rho\,b(\mathbf{u}^h, \mathbf{u}^h, i_h\mathbf{w}) + (p^h, \nabla\cdot i_h\mathbf{w}) + (\mathbf{f}, i_h\mathbf{w})\}\,dt.
\end{aligned}
$$

Adding and subtracting appropriate terms, this becomes

$$
\begin{aligned}
\int_0^T D - D_h\,dt \;=\; & \int_0^T \{\rho\,(\mathbf{u}_t, \mathbf{w} - i_h\mathbf{w}) + \rho\,((\mathbf{u} - \mathbf{u}^h)_t, i_h\mathbf{w}) + 2\,\nu(\nabla^s\,\mathbf{u}, \nabla^s\,(\mathbf{w} - i_h\mathbf{w})) \\
& + 2\,\nu(\nabla^s\,(\mathbf{u} - \mathbf{u}^h), \nabla^s\,i_h\mathbf{w}) + \rho\,b(\mathbf{u}, \mathbf{u}, \mathbf{w} - i_h\mathbf{w}) + \rho\,b(\mathbf{u}, \mathbf{u}, i_h\mathbf{w}) \\
& - \rho\,b(\mathbf{u}^h, \mathbf{u}^h, i_h\mathbf{w}) - (p, \nabla\cdot(\mathbf{w} - i_h\mathbf{w})) \\
& - (p - p^h, \nabla\cdot i_h\mathbf{w}) - (\mathbf{f}, \mathbf{w} - i_h\mathbf{w})\}\,dt. \qquad (4.2.4)
\end{aligned}
$$

Observe now that the term containing $(\mathbf{f}, \mathbf{w} - i_h\mathbf{w})$ in (4.2.4) can be rewritten by multiplying (4.2.1) by $\mathbf{w} - i_h\mathbf{w}$ and integrating:

$$
\begin{aligned}
(\mathbf{f}, \mathbf{w} - i_h\mathbf{w}) \;=\; & \rho\,(\mathbf{u}_t, \mathbf{w} - i_h\mathbf{w}) + 2\,\nu(\nabla^s\,\mathbf{u}, \nabla^s\,(\mathbf{w} - i_h\mathbf{w})) \\
& + \rho\,b(\mathbf{u}, \mathbf{u}, \mathbf{w} - i_h\mathbf{w}) - (p, \nabla\cdot(\mathbf{w} - i_h\mathbf{w})). \qquad (4.2.5)
\end{aligned}
$$

Hence, (4.2.4) and (4.2.5) together give

$$
\begin{aligned}
\int_0^T D - D_h\,dt \;=\; & \int_0^T \{\rho\,((\mathbf{u} - \mathbf{u}^h)_t, i_h\mathbf{w}) + 2\,\nu(\nabla^s\,(\mathbf{u} - \mathbf{u}^h), \nabla^s\,i_h\mathbf{w}) \\
& + \rho\,b(\mathbf{u}, \mathbf{u}, i_h\mathbf{w}) - \rho\,b(\mathbf{u}^h, \mathbf{u}^h, i_h\mathbf{w}) + (p - p^h, \nabla\cdot i_h\mathbf{w})\}\,dt. \quad (4.2.6)
\end{aligned}
$$

Let $\mathbf{e} = \mathbf{u} - \mathbf{u}^h$ and divide each term in (4.2.6) by T. The first term on the right hand side yields, with the time independence of $i_h\mathbf{w}$,

$$\frac{1}{T}(\mathbf{e}(T) - \mathbf{e}(0), i_h\mathbf{w}) \;\leq\; \frac{C_{PF}}{T}\,(\|\mathbf{e}(T)\| + \|\mathbf{e}(0)\|)\,\|\nabla i_h\mathbf{w}\|.$$

36

Now, by (2.3.3),

$$< (\nabla^s \mathbf{e}, \nabla^s i_h \mathbf{w}) >_T \; \leq \; < ||\nabla \mathbf{e}||^2 >_T^{1/2} \; ||\nabla i_h \mathbf{w}||.$$

Next, consider the nonlinear term

$$< b(\mathbf{u}, \mathbf{u}, i_h \mathbf{w}) - b(\mathbf{u}^h, \mathbf{u}^h, i_h \mathbf{w}) >_T$$

$$= \quad < b(\mathbf{u}, \mathbf{e}, i_h \mathbf{w}) + b(\mathbf{e}, \mathbf{u}^h, i_h \mathbf{w}) >_T$$

$$\leq \quad M < (||\nabla \mathbf{u}|| + ||\nabla \mathbf{u}^h||) ||\nabla \mathbf{e}|| ||\nabla i_h \mathbf{w}|| >_T$$

$$\overset{(2.3.3)}{\leq} \quad C||\nabla i_h \mathbf{w}|| < (||\nabla \mathbf{u}|| + ||\nabla \mathbf{u}^h||)^2 >_T^{1/2} < ||\nabla \mathbf{e}||^2 >_T^{1/2}$$

$$\leq \quad C||\nabla i_h \mathbf{w}|| < ||\nabla \mathbf{u}||^2 + ||\nabla \mathbf{u}^h||^2 >_T^{1/2} < ||\nabla \mathbf{e}||^2 >_T^{1/2}$$

For the pressure term, we obtain, with the time independence of $i_h \mathbf{w}$ and the Cauchy-Schwarz inequality,

$$< (p - p^h, \nabla \cdot i_h \mathbf{w}) >_T \quad = \quad (< p - p^h >_T, \nabla \cdot i_h \mathbf{w}) \leq C \, || < p - p^h >_T \, || \, ||\nabla i_h \mathbf{w}||.$$

Putting everything together, equation (4.2.6) becomes

$$| < D - D_h >_T | \quad \leq \quad \rho \frac{C_{PF}}{T} \left(||\mathbf{e}(T)|| + ||\mathbf{e}(0)|| \right) ||\nabla i_h \mathbf{w}||$$

$$+ \quad (\nu + \rho < ||\nabla \mathbf{u}||^2 + ||\nabla \mathbf{u}^h||^2 >_T^{1/2}) \; < ||\nabla \mathbf{e}||^2 >_T^{1/2} \; ||\nabla i_h \mathbf{w}||$$

$$+ \quad C \, || < p - p^h >_T \, || \, ||\nabla i_h \mathbf{w}||,$$

Taking *limsup* on both sides of the inequality, we have

$$\limsup_{T \to \infty} | < D - D_h >_T | \quad \leq \quad (\nu + \rho < ||\nabla \mathbf{u}||^2 + ||\nabla \mathbf{u}^h||^2 >^{1/2}) \; < ||\nabla \mathbf{e}||^2 >^{1/2} \; ||\nabla i_h \mathbf{w}||$$

$$+ \quad C \limsup_{T \to \infty} || < p - p^h >_T \, || \, ||\nabla i_h \mathbf{w}||.$$

This gives the statement of the theorem, since the terms multiplying $< ||\nabla \mathbf{e}||^2 >^{1/2}$ are bounded by Proposition 4.1.1, the left hand side is lower bounded by $| < D - D_h > |$, and $||\nabla i_h \mathbf{w}|| \leq 2 ||\mathbf{w}||_{H^2(\Omega)} = C$. $\qquad \square$

Corollary 4.2.1. *If, in addition to the assumptions of Theorem 4.2.1, (4.1.10) holds, then*

$$| < D - D_h > |, \; | < L - L_h > | \quad \leq \quad C \left(\nu ||\nabla(\mathbf{u}^* - \mathbf{u}^{*h})|| + \limsup_{T \to \infty} || < p - p^h >_T \, || \right).$$

In the next section we investigate properties of the approximate solution of shear flows.

4.3   PERSISTENT SHEAR FLOWS

We have seen in the previous sections that, provided the portion of the body force driving the flow that persists is small, statistics, such as the time averaged energy dissipation rate, can be accurately predicted by a flow simulation. This accuracy holds quite generally without any of the further assumptions on $\mathbf{u}_0$, ν and Re typically needed to prove accuracy over bounded time intervals.

The case when the persistent forces driving the flow are not small is much more difficult; we shall prove in this section that the analogous estimate of time averaged energy dissipation rate is physically reasonable under a condition on the finite element mesh near the walls. Briefly, we consider the finite element approximation to the following shear flow problem: let $\Omega = [0, L]^3$

$$
\begin{aligned}
\frac{\partial \mathbf{u}}{\partial t} + \mathbf{u} \cdot \nabla \mathbf{u} + \nabla p - \nu \Delta \mathbf{u} &= 0 & \text{in } \Omega \times (0, T] \\
\nabla \cdot \mathbf{u} &= 0 & \text{in } \Omega \times (0, T] \\
\mathbf{u} &= \mathbf{u}_0 & \text{at } t = 0 \\
\mathbf{u}(x_1, x_2, x_3, t) &= \boldsymbol{\phi}(x_3) & \text{for } x_3 \in \partial \Omega \\
\mathbf{u}(x_1, x_2, x_3, t) &= \mathbf{u}(x_1 + L, x_2, x_3, t) & \text{for } x_1 \in \partial \Omega \\
\mathbf{u}(x_1, x_2, x_3, t) &= \mathbf{u}(x_1, x_2 + L, x_3, t) & \text{for } x_2 \in \partial \Omega
\end{aligned}
$$

where

$$
\boldsymbol{\phi}(x_3) = \begin{pmatrix} 0 \\ 0 \\ 0 \end{pmatrix} \text{ if } x_3 = 0 \text{ and } \boldsymbol{\phi}(x_3) = \begin{pmatrix} U \\ 0 \\ 0 \end{pmatrix} \text{ if } x_3 = L,
$$

see Figure 1.

In this problem, the persistent force driving the flow is clearly the motion of the top wall and the time averaged energy dissipation rate must balance the drag exerted by the walls

38
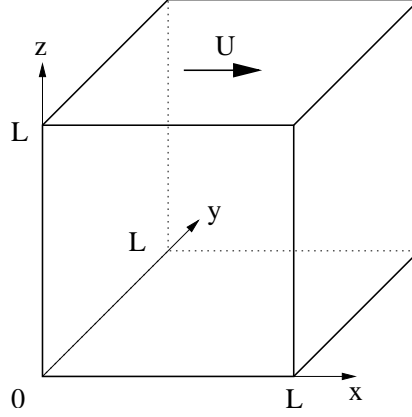
Figure 1: The shear flow problem.

on the fluid. For such problems, the Richardson-Kolmogorov energy cascade predicts quite simply [1]

$$< \varepsilon(\mathbf{u}) > \approx \frac{U^3}{L}$$

independent of ν and Re, respectively.

Remarkably, the upper estimate has also been proven for weak solutions of the Navier-Stokes equations in full generality:

$$< \varepsilon(\mathbf{u}) > \leq C \frac{U^3}{L}$$

by Constantin and Doering [16] and Wang [88].

Herein, we show in essence that provided the first mesh line of the finite element space is within $O(1/Re)$ of the top and bottom walls then

$$< \varepsilon(\mathbf{u}^h) > \leq C \frac{U^3}{L},$$

---

[1]Briefly: the largest coherent structures are associated with the motion of the upper wall. They thus have length scale L and characteristic velocity U. Their local Reynolds number is thus $(\frac{U L}{\nu}(= Re))$ and viscous dissipation is negligible on them. These break up into smaller eddies (velocity $\mathbf{u}$, length l, $Re\,(l) = \frac{\mathbf{u}\,(l)\,l}{\nu}$) until $Re\,(l)$ is small enough for viscous dissipation to drive their kinetic energy to zero exponentially fast. Since viscous dissipation is negligible through this cascade, the energy dissipation rate is related then to the power input to the largest scales at the first step in the cascade. These largest eddies have energy $\frac{1}{2}U^2$ and time scale $\tau = \frac{L}{U}$ so the rate of energy transfer is $O(\frac{U^2}{\tau}) = O(\frac{U^3}{L})$.

i.e. the computed energy dissipation has the correct mathematical and physical scaling.

Since the proof adapts the ideas of Wang [88] we expect that a similar analysis would hold for other variational methods as well.

Let

$$
\begin{aligned}
\mathbf{X} \ = \ & \{\mathbf{v} \in H^1(\Omega) \ : \ \mathbf{v}(x_1, x_2, x_3, t) = \mathbf{v}(x_1 + L, x_2, x_3, t) \text{ for } x_1 \in \partial\Omega, \\
& \mathbf{v}(x_1, x_2, x_3, t) = \mathbf{v}(x_1, x_2 + L, x_3, t) \text{ for } x_2 \in \partial\Omega, \mathbf{v}(x_1, x_2, x_3, t) = \phi(x_3) \text{ for } x_3 \in \partial\Omega\}, \\
\mathbf{X}_0 \ = \ & \{\mathbf{v} \in H^1(\Omega) \ : \ \mathbf{v}(x_1, x_2, x_3, t) = \mathbf{v}(x_1 + L, x_2, x_3, t) \text{ for } x_1 \in \partial\Omega, \\
& \mathbf{v}(x_1, x_2, x_3, t) = \mathbf{v}(x_1, x_2 + L, x_3, t) \text{ for } x_2 \in \partial\Omega, \mathbf{v}(x_1, x_2, x_3, t) = 0 \text{ for } x_3 \in \partial\Omega\}, \\
Q \ = \ & L_0^2(\Omega)
\end{aligned}
$$

and denote corresponding conforming finite element spaces with a superscript h. We assume that the finite element space for the velocity contains linears.

The finite element problem reads as follow: find $\mathbf{u}^h : [0, T) \to \mathbf{X}^h$, $p^h : [0, T) \to Q^h$ such that

$$
(\mathbf{u}_t^h, \mathbf{v}^h) + \nu(\nabla\mathbf{u}^h, \nabla\mathbf{v}^h) + b(\mathbf{u}^h, \mathbf{u}^h, \mathbf{v}^h) - (p^h, \nabla \cdot \mathbf{v}^h) \ = \ 0 \quad \forall \mathbf{v}^h \in \mathbf{X}_0^h \quad (4.3.1)
$$

$$
(\nabla \cdot \mathbf{u}^h, q^h) \ = \ 0 \quad \forall q^h \in Q^h \quad (4.3.2)
$$

$$
(\mathbf{u}(x, 0) - \mathbf{u}_0(x), \mathbf{v}) \ = \ 0 \quad \forall \mathbf{v}^h \in \mathbf{X}_0^h \quad (4.3.3)
$$

Consider the background flow (an extension of the boundary condition ϕ to the interior of Ω) given by

$$
\tilde{\phi}(x_3) = \begin{cases} 0, & \text{if } x_3 \in [0, L - \beta L] \\ \frac{U}{\beta L}(x_3 - (L - \beta L)), & \text{if } x_3 \in [L - \beta L, L] \end{cases}
$$

and

$$
\Phi = \begin{bmatrix} \tilde{\phi}(x_3) \\ 0 \\ 0 \end{bmatrix},
$$

where β is a positive number. For $\beta > 0$ this function is piecewise linear, continuous and satisfies the boundary conditions.

We shall select β appropriately so that $\boldsymbol{\Phi}$ belongs to the finite element space and then take $\mathbf{v}^h = \mathbf{u}^h - \boldsymbol{\Phi}$ in (4.3.1) to get

$$(\mathbf{u}_t^h, \mathbf{u}^h) - (\mathbf{u}_t^h, \boldsymbol{\Phi}) + \nu \, || \, \nabla \mathbf{u}^h \, ||^2 - \nu \, (\nabla \, \mathbf{u}^h, \nabla \, \boldsymbol{\Phi}) - b(\mathbf{u}^h, \mathbf{u}^h, \boldsymbol{\Phi}) = 0 \qquad (4.3.4)$$

since $b(\cdot, \cdot, \cdot)$ is skew symmetric and $\boldsymbol{\Phi}$ is divergence free.

Observing that $(\mathbf{u}_t^h, \boldsymbol{\Phi}) = \frac{\partial}{\partial t}(\mathbf{u}^h, \boldsymbol{\Phi})$, since $\frac{\partial \boldsymbol{\Phi}}{\partial t} = 0$, we rewrite (4.3.4) as

$$\frac{1}{2}\frac{d}{dt}|| \, \mathbf{u}^h \, ||^2 + \nu \, || \, \nabla \mathbf{u}^h \, ||^2 = \frac{\partial}{\partial t}(\mathbf{u}^h, \boldsymbol{\Phi}) + b(\mathbf{u}^h, \mathbf{u}^h, \boldsymbol{\Phi}) + \nu \, (\nabla \, \mathbf{u}^h, \nabla \, \boldsymbol{\Phi})$$

and integrate in time to get

$$\frac{1}{2}|| \, \mathbf{u}^h(T) \, ||^2 - \frac{1}{2}|| \, \mathbf{u}^h(0) \, ||^2 + \nu \int_0^T || \, \nabla \mathbf{u}^h \, ||^2 \, dt$$

$$= \; (\mathbf{u}^h(T), \boldsymbol{\Phi}) - (\mathbf{u}^h(0), \boldsymbol{\Phi}) + \int_0^T b(\mathbf{u}^h, \mathbf{u}^h, \boldsymbol{\Phi}) \, dt + \nu \int_0^T (\nabla \, \mathbf{u}^h, \nabla \, \boldsymbol{\Phi}) \, dt. \quad (4.3.5)$$

We need to estimate each term on the right hand side of (4.3.5). For some of the terms, calculated values of $\boldsymbol{\Phi}$ will be needed:

$$
\begin{aligned}
|| \, \boldsymbol{\Phi} \, ||_{L^\infty(\Omega)} &= \; U, \\
|| \, \nabla \boldsymbol{\Phi} \, ||_{L^\infty(\Omega)} &= \; \frac{U}{\beta \, L}, \\
|| \, \boldsymbol{\Phi} \, ||^2 &= \; L^2 \int_0^L | \, \tilde{\phi}(x_3) \, |^2 \, dx_3 = L^2 \int_{L-\beta L}^L \frac{U^2}{(\beta \, L)^2} \, (\, x_3 - (L - \beta \, L) \,)^2 \, dx_3 = \frac{1}{3} U^2 \, \beta \, L^3, \\
|| \, \nabla \boldsymbol{\Phi} \, ||^2 &= \; \frac{U^2 \, L}{\beta}.
\end{aligned}
$$

For completeness, we include a short proof of the scaling of the constant in the Poincaré-Friedrich's inequality. That will be helpful for the estimation of the nonlinear term.

Lemma 4.3.1. *Let $\mathcal{O}_{\beta L} = \{(x_1, x_2, x_3) \in \Omega : L - \beta L < x_3 < L\}$ be the region close to the upper boundary (where the background flow $\boldsymbol{\Phi}$ does not vanish). Then,*

$$|| \, \mathbf{u}^h - \boldsymbol{\Phi} \, ||_{L^2(\mathcal{O}_{\beta L})} \leq \beta \, L \, || \, \nabla(\mathbf{u}^h - \boldsymbol{\Phi}) \, ||_{L^2(\mathcal{O}_{\beta L})}. \qquad (4.3.6)$$

Proof. First, let $\mathbf{v}$ be a C^1 function on $\mathcal{O}_{\beta L}$ that vanishes for $x_3 \in \partial \mathcal{O}_{\beta L}$. Then, componentwise $(i = 1, 2, 3)$, we have

$$v_i(x_1, x_2, x_3) = v_i(x_1, x_2, L) - \int_{x_3}^{L} \frac{dv_i}{dz}(x_1, x_2, z)dz.$$

Observing that $\mathbf{v}_i(x_1, x_2, L) = 0$, squaring both sides and using the Cauchy-Schwartz inequality, we get

$$v_i^2(x_1, x_2, x_3) \leq \beta L \int_{L-\beta L}^{L} \left(\frac{dv_i}{dz}(x_1, x_2, z) \right)^2 dz.$$

Integrating both sides with respect to x_3 gives

$$\int_{L-\beta L}^{L} v_i^2(x_1, x_2, x_3)dx_3 \leq (\beta L)^2 \int_{L-\beta L}^{L} \left(\frac{dv_i}{dz}(x_1, x_2, z) \right)^2 dz.$$

Then, integrating with respect to x_1 and x_2, and summing from $i = 1$ to 3, we have

$$\| \mathbf{v} \|_{L^2(\mathcal{O}_{\beta L})}^2 \leq (\beta L)^2 \| \nabla \mathbf{v} \|_{L^2(\mathcal{O}_{\beta L})}^2,$$

which proves the lemma in the case of a C^1 function. The case $\mathbf{v} \in \mathbf{X}^h \subset H^1(\Omega)$ follows by density. Finally, just take $\mathbf{v}^h = \mathbf{u}^h - \mathbf{\Phi}$. $\qquad\square$

Next, we use the estimates above to derive upper bounds for the following terms:

$$(\mathbf{u}^h(T), \mathbf{\Phi}) \leq \| \mathbf{u}^h(T) \| \, \| \mathbf{\Phi} \| \leq \sqrt{\frac{\beta}{3}} U L^{3/2} \| \mathbf{u}^h(T) \|,$$

$$(\mathbf{u}^h(0), \mathbf{\Phi}) \leq \| \mathbf{u}^h(0) \| \, \| \mathbf{\Phi} \| \leq \sqrt{\frac{\beta}{3}} U L^{3/2} \| \mathbf{u}^h(0) \|,$$

$$\nu \int_0^T (\nabla \mathbf{u}^h, \nabla \mathbf{\Phi}) \, dt \leq \frac{\nu}{2} \int_0^T \| \nabla \mathbf{u}^h \|^2 \, dt + \frac{\nu}{2} \int_0^T \| \nabla \mathbf{\Phi} \|^2 \, dt$$

$$\leq \frac{\nu}{2} \int_0^T \| \nabla \mathbf{u}^h \|^2 \, dt + \frac{\nu}{2\beta} L U^2 T.$$

For the nonlinear term, we add and subtract terms, and use the fact that $b(\cdot, \cdot, \cdot)$ is skew-symmetric, to write

$$b(\mathbf{u}^h, \mathbf{u}^h, \mathbf{\Phi}) = \frac{1}{2}((\mathbf{u}^h - \mathbf{\Phi}) \cdot \nabla(\mathbf{u}^h - \mathbf{\Phi}), \mathbf{\Phi}) - \frac{1}{2}((\mathbf{u}^h - \mathbf{\Phi}) \cdot \nabla \mathbf{\Phi}, \mathbf{u}^h - \mathbf{\Phi})$$

$$+ \frac{1}{2}(\mathbf{\Phi} \cdot \nabla(\mathbf{u}^h - \mathbf{\Phi}), \mathbf{\Phi}) - \frac{1}{2}(\mathbf{\Phi} \cdot \nabla \mathbf{\Phi}, \mathbf{u}^h - \mathbf{\Phi}) \qquad (4.3.7)$$

We use Lemma 4.3.1 together with the calculated values of $\mathbf{\Phi}$ to analyze one term at a time in (4.3.7). In all cases, integration is restricted to $\mathcal{O}_{\beta L}$, since $\text{supp}(\mathbf{\Phi}) \subset \overline{\mathcal{O}}_{\beta L}$.

$$
\begin{aligned}
((\mathbf{u}^h - \mathbf{\Phi}) \cdot \nabla(\mathbf{u}^h - \mathbf{\Phi}), \mathbf{\Phi}) \; &\leq \; ||\,\mathbf{\Phi}\,||_{L^\infty(\mathcal{O}_{\beta L})} ||\,\nabla(\mathbf{u}^h - \mathbf{\Phi})\,||_{L^2(\mathcal{O}_{\beta L})} ||\,\mathbf{u}^h - \mathbf{\Phi}\,||_{L^2(\mathcal{O}_{\beta L})} \\
&\leq \; U\,\beta\,L\,||\,\nabla(\mathbf{u}^h - \mathbf{\Phi})\,||^2_{L^2(\mathcal{O}_{\beta L})} \\
&\leq \; 2\,U\,\beta\,L\,||\,\nabla\mathbf{u}^h\,||^2 + 2\,U^3 L^2,
\end{aligned}
\tag{4.3.8}
$$

$$
\begin{aligned}
((\mathbf{u}^h - \mathbf{\Phi}) \cdot \nabla\mathbf{\Phi}, \mathbf{u}^h - \mathbf{\Phi}) \; &\leq \; ||\,\nabla\mathbf{\Phi}\,||_{L^\infty(\mathcal{O}_{\beta L})} ||\,\mathbf{u}^h - \mathbf{\Phi}\,||^2_{L^2(\mathcal{O}_{\beta L})} \\
&\leq \; U\,\beta\,L\,||\,\nabla(\mathbf{u}^h - \mathbf{\Phi})\,||^2 \\
&\leq \; 2\,U\,\beta\,L\,||\,\nabla\mathbf{u}^h\,||^2 + 2\,U^3 L^2,
\end{aligned}
\tag{4.3.9}
$$

$$
\begin{aligned}
(\mathbf{\Phi} \cdot \nabla(\mathbf{u}^h - \mathbf{\Phi}), \mathbf{\Phi}) \; &\leq \; ||\,\mathbf{\Phi}\,||_{L^\infty(\mathcal{O}_{\beta L})} ||\,\mathbf{\Phi}\,||_{L^2(\mathcal{O}_{\beta L})} ||\,\nabla(\mathbf{u}^h - \mathbf{\Phi})\,||_{L^2(\mathcal{O}_{\beta L})} \\
&\leq \; U\left(\frac{1}{3}U^2\beta L^3\right)^{1/2} ||\,\nabla\mathbf{u}^h\,|| + U\left(\frac{1}{3}U^2\beta L^3\right)^{1/2}\left(\frac{U^2 L}{\beta}\right)^{1/2} \\
&\leq \; \frac{1}{2}U\,\beta\,L\,||\,\nabla\mathbf{u}^h\,||^2 + \frac{5}{6}\,U^3 L^2,
\end{aligned}
\tag{4.3.10}
$$

$$
\begin{aligned}
(\mathbf{\Phi} \cdot \nabla\mathbf{\Phi}, \mathbf{u}^h - \mathbf{\Phi}) \; &\leq \; ||\,\mathbf{\Phi}\,||_{L^\infty(\mathcal{O}_{\beta L})} ||\,\nabla\mathbf{\Phi}\,||_{L^2(\mathcal{O}_{\beta L})} ||\,\mathbf{u}^h - \mathbf{\Phi}\,||_{L^2(\mathcal{O}_{\beta L})} \\
&\leq \; U\,\beta\,L\left(\frac{U^2 L}{\beta}\right)^{1/2} ||\,\nabla\mathbf{u}^h\,|| + U\,\beta\,L\left(\frac{U^2 L}{\beta}\right)^{1/2}\left(\frac{U^2 L}{\beta}\right)^{1/2} \\
&\leq \; \frac{1}{2}U\,\beta\,L\,||\,\nabla\mathbf{u}^h\,||^2 + \frac{3}{2}\,U^3 L^2.
\end{aligned}
\tag{4.3.11}
$$

Putting (4.3.8) to (4.3.11) together, equation (4.3.7) gives

$$
b(\mathbf{u}^h, \mathbf{u}^h, \mathbf{\Phi}) \leq \frac{5}{2}U\,\beta\,L\,||\,\nabla\mathbf{u}^h\,||^2 + \frac{19}{6}U^3 L^2,
$$

so that equation (4.3.5) becomes

$$
\begin{aligned}
\frac{1}{2}||\,\mathbf{u}^h(T)\,||^2 \; - \; &\frac{1}{2}||\,\mathbf{u}^h(0)\,||^2 + \nu \int_0^T ||\,\nabla\mathbf{u}^h\,||^2\,dt \leq \sqrt{\frac{\beta}{3}}UL^{3/2}||\,\mathbf{u}^h(T)\,|| \\
&+ \; \sqrt{\frac{\beta}{3}}UL^{3/2}||\,\mathbf{u}^h(0)\,|| + \frac{\nu}{2}\int_0^T ||\,\nabla\mathbf{u}^h\,||^2\,dt + \frac{\nu}{2\beta}L\,U^2\,T \\
&+ \; \frac{5}{2}\beta\,L\,U \int_0^T ||\,\nabla\mathbf{u}^h\,||^2\,dt + \frac{19}{6}U^3 L^2\,T.
\end{aligned}
$$

Divide by T, take $limsup$ as $T \to \infty$ and use $|\Omega| = L^3$, together with Lemma 4.1.2. If

$$\beta < \frac{1}{5\,Re}, \qquad \text{where} \quad Re = \frac{U\,L}{\nu},$$

then

$$L^3 \left(\frac{1}{2} - \frac{5}{2}\frac{L\,\beta\,U}{\nu} \right) < \varepsilon(\mathbf{u}^h) > \quad \leq \quad \frac{\nu}{2\,\beta} L\,U^2 + \frac{19}{6} U^3 L^2,$$

which gives

$$< \varepsilon(\mathbf{u}^h) > \quad \leq \quad C\frac{U^3}{L}.$$

5.0 LARGE EDDY SIMULATION AND APPROXIMATE DECONVOLUTION MODELS

The famous estimate that $O(Re^{9/4})$ mesh points are required to resolve all the scales of a three dimensional turbulent flow indicates that direct numerical simulation (DNS) is not feasible for high Reynolds number flows and other approaches/turbulence models must be introduced. An alternative to DNS are the Reynolds-stress models, which attempt to model turbulence by time averaging. These models can be very accurate, but they are not suitable for transient flows, because many features of the time dependent solution could disappear under time averaging.

Motivated by the limitations of these two approaches, Large Eddy Simulation (LES) has emerged as one of the most promising approaches in simulation of turbulent flows. Its goal is to compute the large structures of a flow by modeling the effects of small scale structures on the large structures. This is a clever idea, because the large structures, being created by external forces and boundary effects, are specific to each flow, whereas the small structures have a universal behavior and do not need to be accurately represented. This is achieved by applying a space filtering/averaging operation to the Navier-Stokes equations, sifting out the small scales, i.e. those which are of size smaller than the filter width, denoted by δ. LES is not so computationally expensive as DNS (the cost of computing small scales is avoided) and can be expected to be more accurate then the Reynolds-stress models for transient flows (such as vortex shedding and unsteady separation). There are a number of LES models in the literature, and examples of earlier models are the works of Smagorinsky [78], Lily [62] and Deardorff [18].

Traditionally, the derivation of an LES model involves four steps, e.g. Pope [72]:

- Decomposition of the velocity field as $\mathbf{u} = \overline{\mathbf{u}} + \mathbf{u}'$, where $\overline{\mathbf{u}}$ represents the filtered velocity (motion of large scales) and $\mathbf{u}'$, the fluctuations. Typically, $\overline{\mathbf{u}} = G\mathbf{u}$, where G is the filter/averaging operator.

- Averaging of the Navier-Stokes equations gives the non-closed space filtered system, for the new variable $\overline{\mathbf{u}}$:

$$\overline{\mathbf{u}}_t + \nabla \cdot (\overline{\mathbf{u}}\,\overline{\mathbf{u}}) - \nu \Delta \overline{\mathbf{u}} + \nabla \overline{p} = \overline{\mathbf{f}} \qquad \text{and} \qquad \nabla \cdot \overline{\mathbf{u}} = 0. \qquad (5.0.1)$$

  Assume for the moment that differentiation and averaging commute, otherwise, we would have $\overline{\nabla \cdot (\mathbf{u}\,\mathbf{u})}$, instead of $\nabla \cdot (\overline{\mathbf{u}}\,\overline{\mathbf{u}})$ (and similarly for the other terms).

- Closure is obtained by modeling $\mathbf{u}$ in terms of $\overline{\mathbf{u}}$.

- Discretization of the resulting equations, which are then solved numerically.

Examining this list, one can infer that the derivation of a good LES model depends a great deal on the choice of filter and closure model. Moreover, one cannot fail to notice that the new equations to be solved are equations for $\overline{\mathbf{u}}$, and not for $\mathbf{u}$ anymore, thus requiring the imposition of appropriate boundary conditions. This is a matter of great discussion in LES. Put simply, the problem is that the unknowns in the model are all averaged quantities; so the averaged velocity, for instance, must be specified at the boundary. However, most of the time, only the velocity itself is known, not its average. One possibility is to resolve this issue by choosing a specific filter.

There are many filter kernels commonly used in the literature. Some of them are the ideal low pass filter, the box filter and the Gaussian filter, see e.g. Aldama [3], Sagaut [74], John [40], but perhaps the most popular is the Gaussian filter. Its application to the Stokes and the steady state Navier-Stokes equations has been reviewed in Dunca, John and Layton [24] and John and Layton [44]. These are used as convolution kernels for filtering when the domain is the whole space or in the presence of periodic boundary conditions. A major advantage is that filtering and differentiation commute. However, the correct extension for wall bounded domains is not clear: commutation is not possible anymore, unless an extra correction term is introduced in the equations, according to Dunca, John and Layton [25].

An alternative has been proposed by Germano [29]: the use of a differential filter. In that case, $\overline{\mathbf{u}}$ is the solution of a Poisson (or Stokes) problem with right-hand side $\mathbf{u}$, subject to

$\overline{\mathbf{u}} = \mathbf{u}$ on $\partial\Omega$. This seems to be the correct extension of filtering by convolution to bounded domains, providing a simple choice of boundary conditions. It also carries some similarity to filtering in the interior of Ω, since the Poisson kernel is a Gaussian. See Berselli, Iliescu and Layton [6] for a thorough discussion on boundary conditions and LES models.

The closure problem arises because the average of the product is not the product of the averages, i.e $\overline{\mathbf{u}\,\mathbf{u}} \neq \overline{\mathbf{u}}\,\overline{\mathbf{u}}$. In fact, given that $\mathbf{u} = \overline{\mathbf{u}} + \mathbf{u}'$, $\overline{\mathbf{u}\,\mathbf{u}} = \overline{\overline{\mathbf{u}}\,\overline{\mathbf{u}}} + \overline{\overline{\mathbf{u}}\mathbf{u}' + \mathbf{u}'\overline{\mathbf{u}}} + \overline{\mathbf{u}'\mathbf{u}'}$, since $\overline{\mathbf{u}'} \neq \mathbf{0}$ and, in general, $\overline{\overline{\mathbf{u}}} \neq \overline{\mathbf{u}}$. Solving the closure problem means solving the deconvolution problem, i.e. finding useful approximations of $\mathbf{u}$ (since $\overline{\mathbf{u}} = G\mathbf{u}$, this means finding an inverse of G). For most averaging operators, G is symmetric, positive semi-definite and not stably invertible. Thus, the deconvolution problem is generically ill-posed and we resort to approximate deconvolution.

A very simple closure model, perhaps the simplest, is to replace $\mathbf{u}$ by $\overline{\mathbf{u}}$, which is exact on constant flows (since the fluctuation $\mathbf{u}'$ is taken to be zero). However, it is a very rough approximation. Recall the properties of turbulent flows! Nevertheless, this is the simplest model in a specific class of higher order closure models (and systematic definition), the family $(N = 0, 1, 2, \ldots)$ of Approximate Deconvolution Models (ADM), introduced by Adams and Stolz [82, 1]. These models have performed well in practical computations, such as the incompressible channel flow and the supersonic compression-ramp flow, see Stolz, Adams and Kleiser [81, 80]. Their mathematical theory has flourished in the last couple of years, confirming their effectiveness in the works of Dunca and Epshteyn [22] and Layton and Lewandowski [61].

5.1 PROPERTIES OF THE APPROXIMATE DECONVOLUTION OPERATORS

We focus on the case where averaging is performed by differential filters and Ω is periodic.[1] Thus, given $\mathbf{u}$, $\overline{\mathbf{u}}$ is the unique periodic solution of

$$- \delta^2 \Delta\overline{\mathbf{u}} + \overline{\mathbf{u}} = \mathbf{u}, \qquad \text{in } \Omega. \tag{5.1.1}$$

---

[1]In Chapters 6, 7 and 8, when we study discretizations, we do not assume periodicity of Ω.

We then let $G = (-\delta^2 \Delta + I)^{-1}$, so that $\overline{\mathbf{u}} = (-\delta^2 \Delta + I)^{-1} \mathbf{u}$.

Lemma 5.1.1. *G is a symmetric positive operator with eigenvalues*

$$\lambda(G) = \frac{1}{\delta^2 k^2 + 1}, \qquad k = 1, 2, \dots.$$

Proof. The Laplacian operator is symmetric positive definite, and so are $-\delta^2 \Delta + I$ and its inverse, G. Similarly, the eigenvalues of G are the inverse of the eigenvalues of $-\delta^2 \Delta + 1$. $\quad\square$

The approximate deconvolution operators we study are based on the following algorithm, studied by van Cittert, e.g. Bertero and Boccacci [7].

Algorithm 5.1.1 (van Cittert approximate deconvolution algorithm)**.** $\mathbf{u}_0 = \overline{\mathbf{u}}$*, where*

    for n=1,2,...,N-1, perform

$\mathbf{u}_{n+1} = \mathbf{u}_n + \{\overline{\mathbf{u}} - G\mathbf{u}_n\}$

This algorithm may be compactly rewritten as $\mathbf{u}_N = D_N \overline{\mathbf{u}}$, where the Nth deconvolution operator D_N is

$$D_N \overline{\mathbf{u}} := \sum_{n=0}^{N} (I - G)^n \overline{\mathbf{u}}. \tag{5.1.2}$$

The operators corresponding to $N = 0, 1, 2$, for example, are $D_0 \overline{\mathbf{u}} = \overline{\mathbf{u}}$, and $D_1 \overline{\mathbf{u}} = 2\overline{\mathbf{u}} - \overline{\overline{\mathbf{u}}}$, and $D_2 \overline{\mathbf{u}} = 3\overline{\mathbf{u}} - 3\overline{\overline{\mathbf{u}}} + \overline{\overline{\overline{\mathbf{u}}}}$. Let us now give some key properties of these operators and show how they renorm the energy.

Lemma 5.1.2. *[Stability of approximate deconvolution]Let averaging be defined by the differential filter (5.1.1). Then D_N is a self-adjoint, positive definite operator on $L^2(\Omega)$ with norm*

$$||D_N|| := \sup_{\phi \in L^2(\Omega)} \frac{||D_N \phi||}{||\phi||} = N + 1.$$

Proof. We summarize the proof from Berselli, Iliescu and Layton [6] for completeness. Recall from Lemma 5.1.1 that the eigenvalues of G are between zero and one, accumulating at zero. Since $D_N := \sum_{n=0}^{N} (I - G)^n$ is a function of G, it is also self-adjoint. By the spectral mapping theorem

$$\lambda(D_N) = \sum_{n=0}^{N} \lambda(I - G)^n = \sum_{n=0}^{N} (1 - \lambda(G))^n.$$

Thus,

$$\lambda(D_N) = \sum_{n=0}^{N} \lambda(I - G)^n = \sum_{n=0}^{N}(1 - \lambda(G))^n, \quad \text{and} \quad 0 < \lambda(G) \leq 1$$

imply that $1 \leq \lambda(D_N) \leq N + 1$, i.e. $\lambda(D_N) > 0$ and D_N is also positive definite. Since D_N is self-adjoint, the operator norm $||D_N||$ is also easily bounded by the spectral mapping theorem by

$$||D_N|| = \sum_{n=0}^{N} \lambda_{\max}(I - G)^n = \sum_{n=0}^{N}(1 - \lambda_{\min}(G))^n = N + 1. \tag{5.1.3}$$

$\square$

Definition 5.1.1. *The deconvolution weighted norm and inner product are*

$$\|\phi\|_N = \sqrt{(\phi, D_N\phi)} \qquad and \qquad (\phi, \psi)_N := (\phi, D_N\psi).$$

for $\phi, \psi \in L^2(\Omega)$.

Lemma 5.1.3. *We have*

$$||\phi||^2 \leq \|\phi\|_N^2 \leq (N + 1)||\phi||^2, \quad \forall \phi \in L^2(\Omega) . \tag{5.1.4}$$

Proof. As in the proof of Lemma 5.1.2, $1 \leq \lambda(D_N) \leq N + 1$. Since D_N is a self-adjoint operator (and its eigenvectors form an orthonormal basis of $L^2(\Omega)$), this proves the above equivalence of norms. $\square$

It is insightful to consider the Cauchy problem or the periodic problem and visualize the approximate deconvolution operators D_N in wave number space (re-scaled by $k \leftarrow \delta k$). This shows how the N norm reweights the usual $L^2(\Omega)$ norm. Let $\widehat{D}_N$ be the symbol or the transfer function of D_N, given by

$$\widehat{D}_N(k) = \sum_{k=0}^{N}(\widehat{I - G})^n = \sum_{k=0}^{N}\left(\frac{k^2}{1 + k^2}\right)^n. \tag{5.1.5}$$

49
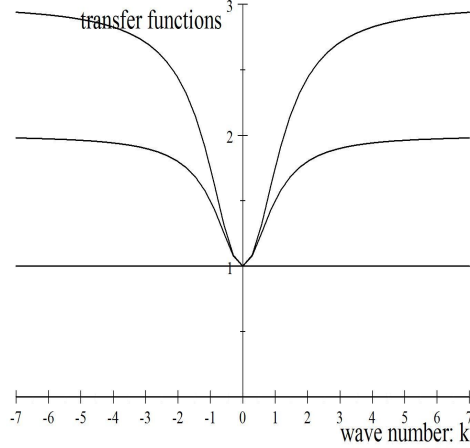
Figure 2: Approximate de-convolution operators, N=0,1,2.

Examples of the first three are

$$\widehat{D}_0 = 1,$$

$$\widehat{D}_1 = 1 + \frac{k^2}{k^2 + 1}, \text{ and}$$

$$\widehat{D}_2 = 1 + \frac{k^2}{k^2 + 1} + \left(\frac{k^2}{k^2 + 1}\right)^2,$$

and their transfer functions are plotted in Figure 2.

Note that the plot of $\widehat{D}_N(k)$ is consistent with (5.1.4): the transfer functions are bounded below by 1, positive and uniformly bounded by $N+1$. Figure 2 also reveals that the weighted norm is very close to the usual norm on the largest spacial scales but then overweights (by at most $N+1$) smaller scales. The large scales are associated with the smooth components and with the wave numbers near zero (i.e., $|\mathbf{k}|$ small). Thus, the fact that D_N is a very accurate solution of the deconvolution problem for the large scales is reflected in the above graph in that the transfer functions $\widehat{D}_N(k)$ have high order contact with $\widehat{G^{-1}} = 1 + k^2$ near $k = 0$.

Lemma 5.1.4 (Error in approximate de-convolution). *For any $\phi \in L^2(\Omega)$,*

$$\begin{aligned} \phi - D_N\overline{\phi} &= (I - G)^{N+1}\phi \\ &= (-1)^{N+1}\delta^{2N+2}\Delta^{N+1}G^{(N+1)}\phi, \end{aligned}$$

50

i.e., for smooth ϕ, $\phi = D_N\overline{\phi} + O(\delta^{2N+2})$.

Proof. See Dunca and Epshteyn [22]. □

Proposition 5.1.1. *For ϕ smooth and N fixed,*

$$\|\phi\|_N^2 = \|\phi\|^2 + O(\delta^2).$$

Proof. A short proof using $\phi - \overline{\phi} = O(\delta^2)$ and $\phi - D_N\overline{\phi} = O(\delta^{2N+2})$ is as follows:

$$(\phi, D_N\phi) = (\phi, \phi) + (\phi, D_N\overline{\phi} - \phi) + (\phi, D_N(\phi - \overline{\phi})) = \|\phi\|^2 + O(\delta^{2N+2}) + O(\delta^2).$$

□

5.2   PROPERTIES OF THE APPROXIMATE DECONVOLUTION LES MODELS

Let $(\mathbf{w}, q)$ denote approximations to $(\overline{\mathbf{u}}, \overline{p})$, the averaged velocity and pressure of the Navier-Stokes equations. The induced LES model is to find $(\mathbf{w}, q)$ satisfying

$$\mathbf{w}_t + \nabla \cdot (\overline{D_N(\mathbf{w})\, D_N(\mathbf{w})}) - \nu\Delta\mathbf{w} + \nabla q = \overline{\mathbf{f}} \qquad \text{and} \qquad \nabla \cdot \mathbf{w} = 0 \qquad (5.2.1)$$

with initial condition $\mathbf{w}(\mathbf{x}, 0) = \mathbf{w}_0(\mathbf{x}) = \overline{\mathbf{u}}_0(\mathbf{x})$.

These models have been extensively studied from an analytical point of view in the case of periodic boundary conditions. It all started with the Zeroth Order Model (the simplest model, although it provides much insight) when Layton and Lewandowski [53] showed that weak solutions exist and that the model is stable. In Layton and Lewandowski [54] it was further proven that strong solutions exist and are unique, the modeling error, $\|\overline{\mathbf{u}} - \mathbf{w}\|$, was bounded and convergence as $\delta \to 0$ to a solution of the NSE was also established. The methods used in Layton and Lewandowski [53, 54] were extended to the whole ADM family by Dunca and Epshteyn [22] to prove an energy inequality, existence, uniqueness and regularity of strong solutions.

First, let $\mathcal{C}$ denote the d-dimensional cube of size $L > 0$, $\mathcal{C} = (0, L)^d$, and

$$H^m(\mathcal{C}) = \{\mathbf{w} \in H^m_{loc}(\mathbb{R}^d) : \mathbf{w} \text{ periodic with period } \mathcal{C}\} \tag{5.2.2}$$

$$\overline{H}^m(\mathcal{C}) = \left\{\mathbf{w} \in H^m(\mathcal{C}) : \int_{\mathcal{C}} \mathbf{w} \, d\mathbf{x} = 0\right\}. \tag{5.2.3}$$

We recall here, from Dunca and Epstheyn [22], the energy balance of the ADM (5.2.1).

Proposition 5.2.1 (Model's energy balance)**.** *Consider the ADM (5.2.1). For $\mathbf{w}_0 \in \overline{H}^1(\mathcal{C}) \cap H(\mathcal{C})$ and $\mathbf{f} \in L^2(0, T; \mathbf{V}')$, the unique strong solution $\mathbf{w}$ of (5.2.1) satisfies*

$$\frac{1}{2}[\|\mathbf{w}(t)\|_N^2 + \delta^2\|\nabla\mathbf{w}(t)\|_N^2] + \int_0^t \nu\|\nabla\mathbf{w}(t')\|_N^2 + \nu\delta^2\|\Delta\mathbf{w}(t')\|_N^2 \, dt' =$$

$$= \frac{1}{2}[\|\mathbf{w}_0\|_N^2 + \delta^2\|\nabla\mathbf{w}_0\|_N^2] + \int_0^t (\mathbf{f}(t'), \mathbf{w}(t'))_N \, dt'. \tag{5.2.4}$$

Proof. See Dunca and Epshteyn [22]. $\square$

Remark 5.2.1. *From this proposition, we can clearly identify the analogs in the ADM (5.2.1) of the physical quantities of kinetic energy and energy dissipation rate, given next.*

Definition 5.2.1.

$$E_{model}(t) \quad := \quad \frac{1}{2L^3}\{\|\mathbf{w}(t)\|_N^2 + \delta^2\|\nabla\mathbf{w}(t)\|_N^2\} \tag{5.2.5}$$

$$\varepsilon_{model}(t) \quad := \quad \frac{\nu}{L^3}\{\|\nabla\mathbf{w}(t)\|_N^2 + \delta^2\|\Delta\mathbf{w}(t)\|_N^2\}. \tag{5.2.6}$$

Remark 5.2.2. *The energy dissipation in the model*

$$\varepsilon_{model}(t) := \frac{\nu}{L^3}\left\{\|\nabla\mathbf{w}(t)\|_N^2 + \delta^2\Delta\mathbf{w}(t)\|_N^2\right\} \tag{5.2.7}$$

is enhanced by the extra term, which is equivalent to $\nu\delta^2\|\Delta\mathbf{w}(t)\|^2$. This term acts as an irreversible energy drain localized at large local fluctuations. The kinetic energy of the model has an extra term

$$E_{model}(t) := \frac{1}{2L^3}\{\|\mathbf{w}(t)\|_N^2 + \delta^2\|\nabla\mathbf{w}(t)\|_N^2\} \tag{5.2.8}$$

which is uniformly equivalent to $\delta^2\|\nabla\mathbf{w}(t)\|^2$.

The true kinetic energy,

$$E(t) := \frac{1}{2L^3} \|\mathbf{w}(t)\|^2,$$

in regions of large deformations is thus extracted, conserved and stored in the kinetic energy penalty term $\delta^2 \|\nabla \mathbf{w}(t)\|^2$.

Remark 5.2.3. *Recall the definition of energy dissipation rate from Chapter 4. In terms of the model's velocity* $\mathbf{w}$*, it can be expressed as*

$$\varepsilon(t) := \frac{\nu}{L^3} \|\nabla \mathbf{w}(t)\|^2. \tag{5.2.9}$$

Proposition 5.2.2. *For smooth* $\mathbf{w}$*,*

$$E_{model}(t) = E(t) + O(\delta^2), \qquad \varepsilon_{model}(t) = \varepsilon(t) + O(\delta^2).$$

Proof. This follows directly from Definition 5.2.1, Proposition 5.1.1 and Lemma 5.1.4. □

Dunca and Epshteyn [22] also give a rigorous bound on the modeling error, $\|\bar{\mathbf{u}} - \mathbf{w}\| = O(\delta^{2N+2})$ (where $\mathbf{u}$ is assumed to be a unique strong solution of the Navier-Stokes equations). These models also preserve energy in the absence of viscosity and external forces, see Rebholz [73], making it conceivable that they possess an energy cascade, proven in Layton and Neda [56]. Another remarkable property of this family of models is that their time averaged consistency error converges to zero uniformly in the Reynolds number as $O(\delta^{1/3})$ (see Lewandowsky and Layton [61]).

The mathematical properties of these models are superior to those of many other LES models being currently used, so the next natural step is to develop and analyze useful discretizations, for the practical case of bounded, non periodic, domains.

6.0   CONVERGENCE ANALYSIS OF THE FINITE ELEMENT METHOD FOR A FUNDAMENTAL METHOD IN TURBULENCE

One of the most basic models in turbulence is the Zeroth Order Model. It has been studied analytically and has good properties, such as existence and uniqueness of strong solutions, Layton and Lewandowski [53, 54] (unlike the Navier-Stokes equations). Our motivation is to use the finite element method to derive a good discretization for this model. Despite being the lowest order of the Approximate Deconvolution Models, it is the key to understanding the higher order members.

Interestingly, this seemingly straightforward idea is far more intricate than it appears. It demands the study of a correct interpretation of averaging on bounded domains. This is the first step in devising stable discretizations for the model, and is strongly influenced by how filtering is ultimately defined in the computational framework. We find that solving the filter equation in a mesh finer than the one used to solve the model itself does not offer any clear advantages, may even be unstable and, of course, increases the computational effort. We also present convergence studies for the discretizations we propose.

In our derivation of the Zeroth Order Model, with the filter chosen, the commutation error (e.g. $\overline{\nabla \cdot \mathbf{u}} \approx \nabla \cdot \overline{\mathbf{u}}$) is within the modeling error of $O(\delta^2)$, so it can be safely ignored. The imposition of correct boundary conditions also has a lot to do with the filter selection. We have chosen to use a differential filter, because that seems to provide a reasonable extension of filtering by convolution to bounded domains. It also gives us somewhat more freedom: loosely speaking, since in the finite element method all equations are treated weakly, we can impose boundary conditions only on the component of the averaged value that lies in the space we are working with.

We investigate stability and convergence of a semidiscretization of the Zeroth Order

Model. In order to assess its accuracy, the numerical error, $\mathbf{w} - \mathbf{w}^h$, is considered, where $\mathbf{w}^h$ is an approximation to $\mathbf{w}$. We analyze two types of schemes, depending on the discretization of the differential filter equation (which can be done on the same mesh as the solution of the problem or on a finer one). When the filtering operation is performed on the same mesh, $\mathbf{w}^h$ is stable and we can prove that an optimal error estimate holds, whereas if it is performed on a finer mesh, we can show only that $\mathbf{w}^h$ is stable for a small finite interval of time. In addition, the convergence results assume strong regularity properties on the true solution $\mathbf{w}$ and require strong conditions on the body forces and the mesh size h. Computationally, this means that solving the filtering equation in the same mesh used to compute the solution is the best approach, since it is both more economical and stable.

In Section 6.1, we give a brief derivation of the model. Properties of the differential filter are presented in Section 6.2. The stability and error analysis of the model with respect to both discretizations of the filtering equations are studied in Section 6.3.

6.1   DERIVATION OF THE MODEL

The Zeroth Order Model is arguably the simplest LES model for the incompressible Navier-Stokes equations, presented in (3.1.1) and recalled here:

$$
\begin{aligned}
\mathbf{u}_t + \nabla \cdot (\mathbf{u}\mathbf{u}) - \nu \Delta \mathbf{u} + \nabla p &= \mathbf{f} & \text{in } (0, T] \times \Omega, \\
\nabla \cdot \mathbf{u} &= 0 & \text{in } [0, T] \times \Omega, \\
\mathbf{u} &= \mathbf{0} & \text{in } [0, T] \times \partial\Omega, \\
\mathbf{u}(0, \mathbf{x}) &= \mathbf{u}_0(\mathbf{x}) & \text{in } \Omega \\
\int_\Omega p \, d\mathbf{x} &= 0,
\end{aligned} \tag{6.1.1}
$$

where $\Omega \subset \mathbb{R}^d$, $d = 2, 3$ is a bounded, regular domain, $\mathbf{u}$ is the fluid velocity, p is the fluid pressure, $\mathbf{f}$ is the body force driving the flow and ν is the kinematic viscosity. The Reynolds number, Re, is inversely proportional to ν ($Re = LU/\nu$, where L and U are characteristic length and velocity scales, respectively).

Spacial filtering is achieved by an averaging process (here, the solution of a Poisson problem) which requires $\mathbf{u}$ to be defined in terms of $\overline{\mathbf{u}}$ (closure problem). We shall work with a filter that (minimally) satisfies

$$\mathbf{u} = \overline{\mathbf{u}} + O(\delta^2),$$

for smooth $\mathbf{u}$.

Applying this spacial averaging operator to (6.1.1) gives the space filtered Navier-Stokes equations (imposition of zero boundary condition is explained in Section 6.2)

$$
\begin{aligned}
\overline{\mathbf{u}}_t + \overline{\nabla \cdot (\overline{\mathbf{u}}\,\overline{\mathbf{u}} + O(\delta^2))} - \nu \Delta \overline{\mathbf{u}} + \overline{\nabla p} &= \overline{\mathbf{f}} && \text{in } (0,T] \times \Omega, \\
\nabla \cdot \overline{\mathbf{u}} + O(\delta^2) &= 0 && \text{in } [0,T] \times \Omega, \\
\overline{\mathbf{u}} &= 0 && \text{on } [0,T] \times \partial\Omega, \\
\overline{\mathbf{u}}(0,\mathbf{x}) &= \overline{\mathbf{u}}_0(\mathbf{x}) && \text{in } \Omega.
\end{aligned}
\tag{6.1.2}
$$

Letting $\mathbf{w}$ denote the approximation to $\overline{\mathbf{u}}$ induced by this closure model, and dropping the $O(\delta^2)$ terms, system (6.1.2) gives that $(\mathbf{w}, p)$ satisfies

$$
\begin{aligned}
\mathbf{w}_t + \overline{\nabla \cdot (\mathbf{w}\mathbf{w})} - \nu \Delta \mathbf{w} + \overline{\nabla p} &= \overline{\mathbf{f}} && \text{in } (0,T] \times \Omega, \\
\nabla \cdot \mathbf{w} &= 0 && \text{in } [0,T] \times \Omega, \\
\mathbf{w} &= 0 && \text{on } [0,T] \times \partial\Omega, \\
\mathbf{w}(0,\mathbf{x}) &= \overline{\mathbf{u}}_0(\mathbf{x}) && \text{in } \Omega.
\end{aligned}
\tag{6.1.3}
$$

Once again, we remark that, for this model, we assume that the differentiation and averaging operators commute up to the modeling error of $O(\delta^2)$. We commute operators or not, according to which yields a stable model. For example, we can impose $\nabla \cdot \mathbf{w} = 0$ as in (6.1.3) (to preserve incompressibility), or use $\nabla \overline{p}$ instead of $\overline{\nabla p}$, (see Section 6.3 for details).

6.2   PROPERTIES OF DIFFERENTIAL FILTERS

We focus on the differential filter, introduced by Germano [29], since the differential equation can be supplemented with appropriate boundary conditions, which seems to be a natural extension of filtering on the whole space to a bounded domain.

We work with the following Poisson problem: given ϕ, its differential filter $\overline{\phi}$ is the solution of

$$-\delta^2 \Delta \overline{\phi} + \overline{\phi} = \phi$$

subject to zero boundary condition.

Remark 6.2.1. *From here on, as an alternative to the usual notation of overbar to indicate averaging, we introduce a new variable. For clarity, instead of denoting the differential filter of ϕ by $\overline{\phi}$, we will denote it by ψ.*

Given $\phi \in L^2(\Omega)$, $\psi \in \mathbf{X}$ satisfies

$$\delta^2(\nabla\psi, \nabla\mathbf{v}) + (\psi, \mathbf{v}) = (\phi, \mathbf{v}) \quad \forall\, \mathbf{v} \in \mathbf{X}, \tag{6.2.1}$$

with solution operator $T : L^2(\Omega) \to \mathbf{X}$ such that $T\phi = \psi$. It is well known that given $\phi \in L^2(\Omega)$, (6.2.1) has a unique solution and that if Ω is a convex polygon, then $\psi \in H^2(\Omega)$. In general, if $\phi \in H^k(\Omega)$, then $\psi \in H^{k+2}(\Omega)$ (see Grisvard [32]).

Similarly, the discrete filter $\psi^h \in \mathbf{X}^h$ is given by

$$\delta^2(\nabla\psi^h, \nabla\mathbf{v}) + (\psi^h, \mathbf{v}) = (\phi, \mathbf{v}) \quad \forall\, \mathbf{v} \in \mathbf{X}^h, \tag{6.2.2}$$

with solution operator $T^h : L^2(\Omega) \to \mathbf{X}^h$ satisfying $T^h\phi = \psi^h$.

Next we describe some of the properties of differential filters to be used in the error estimation in Section 6.3.1. Similar properties are given in Dunca and John [23] and are included here for completeness.

Lemma 6.2.1. *If $\phi \in L^2(\Omega)$, the following stability estimate for problem (6.2.1) holds:*

$$\delta^2 \|\nabla\psi\|^2 + \frac{1}{2}\|\psi\|^2 \leq \frac{1}{2}\|\phi\|^2.$$

Proof. In (6.2.1), choose $\mathbf{v} = \boldsymbol{\psi}$, then apply the Cauchy-Schwarz and Young's inequality on the right-hand side. □

Lemma 6.2.2. *The operator* $T : L^2(\Omega) \to \mathbf{X}$ *is self-adjoint on* $L^2(\Omega)$.

Proof. Let $\mathbf{v} \in L^2(\Omega)$. Then $T\mathbf{v} \in \mathbf{X}$ and from (6.2.1) and symmetry of inner products, we have

$$(\boldsymbol{\phi}, T\mathbf{v}) = \delta^2(\nabla(T\boldsymbol{\phi}), \nabla(T\mathbf{v})) + (T\boldsymbol{\phi}, T\mathbf{v}) = (T\boldsymbol{\phi}, \mathbf{v}).$$

□

Lemma 6.2.3. *If* $\nabla \boldsymbol{\phi} \in L^2(\Omega)$ *and* $\boldsymbol{\psi}$ *satisfies (6.2.1), then*

$$\frac{\delta^2}{2} \| \nabla(\boldsymbol{\phi} - \boldsymbol{\psi}) \|^2 + \| \boldsymbol{\phi} - \boldsymbol{\psi} \|^2 \leq \frac{\delta^2}{2} \| \nabla \boldsymbol{\phi} \|^2, \tag{6.2.3}$$

If, additionally, $\Delta \boldsymbol{\phi} \in L^2(\Omega)$, *then*

$$\delta^2 \| \nabla(\boldsymbol{\phi} - \boldsymbol{\psi}) \|^2 + \frac{1}{2} \| \boldsymbol{\phi} - \boldsymbol{\psi} \|^2 \leq \frac{\delta^4}{2} \| \Delta \boldsymbol{\phi} \|^2. \tag{6.2.4}$$

Proof. Add and subtract $\delta^2(\nabla\boldsymbol{\phi}, \nabla\mathbf{v})$ to (6.2.1), then choose $\mathbf{v} = \boldsymbol{\psi} - \boldsymbol{\phi}$. Applying the Cauchy-Schwarz and Young's inequalities proves the first assertion.

Note that for $\Delta\boldsymbol{\phi} \in L^2(\Omega)$, integration by parts implies that

$$\delta^2(\nabla\boldsymbol{\phi}, \nabla\mathbf{v}) + (\boldsymbol{\phi}, \mathbf{v}) = (-\delta^2\Delta\boldsymbol{\phi} + \boldsymbol{\phi}, \mathbf{v}) \quad \forall \mathbf{v} \in \mathbf{X}. \tag{6.2.5}$$

Subtracting (6.2.1) for $\mathbf{v} \in \mathbf{X}$ from (6.2.5),

$$\delta^2(\nabla(\boldsymbol{\phi} - \boldsymbol{\psi}), \nabla\mathbf{v}) + (\boldsymbol{\phi} - \boldsymbol{\psi}, \mathbf{v}) = -\delta^2(\Delta\boldsymbol{\phi}, \mathbf{v}). \tag{6.2.6}$$

Letting $\mathbf{v} = \boldsymbol{\phi} - \boldsymbol{\psi}$ and using Cauchy Schwarz, followed by Young's inequality, gives the second claim. □

Lemma 6.2.4. *The operator* $T^h : L^2(\Omega) \to \mathbf{X}^h$ *is self-adjoint and positive semi-definite on* $L^2(\Omega)$ *and positive definite on* $\mathbf{X}^h$.

Proof. Self-adjointness follows as in the continuous case. T^h is positive semi-definite on $L^2(\Omega)$, since

$$(\boldsymbol{\phi}, T^h \boldsymbol{\phi}) = \delta^2 ||\nabla(T^h \boldsymbol{\phi})||^2 + ||T^h \boldsymbol{\phi}||^2 \geq 0.$$

Now, for $\boldsymbol{\phi}^h \in \mathbf{X}^h$ with $T^h \boldsymbol{\phi}^h = 0$, using (6.2.2) we have

$$(\boldsymbol{\phi}^h, \boldsymbol{\phi}^h) = \delta^2(\nabla(T^h \boldsymbol{\phi}^h), \nabla \boldsymbol{\phi}^h) + (T^h \boldsymbol{\phi}^h, \boldsymbol{\phi}^h) = 0,$$

which proves the last claim. □

This guarantees that $T^h : L^2(\Omega) \to \mathbf{X}^h$ is invertible on $\mathbf{X}^h$. Let $A^h : \mathbf{X}^h \to \mathbf{X}^h$ be the inverse of T^h on $\mathbf{X}^h$. Then, it is easy to show that $A^h := -\delta^2 \Delta^h + I$ (recall Definition 2.2.1).

Next, we prove an error estimate for problems (6.2.1) and (6.2.2).

Theorem 6.2.1. *Let $\boldsymbol{\psi}$ and $\boldsymbol{\psi}^h$ be solutions of problems (6.2.1) and (6.2.2), respectively and assume that approximation property (2.2.2) holds. Then,*

$$\delta ||\nabla(\boldsymbol{\psi} - \boldsymbol{\psi}^h)|| + ||\boldsymbol{\psi} - \boldsymbol{\psi}^h|| \leq Ch^k(\delta + h)||\boldsymbol{\psi}||_{k+1}. \tag{6.2.7}$$

Proof. From the usual finite element analysis, we get

$$\delta ||\nabla(\boldsymbol{\psi} - \boldsymbol{\psi}^h)|| + ||\boldsymbol{\psi} - \boldsymbol{\psi}^h|| \leq C \inf_{\tilde{\boldsymbol{\psi}} \in \mathbf{X}^h} \left(\delta ||\nabla(\boldsymbol{\psi} - \tilde{\boldsymbol{\psi}})|| + ||\boldsymbol{\psi} - \tilde{\boldsymbol{\psi}}|| \right),$$

where $\tilde{\boldsymbol{\psi}}$ is an approximation to $\boldsymbol{\psi} \in \mathbf{X}^h$. □

Examining the right hand side, the optimal parameter selection is $\delta = O(h)$. In this case, we have the following.

Corollary 6.2.1. *If, in addition to the assumptions of Theorem 6.2.1, we choose $\delta = O(h)$, the following is true:*

$$\delta ||\nabla(\boldsymbol{\psi} - \boldsymbol{\psi}^h)|| + ||\boldsymbol{\psi} - \boldsymbol{\psi}^h|| \leq Ch^{k+1}||\boldsymbol{\psi}||_{k+1}. \tag{6.2.8}$$

Before going on to the numerical analysis, let us first say a few words on how we define averaging.

Remark 6.2.2. *Recall formulations (6.2.1) and (6.2.2). These may seem like odd choices for many terms in the filtered equations of Section 6.3. For example, even if $\boldsymbol{\phi} \neq 0$ on $\partial\Omega$, we would still have $T^h\boldsymbol{\phi} = 0$ and $T\boldsymbol{\phi} = 0$ on $\partial\Omega$. The reasons are that in a weak formulation, these terms occur as $(T\boldsymbol{\phi}, \mathbf{v})$, $\mathbf{v} \in \mathbf{X}$ and $(T^h\boldsymbol{\phi}, \mathbf{v}^h)$, $\mathbf{v}^h \in \mathbf{X}^h$. Thus, the component of $\boldsymbol{\phi}$ (for example) outside of $\mathbf{X}$ or $\mathbf{X}^h$, respectively, will not influence the weak formulation. In other words, if $-\Delta^h : \mathbf{X}^h \to \mathbf{X}^h$ denotes the discrete Laplacian and Π^h, the L^2 projection into $\mathbf{X}^h$, (6.2.2), for example, implies that $T^h\boldsymbol{\phi} = T^h(\Pi^h\boldsymbol{\phi})$. Moreover, for stability, it is important that all averaging operators have common domains, and then the same boundary conditions.*

Remark 6.2.3. *Another important possibility is filtering as the solution of a Stokes problem, rather than a Poisson problem. The motivation for that is to preserve incompressibility exactly (not simply up to $O(\delta^2)$). This type of averaging deserves to be further investigated.*

6.3   STABILITY AND ERROR ANALYSIS OF THE MODEL

In this section, we propose two semi discretizations of (6.1.3) and discuss their stability and convergence properties. The basic difference between the two formulations is the manner in which the filtering operation is performed.

Consider the problem: Find $(\mathbf{w}, p) \in (\mathbf{X}, Q)$ such that $\mathbf{w}(0, \mathbf{x})$ is an approximation of $\overline{\mathbf{u}}_0(\mathbf{x})$ and

$$(\mathbf{w}_t, \mathbf{v}) + (\overline{\nabla \cdot (\mathbf{ww})}, \mathbf{v}) + \nu(\nabla\mathbf{w}, \nabla\mathbf{v}) + (\overline{\nabla p}, \mathbf{v}) = (\overline{\mathbf{f}}, \mathbf{v}), \qquad \forall \mathbf{v} \in \mathbf{X}$$

$$(\nabla \cdot \mathbf{w}, q) = 0, \quad \forall q \in Q \tag{6.3.1}$$

Ultimately, since we are performing a numerical analysis, all filters must be discrete. The discretization of (6.3.1) calls for a decision on whether the computation of $\overline{\nabla \cdot (\mathbf{w}\,\mathbf{w})}$, for example, should be performed in the same mesh used to calculate $\mathbf{w}$. In other words, should the filtering operation be carried out in the same mesh used to approximate the solution of the problem, or in a finer mesh? We investigate the two possibilities.

We regard the case in which filtering and computation of $\mathbf{w}$ are performed in the same mesh as "discrete filter". When filtering/averaging is performed by solving the filtering problem on a finer mesh, we call it "exact filter". In order to keep the notation clear, we use the operators T and T^h (as defined in Section 6.2) instead of *overbar*. If $\boldsymbol{\zeta}$ is the quantity to be filtered, then $T(\boldsymbol{\zeta})$ means that $\overline{\boldsymbol{\zeta}}$ is computed in a finer mesh and $T^h(\boldsymbol{\zeta})$ means that $\overline{\boldsymbol{\zeta}}$ is computed on the same mesh. Based on Remark 6.2.2, we will omit the use of projections into $\mathbf{X}$ and $\mathbf{X}^h$ from now on. For instance, we will write $T^h(\boldsymbol{\zeta})$ instead of $T^h(\Pi^h\boldsymbol{\zeta})$, since these are equivalent.

Different filters will lead to different schemes. Note that Cases I and II (discrete and exact filter, respectively, discussed below) require (for stability) a different formulation of the pressure term in the momentum equation, $(\overline{\nabla p^h}, \mathbf{v}^h)$ versus $(\lambda^h, \nabla \cdot \mathbf{v}^h)$. In the two formulations, p^h is an approximation to p (Navier-Stokes pressure), while λ^h is an approximation to $\overline{p}$. This means that, in Case II, we are introducing a commutation error (within $O(\delta^2)$ of the modeling error, due to the non commutativity of filtering and differentiation in bounded domains).

We need to introduce two new skew symmetric forms on $\mathbf{X} \times \mathbf{X} \times \mathbf{X}$. For $\mathbf{u} \cdot \nabla \mathbf{v} \in L^2(\Omega)$ and $(\nabla \cdot \mathbf{u})\mathbf{v} \in L^2(\Omega)$, the bilinear forms are:

$$B(\mathbf{u}, \mathbf{v}, \mathbf{w}) = (T(\mathbf{u} \cdot \nabla \mathbf{v}), \mathbf{w}) + \frac{1}{2}(T((\nabla \cdot \mathbf{u})\mathbf{v}), \mathbf{w}) \qquad (6.3.2)$$

and

$$B^h(\mathbf{u}, \mathbf{v}, \mathbf{w}) = (T^h(\mathbf{u} \cdot \nabla \mathbf{v}), \mathbf{w}) + \frac{1}{2}(T^h((\nabla \cdot \mathbf{u})\mathbf{v}), \mathbf{w}). \qquad (6.3.3)$$

These bilinear forms have some important properties.[1]

Lemma 6.3.1. *For all* $\mathbf{u}, \mathbf{v}, \mathbf{w} \in \mathbf{X}$,

$$B(\mathbf{u}, \mathbf{v}, \mathbf{w}) = b(\mathbf{u}, \mathbf{v}, T(\mathbf{w})).$$

---

[1]Recall from Remark 2.1.1 that $b(\cdot, \cdot, \cdot) = b^*(\cdot, \cdot, \cdot)$.

Proof. Let $\hat{\mathbf{w}} = T(\mathbf{w})$ and since $\mathbf{w} \in \mathbf{X}$, $\hat{\mathbf{w}} \in \mathbf{X}$. From (6.3.2) and the self-adjointness of the operator T, we can write

$$B(\mathbf{u}, \mathbf{v}, \mathbf{w}) = (\mathbf{u} \cdot \nabla \mathbf{v}, \hat{\mathbf{w}}) + \frac{1}{2}((\nabla \cdot \mathbf{u})\mathbf{v}, \hat{\mathbf{w}}),$$

and integration by parts gives that

$$((\nabla \cdot \mathbf{u})\mathbf{v}, \hat{\mathbf{w}}) = -(\mathbf{u} \cdot \nabla \mathbf{v}, \hat{\mathbf{w}}) - (\mathbf{u} \cdot \nabla \hat{\mathbf{w}}, \mathbf{v}).$$

$\square$

Lemma 6.3.2. *For all* $\mathbf{u}, \mathbf{v} \in \mathbf{X}$ *and* $\mathbf{w}^h \in \mathbf{X}^h$,

$$B^h(\mathbf{u}, \mathbf{v}, A^h \mathbf{w}^h) = b(\mathbf{u}, \mathbf{v}, \mathbf{w}^h).$$

Proof. From (6.3.3) and the self-adjointness of $T^h : L^2(\Omega) \to \mathbf{X}^h$, we have

$$B^h(\mathbf{u}, \mathbf{v}, A^h \mathbf{w}^h) = (\mathbf{u} \cdot \nabla \mathbf{v}, T^h A^h \mathbf{w}^h) + \frac{1}{2}((\nabla \cdot \mathbf{u})\mathbf{v}, T^h A^h \mathbf{w}^h).$$

Since $T^h A^h \mathbf{w}^h = \mathbf{w}^h$ on $\mathbf{X}^h$, integration by parts gives

$$(\mathbf{u} \cdot \nabla \mathbf{v}, T^h A^h \mathbf{w}^h) + \frac{1}{2}((\nabla \cdot \mathbf{u})\mathbf{v}, T^h A^h \mathbf{w}^h) = b(\mathbf{u}, \mathbf{v}, \mathbf{w}^h).$$

$\square$

Corollary 6.3.1. *For all* $\mathbf{u}^h, \mathbf{v}^h \in \mathbf{X}^h$,

$$B^h(\mathbf{u}^h, \mathbf{v}^h, A^h \mathbf{v}^h) = 0.$$

Proof. Follows directly from Lemma 6.3.2 and the property that $b(\mathbf{u}^h, \mathbf{v}^h, \mathbf{v}^h) = 0$. $\square$

Using (6.3.2), the Zeroth Order Model (6.1.3) can be rewritten as: Find $(\mathbf{w}, p) \in (\mathbf{X}, Q)$ such that $\mathbf{w}(0, \mathbf{x}) = \bar{\mathbf{u}}_0(\mathbf{x})$

$$(\mathbf{w}_t, \mathbf{v}) + B(\mathbf{w}, \mathbf{w}, \mathbf{v}) + \nu(\nabla \mathbf{w}, \nabla \mathbf{v}) + (T(\nabla p), \mathbf{v}) = (T(\mathbf{f}), \mathbf{v}), \qquad \forall \, \mathbf{v} \in \mathbf{X}$$

$$(\nabla \cdot \mathbf{w}, q) = 0, \quad \forall \, q \in Q \tag{6.3.4}$$

In the next pages, we show that the solution computed with the discrete filter is stable and convergent. However, in the exact filter case, it appears that the solution is stable only for a finite time, which raises some issues on how well the computed solution approximates the exact solution.

6.3.1 Case I: Discrete Differential Filter

Consider a semi-discretization of the Zeroth Order Model (6.3.1): Find $\mathbf{w}^h : [0, T] \to \mathbf{X}^h$, $p^h : (0, T] \to Q^h$ satisfying

$$
\begin{aligned}
(\mathbf{w}_t^h, \mathbf{v}^h) \;+\;& B^h(\mathbf{w}^h, \mathbf{w}^h, \mathbf{v}^h) \\
&+\; \nu(\nabla \mathbf{w}^h, \nabla \mathbf{v}^h) + (T^h(\nabla p^h), \mathbf{v}^h) = (T^h(\mathbf{f}), \mathbf{v}^h), \qquad \forall \, \mathbf{v}^h \in \mathbf{X}^h \\
&(\nabla \cdot \mathbf{w}^h, q^h) = 0, \quad \forall \, q^h \in Q^h
\end{aligned} \tag{6.3.5}
$$

where $\mathbf{w}^h(0, \mathbf{x})$ is an approximation of $\bar{\mathbf{u}}_0(\mathbf{x})$.

Lemma 6.3.3 (Stability of the semi-discrete solution). *Assume $\mathbf{w}^h$ satisfies (6.3.5) and $\mathbf{f} \in L^2(0, T, H^{-1}(\Omega))$. Then,*

$$
\begin{aligned}
\frac{1}{2} \| \mathbf{w}^h \|_{L^\infty(0,T,L^2(\Omega))}^2 \;+\;& \frac{\delta^2}{2} \| \nabla \mathbf{w}^h \|_{L^\infty(0,T,L^2(\Omega))}^2 \\
&+\; \frac{\nu}{2} \| \nabla \mathbf{w}^h \|_{L^2(0,T,L^2(\Omega))}^2 + \nu \delta^2 \| \Delta^h \mathbf{w}^h \|_{L^2(0,T,L^2(\Omega))}^2 \\
&\leq\; \frac{1}{2} (\| \mathbf{w}^h(0) \|^2 + \delta^2 \| \nabla \mathbf{w}^h(0) \|^2) + \frac{1}{2\nu} \| \mathbf{f} \|_{L^2(0,T;H^{-1}(\Omega))}^2.
\end{aligned}
$$

Proof. Consider the variational formulation (6.3.5) and take $\mathbf{v}^h = A^h \mathbf{w}^h$ and $q^h = p^h$. Adding the two equations, using the self-adjointness of T^h, the definitions of A^h and Π^h and Corollary 6.3.1, this is the same as

$$
\frac{1}{2} \frac{d}{dt} (\| \mathbf{w}^h \|^2 + \delta^2 \| \nabla \mathbf{w}^h \|^2) + \nu(\nabla \mathbf{w}^h, \nabla(A^h \mathbf{w}^h)) = (\mathbf{f}, \mathbf{w}^h).
$$

From this, the Cauchy-Schwarz and Young's inequalities give

$$
\frac{1}{2} \frac{d}{dt} (\| \mathbf{w}^h \|^2 + \delta^2 \| \nabla \mathbf{w}^h \|^2) + \frac{\nu}{2} \| \nabla \mathbf{w}^h \|^2 + \nu \delta^2 \| \Delta^h \mathbf{w}^h \|^2 \leq \frac{1}{2\nu} \| \mathbf{f} \|_{-1}^2.
$$

The result follows by integrating in time. □

In what follows we give an estimate for the difference between the exact solution, $\mathbf{w}$, and the semi-discrete, $\mathbf{w}^h$.

Theorem 6.3.1 (Accuracy of Discretization)**.** *Assume* $\mathbf{w}$ *satisfies (6.3.4) and* $\mathbf{w}^h$ *satisfies (6.3.5). Assume also that* $\mathbf{w}_t \in L^2(0,T; H^{-1}(\Omega))$, $p \in L^2(0,T; L^2_0(\Omega))$, $\mathbf{w} \cdot \nabla \mathbf{w}$ *and* $\nabla p \in L^2(\Omega)$ *for every* $t \in (0,T)$ *and that* $\nabla \mathbf{w} \in L^4(0,T,L^2(\Omega))$. *Then, the numerical error satisfies:*

$$
\begin{aligned}
||\,\mathbf{w} - \mathbf{w}^h\,||^2_{L^\infty(0,T,L^2(\Omega))} \quad + \quad & \delta^2 ||\,\nabla(\mathbf{w} - \mathbf{w}^h)\,||^2_{L^\infty(0,T,L^2(\Omega))} + \nu ||\,\nabla(\mathbf{w} - \mathbf{w}^h)\,||^2_{L^2(0,T,L^2(\Omega))} \\
\leq\ & C^* \inf_{\tilde{\mathbf{w}} \in \mathbf{X}^h} \left(||\,(\mathbf{w} - \tilde{\mathbf{w}})(0)\,||^2 + \delta^2 ||\,\nabla(\mathbf{w} - \tilde{\mathbf{w}})(0)\,||^2\right) \\
& + C^* \nu^{-1} \inf_{\tilde{\mathbf{w}} \in \mathbf{X}^h, p^h \in Q^h} \Big\{ (1 + \delta^2) \Big(||\,(\mathbf{w} - \tilde{\mathbf{w}})_t\,||^2_{L^2(0,T;L^2(\Omega))} \\
& + ||\,p - p^h\,||^2_{L^2(0,T;L^2(\Omega))} + ||(T - T^h)(\mathbf{w} \cdot \nabla \mathbf{w})\,||^2_{L^2(0,T;L^2(\Omega))} \\
& + ||(T - T^h)(\mathbf{f})\,||^2_{L^2(0,T;L^2(\Omega))} + ||(T - T^h)(\nabla p)\,||^2_{L^2(0,T;L^2(\Omega))} \Big) \\
& + (1 + \delta^2 h^{-2}) ||\nabla(\mathbf{w} - \tilde{\mathbf{w}})\,||^2_{L^4(0,T;L^2(\Omega))} \\
& + ||\,\nabla \mathbf{w}\,||^2_{L^4(0,T;L^2(\Omega))} ||\,\nabla(\mathbf{w} - \tilde{\mathbf{w}})\,||^2_{L^4(0,T;L^2(\Omega))} \\
& + ||\,\mathbf{w}^h\,||_{L^\infty(0,T;L^2(\Omega))} ||\,\nabla \mathbf{w}^h\,||_{L^2(0,T;L^2(\Omega))} ||\,\nabla(\mathbf{w} - \tilde{\mathbf{w}})\,||^2_{L^4(0,T;L^2(\Omega))} \Big\}
\end{aligned}
$$

where $C^* = e^{C\nu^{-3} ||\,\nabla \mathbf{w}\,||^4_{L^4(0,T;L^2(\Omega))}}$.

Proof. Subtracting (6.3.5) from (6.3.4), we have

$$
\begin{aligned}
((\mathbf{w} - \mathbf{w}^h)_t, \mathbf{v}^h) + \nu(\nabla(\mathbf{w} - \mathbf{w}^h), \nabla \mathbf{v}^h) + B(\mathbf{w}, \mathbf{w}, \mathbf{v}^h) \\
- B^h(\mathbf{w}^h, \mathbf{w}^h, \mathbf{v}^h) + (T(\nabla p) - T^h(\nabla p^h), \mathbf{v}^h) = (T(\mathbf{f}) - T^h(\mathbf{f}), \mathbf{v}^h), \qquad \forall\, \mathbf{v}^h \in \mathbf{X}^h.
\end{aligned}
$$

Adding and subtracting $(T^h(\mathbf{w} \cdot \nabla \mathbf{w}), \mathbf{v}^h)$ to the nonlinear terms, we get

$$
\begin{aligned}
B(\mathbf{w}, \mathbf{w}, \mathbf{v}^h) - B^h(\mathbf{w}^h, \mathbf{w}^h, \mathbf{v}^h) \ = \ & ((T - T^h)(\mathbf{w} \cdot \nabla \mathbf{w}), \mathbf{v}^h) \\
& + B^h(\mathbf{w}, \mathbf{w}, \mathbf{v}^h) - B^h(\mathbf{w}^h, \mathbf{w}^h, \mathbf{v}^h),
\end{aligned}
$$

since $\nabla \cdot \mathbf{w} = 0$ weakly. Similarly, adding and subtracting $T^h(\nabla p)$ to the pressure term, we get

$$
(T(\nabla p) - T^h(\nabla p^h), \mathbf{v}^h) = ((T - T^h)(\nabla p), \mathbf{v}^h) + (T^h(\nabla p - \nabla p^h), \mathbf{v}^h)
$$

Then, the error equation becomes

$$((\mathbf{w} - \mathbf{w}^h)_t, \mathbf{v}^h) \ + \ \nu(\nabla(\mathbf{w} - \mathbf{w}^h), \nabla\mathbf{v}^h)$$

$$+ \ ((T - T^h)(\mathbf{w} \cdot \nabla\mathbf{w}), \mathbf{v}^h) + B^h(\mathbf{w}, \mathbf{w}, \mathbf{v}^h) - B^h(\mathbf{w}^h, \mathbf{w}^h, \mathbf{v}^h)$$

$$+ \ ((T - T^h)(\nabla p), \mathbf{v}^h) + (T^h(\nabla p - \nabla p^h), \mathbf{v}^h) = ((T - T^h)(\mathbf{f}), \mathbf{v}^h).$$

Choose an interpolant $\tilde{\mathbf{w}} \in \mathbf{V}^h$ and set $\mathbf{e} = \mathbf{w} - \mathbf{w}^h = (\mathbf{w} - \tilde{\mathbf{w}}) - (\mathbf{w}^h - \tilde{\mathbf{w}}) = \boldsymbol{\eta} - \boldsymbol{\chi}^h$. Then,

$$(\boldsymbol{\chi}_t^h, \mathbf{v}^h) \ + \ \nu(\nabla\boldsymbol{\chi}^h, \nabla\mathbf{v}^h) + ((T - T^h)(\mathbf{w} \cdot \nabla\mathbf{w}), \mathbf{v}^h)$$

$$+ \ B^h(\mathbf{w}, \mathbf{w}, \mathbf{v}^h) - B^h(\mathbf{w}^h, \mathbf{w}^h, \mathbf{v}^h) + ((T - T^h)(\nabla p), \mathbf{v}^h) + (T^h(\nabla p - \nabla p^h), \mathbf{v}^h)$$

$$= \ (\boldsymbol{\eta}_t, \mathbf{v}^h) + \nu(\nabla\boldsymbol{\eta}, \nabla\mathbf{v}^h) + ((T - T^h)(\mathbf{f}), \mathbf{v}^h). \tag{6.3.6}$$

Since $\tilde{\mathbf{w}} \in \mathbf{X}^h$, we can set $\mathbf{v}^h = A^h\boldsymbol{\chi}^h$. From Lemma 6.3.2, we write

$$B^h(\mathbf{w}, \mathbf{w}, A^h\boldsymbol{\chi}^h) - B^h(\mathbf{w}^h, \mathbf{w}^h, A^h\boldsymbol{\chi}^h) = b(\mathbf{w}, \mathbf{w}, \boldsymbol{\chi}^h) - b(\mathbf{w}^h, \mathbf{w}^h, \boldsymbol{\chi}^h),$$

and we also have

$$(T^h(\nabla p - \nabla p^h), A^h\boldsymbol{\chi}^h) = (\nabla p - \nabla p^h, T^h A^h\boldsymbol{\chi}^h) = -(p - p^h, \nabla \cdot \boldsymbol{\chi}^h).$$

For the other terms, we have to use the fact that $A^h = -\delta^2\Delta^h + I$.

Thus, equation (6.3.6) becomes

$$\frac{1}{2}\frac{d}{dt}\left(\|\boldsymbol{\chi}^h\|^2 \ + \ \delta^2\|\nabla\boldsymbol{\chi}^h\|^2\right) + \nu\|\nabla\boldsymbol{\chi}^h\|^2 + \nu\delta^2\|\Delta^h\boldsymbol{\chi}^h\|^2$$

$$= (\boldsymbol{\eta}_t, \boldsymbol{\chi}^h) - \delta^2(\boldsymbol{\eta}_t, \Delta^h\boldsymbol{\chi}^h)$$

$$+ \nu(\nabla\boldsymbol{\eta}, \nabla\boldsymbol{\chi}^h) - \nu\delta^2(\nabla\boldsymbol{\eta}, \nabla(\Delta^h\boldsymbol{\chi}^h))$$

$$+ (p - p^h, \nabla \cdot \boldsymbol{\chi}^h)$$

$$- b(\mathbf{w}, \mathbf{w}, \boldsymbol{\chi}^h) + b(\mathbf{w}^h, \mathbf{w}^h, \boldsymbol{\chi}^h)$$

$$- ((T - T^h)(\mathbf{w} \cdot \nabla\mathbf{w}), \boldsymbol{\chi}^h) + \delta^2((T - T^h)(\mathbf{w} \cdot \nabla\mathbf{w}), \Delta^h\boldsymbol{\chi}^h)$$

$$- ((T - T^h)(\nabla p), \boldsymbol{\chi}^h) + \delta^2((T - T^h)(\nabla p), \Delta^h\boldsymbol{\chi}^h)$$

$$+ ((T - T^h)(\mathbf{f}), \boldsymbol{\chi}^h) - \delta^2((T - T^h)(\mathbf{f}), \Delta^h\boldsymbol{\chi}^h). \tag{6.3.7}$$

65

Next, each of the terms in (6.3.7) is bounded. First, we examine the linear terms (we use an inverse inequality of the form $\|\nabla(\Delta^h \boldsymbol{\chi}^h)\| \le C\, h^{-1} \|\Delta^h \boldsymbol{\chi}^h\|$):

$$(\boldsymbol{\eta}_t, \boldsymbol{\chi}^h) \le \frac{\nu}{14}\|\nabla \boldsymbol{\chi}^h\|^2 + \frac{C}{\nu}\|\boldsymbol{\eta}_t\|^2$$

$$\delta^2(\boldsymbol{\eta}_t, \Delta^h \boldsymbol{\chi}^h) \le \frac{\nu\delta^2}{10}\|\Delta^h \boldsymbol{\chi}^h\|^2 + \frac{C\delta^2}{\nu}\|\boldsymbol{\eta}_t\|^2$$

$$\nu(\nabla \boldsymbol{\eta}, \nabla \boldsymbol{\chi}^h) \le \frac{\nu}{14}\|\nabla \boldsymbol{\chi}^h\|^2 + C\,\nu\,\|\nabla \boldsymbol{\eta}\|^2$$

$$\nu\delta^2(\nabla \boldsymbol{\eta}, \nabla(\Delta^h \boldsymbol{\chi}^h)) \le \frac{\nu\delta^2}{10}\|\Delta^h \boldsymbol{\chi}^h\|^2 + \frac{C\nu\delta^2}{h^2}\|\nabla \boldsymbol{\eta}\|^2$$

$$(p - p^h, \nabla \cdot \boldsymbol{\chi}^h) \le \frac{\nu}{14}\|\nabla \boldsymbol{\chi}^h\|^2 + \frac{C}{\nu}\|p - p^h\|^2$$

$$((T - T^h)(\nabla p), \boldsymbol{\chi}^h) \le \frac{\nu}{14}\|\nabla \boldsymbol{\chi}^h\|^2 + \frac{C}{\nu}\|(T - T^h)(\nabla p)\|^2$$

$$\delta^2((T - T^h)(\nabla p), \Delta^h \boldsymbol{\chi}^h) \le \frac{\nu\delta^2}{10}\|\Delta^h \boldsymbol{\chi}^h\|^2 + \frac{C\delta^2}{\nu}\|(T - T^h)(\nabla p)\|^2$$

$$((T - T^h)(\mathbf{f}), \boldsymbol{\chi}^h) \le \frac{\nu}{14}\|\nabla \boldsymbol{\chi}^h\|^2 + \frac{C}{\nu}\|(T - T^h)(\mathbf{f})\|^2$$

$$\delta^2((T - T^h)(\mathbf{f}), \Delta^h \boldsymbol{\chi}^h) \le \frac{\nu\delta^2}{10}\|\Delta^h \boldsymbol{\chi}^h\|^2 + \frac{C\delta^2}{\nu}\|(T - T^h)(\mathbf{f})\|^2$$

For the nonlinear terms, we have:

$$((T - T^h)(\mathbf{w} \cdot \nabla \mathbf{w}), \boldsymbol{\chi}^h) \le \frac{\nu}{14}\|\nabla \boldsymbol{\chi}^h\|^2 + \frac{C}{\nu}\|(T - T^h)(\mathbf{w} \cdot \nabla \mathbf{w})\|^2$$

$$\delta^2((T - T^h)(\mathbf{w} \cdot \nabla \mathbf{w}), \Delta^h \boldsymbol{\chi}^h) \le \frac{\nu\delta^2}{10}\|\Delta^h \boldsymbol{\chi}^h\|^2 + \frac{C\delta^2}{\nu}\|(T - T^h)(\mathbf{w} \cdot \nabla \mathbf{w})\|^2$$

Lastly, we look at the term $b(\mathbf{w}, \mathbf{w}, \boldsymbol{\chi}^h) - b(\mathbf{w}^h, \mathbf{w}^h, \boldsymbol{\chi}^h)$. Adding and subtracting $b(\mathbf{w}^h, \mathbf{w}, \boldsymbol{\chi}^h)$, it can be rewritten as

$$b(\mathbf{w}, \mathbf{w}, \boldsymbol{\chi}^h) - b(\mathbf{w}^h, \mathbf{w}^h, \boldsymbol{\chi}^h) = b(\boldsymbol{\eta}, \mathbf{w}, \boldsymbol{\chi}^h) - b(\boldsymbol{\chi}^h, \mathbf{w}, \boldsymbol{\chi}^h) + b(\mathbf{w}^h, \boldsymbol{\eta}, \boldsymbol{\chi}^h),$$

where each of the terms is bounded as follows:

$$
\begin{aligned}
b(\boldsymbol{\eta}, \mathbf{w}, \boldsymbol{\chi}^h) \quad &\leq M || \boldsymbol{\eta} ||^{1/2} || \nabla \boldsymbol{\eta} ||^{1/2} || \nabla \mathbf{w} || \, || \nabla \boldsymbol{\chi}^h || \\
&\leq \frac{\nu}{14} || \nabla \boldsymbol{\chi}^h ||^2 + \frac{C}{\nu} || \nabla \boldsymbol{\eta} ||^2 || \nabla \mathbf{w} ||^2
\end{aligned}
$$

$$
\begin{aligned}
b(\boldsymbol{\chi}^h, \mathbf{w}, \boldsymbol{\chi}^h) \quad &\leq M || \boldsymbol{\chi}^h ||^{1/2} || \nabla \boldsymbol{\chi}^h ||^{1/2} || \nabla \mathbf{w} || \, || \nabla \boldsymbol{\chi}^h || \\
&\leq \frac{\nu}{14} || \nabla \boldsymbol{\chi}^h ||^2 + \frac{C}{\nu^3} || \nabla \mathbf{w} ||^4 || \boldsymbol{\chi}^h ||^2
\end{aligned}
$$

$$
\begin{aligned}
b(\mathbf{w}^h, \boldsymbol{\eta}, \boldsymbol{\chi}^h) \quad &\leq M || \mathbf{w}^h ||^{1/2} || \nabla \mathbf{w}^h ||^{1/2} || \nabla \boldsymbol{\eta} || \, || \nabla \boldsymbol{\chi}^h || \\
&\leq \frac{\nu}{14} || \nabla \boldsymbol{\chi}^h ||^2 + \frac{C}{\nu} || \mathbf{w}^h || \, || \nabla \mathbf{w}^h || \, || \nabla \boldsymbol{\eta} ||^2
\end{aligned}
$$

Thus,

$$
\begin{aligned}
b(\mathbf{w}, \mathbf{w}, \boldsymbol{\chi}^h) - b(\mathbf{w}^h, \mathbf{w}^h, \boldsymbol{\chi}^h) \quad \leq \quad & \frac{3\nu}{14} || \nabla \boldsymbol{\chi}^h ||^2 + \frac{C}{\nu} || \nabla \boldsymbol{\eta} ||^2 || \nabla \mathbf{w} ||^2 \\
+ \quad & \frac{C}{\nu^3} || \nabla \mathbf{w} ||^4 || \boldsymbol{\chi}^h ||^2 + \frac{C}{\nu} || \mathbf{w}^h || \, || \nabla \mathbf{w}^h || \, || \nabla \boldsymbol{\eta} ||^2
\end{aligned}
$$

Putting all the estimates together, equation (6.3.7) gives

$$
\begin{aligned}
\frac{1}{2} \frac{d}{dt} \left(|| \boldsymbol{\chi}^h ||^2 \right. \quad + \quad & \left. \delta^2 || \nabla \boldsymbol{\chi}^h ||^2 \right) + \nu || \nabla \boldsymbol{\chi}^h ||^2 + \nu \delta^2 || \Delta^h \boldsymbol{\chi}^h ||^2 \\
&\leq C \nu^{-1} (1 + \delta^2) || \boldsymbol{\eta}_t ||^2 + C \nu^{-1} || p - p^h ||^2 \\
&+ C \nu^{-1} (\nu + \nu \delta^2 h^{-2} + || \nabla \mathbf{w} ||^2 + || \mathbf{w}^h || \, || \nabla \mathbf{w}^h ||) \, || \nabla \boldsymbol{\eta} ||^2 \\
&+ C \nu^{-1} (1 + \delta^2) || (T - T^h)(\mathbf{w} \cdot \nabla \mathbf{w}) ||^2 + C \nu^{-1} (1 + \delta^2) || (T - T^h)(\nabla p) ||^2 \\
&+ C \nu^{-1} (1 + \delta^2) || (T - T^h)(\mathbf{f}) ||^2 + C \nu^{-3} || \nabla \mathbf{w} ||^4 || \boldsymbol{\chi}^h ||^2
\end{aligned}
$$

Using Gronwall's inequality, this becomes

$$
\begin{aligned}
\frac{1}{2} || \boldsymbol{\chi}^h ||^2 + \frac{\delta^2}{2} || \nabla \boldsymbol{\chi}^h ||^2 \quad + \quad & \frac{\nu}{2} \int_0^T (|| \nabla \boldsymbol{\chi}^h ||^2 + \delta^2 || \Delta^h \boldsymbol{\chi}^h ||^2) \\
&\leq \frac{C^*}{2} (|| \boldsymbol{\chi}^h(0) ||^2 + \delta^2 || \nabla \boldsymbol{\chi}^h(0) ||^2) \\
&+ C^* \nu^{-1} \int_0^T \left\{ (1 + \delta^2) || \boldsymbol{\eta}_t ||^2 + || p - p^h ||^2 \right. \\
&+ (\nu + \nu \delta^2 h^{-2} + || \nabla \mathbf{w} ||^2 + || \mathbf{w}^h || \, || \nabla \mathbf{w}^h ||) \, || \nabla \boldsymbol{\eta} ||^2 \\
&+ (1 + \delta^2) || (T - T^h)(\mathbf{w} \cdot \nabla \mathbf{w}) ||^2 \\
&+ (1 + \delta^2) || (T - T^h)(\nabla p) ||^2 + (1 + \delta^2) || (T - T^h)(\mathbf{f}) ||^2 \left. \right\} \, dt,
\end{aligned}
$$

where $C^* = e^{C\nu^{-3}\int_0^T \|\nabla \mathbf{w}\|^4 dt}$. Drop the term that contains the operator Δ^h and the triangle inequality gives the result. $\qquad\square$

Corollary 6.3.2. *Let $\delta = O(h)$. If $\mathbf{w}$, $\mathbf{f}$ and p are regular enough and satisfy the assumptions of Theorem 6.3.1, then*

$$\|\mathbf{w} - \mathbf{w}^h\|^2_{L^\infty(0,T,L^2(\Omega))} + \delta^2 \|\nabla(\mathbf{w} - \mathbf{w}^h)\|^2_{L^\infty(0,T,L^2(\Omega))} + \nu\|\nabla(\mathbf{w} - \mathbf{w}^h)\|^2_{L^2(0,T,L^2(\Omega))}$$
$$\leq C(\mathbf{w}, \mathbf{f}, p, \nu)\, h^{2k}.$$

Proof. Follows from the estimate in Theorem 6.3.1, Corollary 6.2.1 (with $\boldsymbol{\psi} = T(\mathbf{w} \cdot \nabla \mathbf{w})$ and $\boldsymbol{\psi}^h = T^h(\mathbf{w} \cdot \nabla \mathbf{w})$, for instance) and the approximation properties (2.2.2) and (2.2.3). $\qquad\square$

6.3.2 Case II: Exact Differential Filter

In this case, we show that the semi-discrete scheme is stable only under some conditions. Due to the fact that the nonlinear term does not vanish, this extra term will impose restrictions on the stability of the scheme. Briefly, it is a cubic term, which can only be dominated by quadratic terms for a finite time interval; eventually the higher order term will dominate. This also means that the kinetic energy of the model is not likely to be monotonic decreasing. In this context, it is natural to raise questions on the convergence properties of the approximating scheme. According to the subsequent analysis, the scheme does converge over small time intervals at least, provided some regularity properties are considered.

The semi-discrete formulation of (6.3.1) now reads as follows: Find $\mathbf{w}^h : [0,T] \to \mathbf{X}^h$, $\lambda^h : (0,T] \to Q^h$ satisfying $\mathbf{w}^h(0,\mathbf{x}) \approx \overline{\mathbf{u}}_0(\mathbf{x})$ and [2]

$$
\begin{aligned}
(\mathbf{w}^h_t, \mathbf{v}^h) + B(\mathbf{w}^h, \mathbf{w}^h, \mathbf{v}^h) + \nu(\nabla\mathbf{w}^h, \nabla\mathbf{v}^h) - (\lambda^h, \nabla\cdot\mathbf{v}^h) &= (T(\mathbf{f}), \mathbf{v}^h), \quad \forall\, \mathbf{v}^h \in \mathbf{X}^h, \\
(\nabla\cdot\mathbf{w}^h, q^h) &= 0, \qquad\qquad \forall\, q^h \in Q^h.
\end{aligned}
$$
(6.3.8)

We now present a basic á priori estimate for the solution of (6.3.8). The following stability theorem is proven by using an idea similar to the one in Temam [84] (see Lemma 3.2, p. 21).

---

[2]Note that the pressure term is now cast as $(\lambda^h, \nabla \cdot \mathbf{v}^h)$, instead of $(T^h(\nabla p^h), \mathbf{v}^h)$, for stability reasons.

Lemma 6.3.4. *(Stability of $\mathbf{w}^h$) Let $\mathbf{w}^h$ satisfy (6.3.8). Then*

$$\|\mathbf{w}^h(t)\|^2 \leq 2(1 + \|\mathbf{w}^h(0)\|^2)$$

with

$$t \leq T^* = C(f, \nu, T)\frac{\delta^2 h^2}{(1 + \|\mathbf{w}^h(0)\|^2)}.$$

Proof. Restrict $\mathbf{v}^h \in \mathbf{V}^h$ in (6.3.8). Choose $\mathbf{v}^h = \mathbf{w}^h$ and use Cauchy-Schwarz and Young's inequalities

$$\frac{1}{2}\frac{d}{dt}\|\mathbf{w}^h\|^2 + \frac{\nu}{2}\|\nabla\mathbf{w}^h\|^2 \leq \frac{1}{2\nu}\|T(\mathbf{f})\|_{-1}^2 - B(\mathbf{w}^h, \mathbf{w}^h, \mathbf{w}^h). \tag{6.3.9}$$

We first consider the nonlinear term. The first step is to use Lemma 6.3.1, followed by equation (2.1.5) in Lemma 2.1.2. Then, use Lemma 6.2.1 and an inverse inequality of the form $\|\nabla\mathbf{w}^h\| \leq Ch^{-1}\|\mathbf{w}^h\|$. The last step is to apply Young's inequality with conjugate exponents 4 and 4/3.

$$
\begin{aligned}
B(\mathbf{w}^h, \mathbf{w}^h, \mathbf{w}^h) &= b(\mathbf{w}^h, \mathbf{w}^h, T(\mathbf{w}^h)) \\
&\leq M\|\nabla\mathbf{w}^h\|\,\|\nabla\mathbf{w}^h\|\,\|T(\mathbf{w}^h)\|^{1/2}\,\|\nabla(T\mathbf{w}^h)\|^{1/2} \\
&\leq C\delta^{-1/2}h^{-1/2}\|\nabla\mathbf{w}^h\|^{3/2}\|\mathbf{w}^h\|^{3/2} \\
&\leq \frac{\nu}{2}\|\nabla\mathbf{w}^h\|^2 + C\delta^{-2}h^{-2}\nu^{-3}\|\mathbf{w}^h\|^6.
\end{aligned}
$$

Using this last inequality, rewrite (8.1.14), multiply it by 2 and drop the term $\nu\|\nabla\mathbf{w}^h\|^2$. In the resulting differential inequality, set $z(t) = 1 + \|\mathbf{w}^h\|^2$ to get the following:

$$\frac{dz}{dt} \leq C^*\delta^{-2}h^{-2}z^3,$$

where

$$C^* = \max(\nu^{-1}\sup_{t\in[0,T]}\|T(\mathbf{f})\|_{-1}^2, C\nu^{-3}).$$

If we solve the differential inequality and integrate from 0 to t, we derive

$$z(t) \leq \frac{z(0)}{\sqrt{1 - 2C^*h^{-2}\delta^{-2}z^2(0)t}} \tag{6.3.10}$$

with $t < 1/(2C^* h^{-2}\delta^{-2}z^2(0))$. We can verify that $\frac{1}{\sqrt{1-2C^*h^{-2}\delta^{-2}z^2(0)t}} \le 2$ and then equation (6.3.10) becomes

$$1 + \|\mathbf{w}^h\|^2 \le 2(1 + \|\mathbf{w}^h(0)\|^2), \quad \text{with} \quad 0 \le t \le \frac{3}{8C^*}\frac{\delta^2 h^2}{(1 + \|\mathbf{w}^h(0)\|^2)^2}.$$

This concludes the proof of the lemma. □

Lemma 6.3.4 confirms what was expected, according to our discussion in the beginning of this section: the approximate solution $\mathbf{w}^h$ is bounded in terms of the problem data, $\mathbf{w}^h(0)$ and $T(\mathbf{f})$, for a bounded time interval.

The next natural step is to analyze convergence properties of the scheme. The following theorem gives an estimate of the error between $\mathbf{w}$ and its finite element approximation, $\mathbf{w}^h$.

Theorem 6.3.2. *Let* $\mathbf{w}$ *and* $\mathbf{w}^h$ *solve (6.3.4) (with the appropriate modification in the pressure term) and (6.3.8), respectively and assume that* $\nabla\mathbf{w} \in L^\infty(0,T,L^2(\Omega))$, $\mathbf{w}_t \in L^\infty(0,T,H^{-1}(\Omega))$, *and* $\lambda \in L^\infty(0,T,L^2(\Omega))$. *Then the error satisfies*

$$\| \mathbf{w} - \mathbf{w}^h \|^2_{L^\infty(0,T;L^2)} \le C \inf_{\tilde{\mathbf{w}}\in\mathbf{V}^h, \lambda^h\in Q^h} \Big[\nu^{-1}\| \mathbf{w}_t - \tilde{\mathbf{w}}_t \|^2_{L^\infty(0,T;H^{-1})} + \nu\| \nabla(\mathbf{w} - \tilde{\mathbf{w}}) \|^2_{L^\infty(0,T;L^2)}$$
$$+ \nu^{-1}\| \lambda - \lambda^h \|^2_{L^\infty(0,T;L^2)} + \nu^{-1}(\delta+1)\| \nabla(\mathbf{w} - \tilde{\mathbf{w}}) \|^4_{L^\infty(0,T;L^2)}$$
$$+ \nu^{-1}\| \nabla\mathbf{w} \|^2_{L^\infty(0,T;L^2)}\| \nabla(\mathbf{w} - \tilde{\mathbf{w}}) \|^2_{L^\infty(0,T;L^2)} \Big].$$

Proof. In order to get an error equation, we subtract (6.3.8) from (6.3.4) for $\mathbf{v}^h \in \mathbf{V}^h$ and set $\mathbf{e} = \mathbf{w} - \mathbf{w}^h$. Then, the equation for $\mathbf{e}$ becomes

$$(\mathbf{e}_t, \mathbf{v}^h) + \nu(\nabla\mathbf{e}, \nabla\mathbf{v}^h) + B(\mathbf{w},\mathbf{w},\mathbf{v}^h) - B(\mathbf{w}^h,\mathbf{w}^h,\mathbf{v}^h) - (\lambda, \nabla\cdot\mathbf{v}^h) = 0 \quad \mathbf{v}^h \in \mathbf{V}^h.$$

By picking $\tilde{\mathbf{w}}$ to be the best approximation of $\mathbf{w}$ in $\mathbf{V}^h$, we can decompose the error in two parts as: $\mathbf{e} = \boldsymbol{\eta} - \boldsymbol{\chi}^h$ where $\boldsymbol{\eta} = \mathbf{w} - \tilde{\mathbf{w}}$ and $\boldsymbol{\chi}^h = \mathbf{w}^h - \tilde{\mathbf{w}}$. Thus, using the fact that $(\lambda^h, \nabla\cdot\mathbf{v}^h) = 0$ for all $q^h \in Q^h$ and the decomposition of $\mathbf{e}$, the error equation can be reformulated as

$$(\boldsymbol{\chi}^h_t, \mathbf{v}^h) + \nu(\nabla\boldsymbol{\chi}^h, \nabla\mathbf{v}^h) = (\boldsymbol{\eta}_t, \mathbf{v}^h) - \nu(\nabla\boldsymbol{\eta}, \nabla\mathbf{v}^h) + (\lambda - \lambda^h, \nabla\cdot\mathbf{v}^h)$$
$$-B(\mathbf{w},\mathbf{w},\mathbf{v}^h) + B(\mathbf{w}^h,\mathbf{w}^h,\mathbf{v}^h).$$

70

Setting $\mathbf{v}^h = \boldsymbol{\chi}^h$ gives

$$\frac{1}{2}\frac{d}{dt}\|\boldsymbol{\chi}^h\|^2 + \nu\|\nabla\boldsymbol{\chi}^h\|^2 = (\boldsymbol{\eta}_t, \boldsymbol{\chi}^h) - \nu(\nabla\boldsymbol{\eta}, \nabla\boldsymbol{\chi}^h) + (\lambda - \lambda^h, \nabla\cdot\boldsymbol{\chi}^h)$$
$$-B(\mathbf{w}, \mathbf{w}, \boldsymbol{\chi}^h) + B(\mathbf{w}^h, \mathbf{w}^h, \boldsymbol{\chi}^h). \qquad (6.3.11)$$

We now analyze the nonlinear terms on the right hand side of (6.3.11). Using the self adjointness property of differential filter, Lemma 6.3.1 and the skew-symmetry of the trilinear form yields

$$B(\mathbf{w}, \mathbf{w}, \boldsymbol{\chi}^h) - B(\mathbf{w}^h, \mathbf{w}^h, \boldsymbol{\chi}^h) = b(\mathbf{w}, \mathbf{w}, T(\boldsymbol{\chi}^h)) - b(\mathbf{w}^h, \mathbf{w}^h, T(\boldsymbol{\chi}^h))$$
$$= b(\mathbf{w}, \mathbf{e}, T(\boldsymbol{\chi}^h)) - b(\mathbf{e}, \mathbf{e}, T(\boldsymbol{\chi}^h)) + b(\mathbf{e}, \mathbf{w}, T(\boldsymbol{\chi}^h))$$
$$= b(\mathbf{w}, \boldsymbol{\eta}, T(\boldsymbol{\chi}^h)) - b(\mathbf{w}, \boldsymbol{\chi}^h, T(\boldsymbol{\chi}^h)) - b(\boldsymbol{\chi}^h, \boldsymbol{\chi}^h, T(\boldsymbol{\chi}^h))$$
$$-b(\boldsymbol{\eta}, \boldsymbol{\eta}, T(\boldsymbol{\chi}^h)) + b(\boldsymbol{\chi}^h, \boldsymbol{\eta}, T(\boldsymbol{\chi}^h)) + b(\boldsymbol{\eta}, \boldsymbol{\chi}^h, T(\boldsymbol{\chi}^h))$$
$$-b(\boldsymbol{\chi}^h, \mathbf{w}, T(\boldsymbol{\chi}^h)) + b(\boldsymbol{\eta}, \mathbf{w}, T(\boldsymbol{\chi}^h)).$$

With the aid of this result, equation (6.3.11) becomes

$$\frac{1}{2}\frac{d}{dt}\|\boldsymbol{\chi}^h\|^2 + \nu\|\nabla\boldsymbol{\chi}^h\|^2 = (\boldsymbol{\eta}_t, \boldsymbol{\chi}^h) - \nu(\nabla\boldsymbol{\eta}, \nabla\boldsymbol{\chi}^h) + (\lambda - \lambda^h, \nabla\cdot\boldsymbol{\chi}^h)$$
$$-b(\mathbf{w}, \boldsymbol{\eta}, T(\boldsymbol{\chi}^h)) + b(\mathbf{w}, \boldsymbol{\chi}^h, T(\boldsymbol{\chi}^h)) + b(\boldsymbol{\chi}^h, \boldsymbol{\chi}^h, T(\boldsymbol{\chi}^h))$$
$$+b(\boldsymbol{\eta}, \boldsymbol{\eta}, T(\boldsymbol{\chi}^h)) - b(\boldsymbol{\chi}^h, \boldsymbol{\eta}, T(\boldsymbol{\chi}^h)) - b(\boldsymbol{\eta}, \boldsymbol{\chi}^h, T(\boldsymbol{\chi}^h))$$
$$+b(\boldsymbol{\chi}^h, \mathbf{w}, T(\boldsymbol{\chi}^h)) - b(\boldsymbol{\eta}, \mathbf{w}, T(\boldsymbol{\chi}^h)). \qquad (6.3.12)$$

We wish to bound the terms on the right hand side of (6.3.12). Therefore, we use the Cauchy-Schwarz inequality followed by Young's inequality:

$$\frac{1}{2}\frac{d}{dt}\|\boldsymbol{\chi}^h\|^2 + \nu\|\nabla\boldsymbol{\chi}^h\|^2 \leq \frac{C}{\nu}\|\boldsymbol{\eta}_t\|_{-1}^2 + C\nu\|\nabla\boldsymbol{\eta}\|^2 + \frac{C}{\nu}\|\lambda - \lambda^h\|^2 + \frac{3\nu}{14}\|\nabla\boldsymbol{\chi}^h\|^2$$
$$+|b(\mathbf{w}, \boldsymbol{\eta}, T(\boldsymbol{\chi}^h)) + b(\mathbf{w}, \boldsymbol{\chi}^h, T(\boldsymbol{\chi}^h)) + b(\boldsymbol{\chi}^h, \boldsymbol{\chi}^h, T(\boldsymbol{\chi}^h))$$
$$+b(\boldsymbol{\eta}, \boldsymbol{\eta}, T(\boldsymbol{\chi}^h)) - b(\boldsymbol{\chi}^h, \boldsymbol{\eta}, T(\boldsymbol{\chi}^h)) - b(\boldsymbol{\eta}, \boldsymbol{\chi}^h, T(\boldsymbol{\chi}^h))$$
$$+b(\boldsymbol{\chi}^h, \mathbf{w}, T(\boldsymbol{\chi}^h)) - b(\boldsymbol{\eta}, \mathbf{w}, T(\boldsymbol{\chi}^h))|. \qquad (6.3.13)$$

Next, we use standard bounds on each of the trilinear forms (as per Lemma 2.1.2) on the right hand side of (6.3.13). We also make frequent use of Lemma 6.2.1, Lemma 6.2.3

and Young's inequality (with conjugate exponents 2 and 2, or 4/3 and 4); in some cases, we apply an inverse inequality.

$$
\begin{aligned}
b(\mathbf{w}, \boldsymbol{\eta}, T(\boldsymbol{\chi}^h)) &= b(\mathbf{w}, \boldsymbol{\eta}, T(\boldsymbol{\chi}^h) - \boldsymbol{\chi}^h) + b(\mathbf{w}, \boldsymbol{\eta}, \boldsymbol{\chi}^h) \\
&\leq M \|\nabla \mathbf{w}\| \|\nabla \boldsymbol{\eta}\| \|\nabla(T(\boldsymbol{\chi}^h) - \boldsymbol{\chi}^h)\| + M \|\nabla \mathbf{w}\| \|\nabla \boldsymbol{\eta}\| \|\nabla \boldsymbol{\chi}^h\| \\
&\leq C \|\nabla \mathbf{w}\| \|\nabla \boldsymbol{\eta}\| \|\nabla \boldsymbol{\chi}^h\| \\
&\leq \frac{\nu}{14} \|\nabla \boldsymbol{\chi}^h\|^2 + \frac{C}{\nu} \|\nabla \mathbf{w}\|^2 \|\nabla \boldsymbol{\eta}\|^2
\end{aligned}
$$

$$
b(\boldsymbol{\eta}, \mathbf{w}, T(\boldsymbol{\chi}^h)) \leq \frac{\nu}{14} \|\nabla \boldsymbol{\chi}^h\|^2 + \frac{C}{\nu} \|\nabla \mathbf{w}\|^2 \|\nabla \boldsymbol{\eta}\|^2
$$

$$
\begin{aligned}
b(\boldsymbol{\chi}^h, \boldsymbol{\chi}^h, T(\boldsymbol{\chi}^h)) &\leq M \|\boldsymbol{\chi}^h\|^{1/2} \|\nabla \boldsymbol{\chi}^h\|^{3/2} \|\nabla T(\boldsymbol{\chi}^h)\| \\
&\leq \frac{\nu}{14} \|\nabla \boldsymbol{\chi}^h\|^2 + \frac{C}{\nu^3} \|\boldsymbol{\chi}^h\|^2 \|\nabla T(\boldsymbol{\chi}^h)\|^4 \\
&\leq \frac{\nu}{14} \|\nabla \boldsymbol{\chi}^h\|^2 + \frac{C}{\nu^3 \delta^4} \|\boldsymbol{\chi}^h\|^6
\end{aligned}
$$

$$
\begin{aligned}
b(\boldsymbol{\eta}, \boldsymbol{\eta}, T(\boldsymbol{\chi}^h)) &= b(\boldsymbol{\eta}, \boldsymbol{\eta}, T(\boldsymbol{\chi}^h) - \boldsymbol{\chi}^h) + b(\boldsymbol{\eta}, \boldsymbol{\eta}, \boldsymbol{\chi}^h) \\
&\leq M \|\nabla \boldsymbol{\eta}\|^2 \|T(\boldsymbol{\chi}^h) - \boldsymbol{\chi}^h\|^{1/2} \|\nabla(T(\boldsymbol{\chi}^h) - \boldsymbol{\chi}^h)\|^{1/2} + M \|\nabla \boldsymbol{\eta}\|^2 \|\nabla \boldsymbol{\chi}^h\| \\
&\leq C \delta^{1/2} \|\nabla \boldsymbol{\eta}\|^2 \|\nabla \boldsymbol{\chi}^h\| + C \|\nabla \boldsymbol{\eta}\|^2 \|\nabla \boldsymbol{\chi}^h\|, \\
&\leq \frac{\nu}{14} \|\nabla \boldsymbol{\chi}^h\|^2 + \frac{C}{\nu} (\delta + 1) \|\nabla \boldsymbol{\eta}\|^4,
\end{aligned}
$$

$$
\begin{aligned}
b(\boldsymbol{\eta}, \boldsymbol{\chi}^h, T(\boldsymbol{\chi}^h)) &\leq M \|\nabla \boldsymbol{\eta}\| \|\nabla \boldsymbol{\chi}^h\| \|T(\boldsymbol{\chi}^h)\|^{1/2} \|\nabla T(\boldsymbol{\chi}^h)\|^{1/2} \\
&\leq C h^{-1} \delta^{-1/2} \|\nabla \boldsymbol{\eta}\| \|\boldsymbol{\chi}^h\|^2
\end{aligned}
$$

$$
b(\boldsymbol{\chi}^h, \boldsymbol{\eta}, T(\boldsymbol{\chi}^h)) \leq C h^{-1} \delta^{-1/2} \|\nabla \boldsymbol{\eta}\| \|\boldsymbol{\chi}^h\|^2
$$

$$
\begin{aligned}
b(\mathbf{w}, \boldsymbol{\chi}^h, T(\boldsymbol{\chi}^h)) &\leq M \|\nabla \mathbf{w}\| \|\nabla \boldsymbol{\chi}^h\| \|T(\boldsymbol{\chi}^h)\|^{1/2} \|\nabla T(\boldsymbol{\chi}^h)\|^{1/2} \\
&\leq C h^{-1} \delta^{-1/2} \|\nabla \mathbf{w}\| \|\boldsymbol{\chi}^h\|^2
\end{aligned}
$$

$$
\begin{aligned}
b(\boldsymbol{\chi}^h, \mathbf{w}, T(\boldsymbol{\chi}^h)) \;&\leq\; M \|\nabla \mathbf{w}\| \, \|\nabla \boldsymbol{\chi}^h\| \, \|T(\boldsymbol{\chi}^h)\|^{1/2} \, \|\nabla T(\boldsymbol{\chi}^h)\|^{1/2} \\
&\leq\; C h^{-1} \delta^{-1/2} \|\nabla \mathbf{w}\| \, \|\boldsymbol{\chi}^h\|^2
\end{aligned}
$$

Putting everything together and using Poincaré-Friedrich's inequality on the left hand side we get

$$
\begin{aligned}
\frac{1}{2}\frac{d}{dt}\|\boldsymbol{\chi}^h\|^2 \;+\;& C_{PF}^{-2}\frac{\nu}{2}\|\boldsymbol{\chi}^h\|^2 \leq \frac{C}{\nu}\|\boldsymbol{\eta}_t\|_{-1}^2 \\
+\;& C\nu\|\nabla\boldsymbol{\eta}\|^2 + \frac{C}{\nu}\|\lambda - \lambda^h\|^2 + \frac{C}{\nu}(\delta+1)\|\nabla\boldsymbol{\eta}\|^4 + \frac{C}{\nu}\|\nabla\mathbf{w}\|^2\|\nabla\boldsymbol{\eta}\|^2 \\
+\;& C\delta^{-1/2}h^{-1}(\|\nabla\boldsymbol{\eta}\| + \|\nabla\mathbf{w}\|)\|\boldsymbol{\chi}^h\|^2 + \frac{C}{\nu^3\,\delta^4}\|\boldsymbol{\chi}^h\|^6. \qquad (6.3.14)
\end{aligned}
$$

Setting $y(t) = \|\boldsymbol{\chi}^h\|^2$ and combining terms, this equation can be rewritten as

$$
\frac{d}{dt}y(t) + \alpha(t)\,y(t) \leq \beta\,y(t)^3 + \gamma,
$$

where $\alpha(t)$ is the coefficient of $\|\boldsymbol{\chi}^h\|^2$, β is the coefficient of $\|\boldsymbol{\chi}^h\|^6$ and γ is the maximum over $[0, T]$ of all the remaining terms on the right hand side of (6.3.14). With a suitable choice of $\tilde{\mathbf{w}}$, we also have $0 \leq \|\boldsymbol{\chi}^h(0)\| \leq \gamma$.

The Continuation Lemma (Lemma 2.4.1) implies that there exists a constant $M \geq 1$ and $\gamma_0 > 0$ such that for $\gamma \leq \gamma_0$,

$$
y(t) \leq M\gamma, \qquad (6.3.15)
$$

for $0 \leq t \leq T$. In other words,

$$
\begin{aligned}
\|\boldsymbol{\chi}^h\|^2 \leq C \max_{0 \leq t \leq T}\Big[\nu^{-1}\|\boldsymbol{\eta}_t\|_{-1}^2 + \nu\|\nabla\boldsymbol{\eta}\|^2 + \nu^{-1}\|\lambda - \lambda^h\|^2 + (\delta+1)\nu^{-1}\|\nabla\boldsymbol{\eta}\|^4 \\
+ \nu^{-1}\|\nabla\mathbf{w}\|^2\|\nabla\boldsymbol{\eta}\|^2 \Big].
\end{aligned}
$$

Applying the triangle inequality and taking the infimum over $\tilde{\mathbf{w}} \in \mathbf{V}^h$ and $\lambda^h \in Q^h$, gives the required result. $\qquad\square$

7.0   NUMERICAL EXPERIMENTS

The theory developed in the previous chapter deserves to be complemented with numerical validation. We chose a few examples to test mainly stability and physical fidelity of that discretization.

We use the software *FreeFem++* [35] to run the numerical tests. Systems (6.3.5) and (6.3.8) are discretized according to the following:

- time stepping scheme: Backward Euler (first order, implicit);
- linearization: fixed point iteration
- discretization in space: Taylor-Hood element (continuous piecewise quadratic polynomials for the velocity and linear for the pressure).

The first goal is to show in an example that the exact filter can actually develop instabilities that lead to blow up of the solution in finite time.

7.1   THE FAILURE OF THE EXACT FILTER

We investigate the kinetic energy of the exact filter versus discrete filter discretization, given respectively by:

$$E_E(\mathbf{w}^h) = \frac{1}{2}||\mathbf{w}^h||^2, \quad \text{for } t \in [0, T].$$

and

$$E_D(\mathbf{w}^h) = \frac{1}{2}||\mathbf{w}^h||^2 + \frac{\delta^2}{2}||\nabla\mathbf{w}^h||^2, \quad \text{for } t \in [0, T].$$

The kinetic energy is one of the indicators of whether a model is useful for turbulent flow computations, e.g. John [40]. Notice that E_D has an extra term, justified by the energy inequality in Lemma 6.3.3. In order to be able to compare these two cases, we normalize the results and present graphs of $E_E/E_E^{initial}$ and $E_D/E_D^{initial}$ in Figures 3 and 4.

Our test problem is determined by the following choices:

$$\Omega = (0,1) \times (0,1) \qquad \mathbf{w}^h|_{\partial \Omega} = 0 \qquad \bar{\mathbf{f}} = \mathbf{0}.$$

A nonzero divergence free initial condition is obtained by construction. Let

$$\psi(x,y) = 10 \sin(100xy^2)x^2(1-x)^2y^2(1-y)^2 \qquad (7.1.1)$$

and set

$$\mathbf{w}_0 = \begin{bmatrix} \psi_y \\ -\psi_x \end{bmatrix}.$$

Then, $\nabla \cdot \mathbf{w}_0 = 0$.

We have proven that the kinetic energy for the exact filter scheme is bounded for a finite time interval. Here, we show numerically that it actually blows up after a certain time by computing the total kinetic energy of the approximated velocity.

Let n_Z be the number of mesh points used in the discretization of the Zeroth Order Model equation and n_F, the corresponding number for the filtering problem. Considering that the boundary conditions and the forcing term, $\bar{\mathbf{f}}$, are zero, one would expect that after some transient time period, where the effects of the nonzero initial condition are still important, the solution would tend to zero.

Figure 3 shows that the kinetic energy computed with the exact filter does not correspond to the expected true kinetic energy. It not only does not go to zero, but blows up. This can be verified by dividing the time step by 2, which gives the same qualitative result. On the other hand, the kinetic energy of the discrete filter scheme is consistent with what we expect and tends to zero asymptotically and monotonically, as shown in Figure 4.
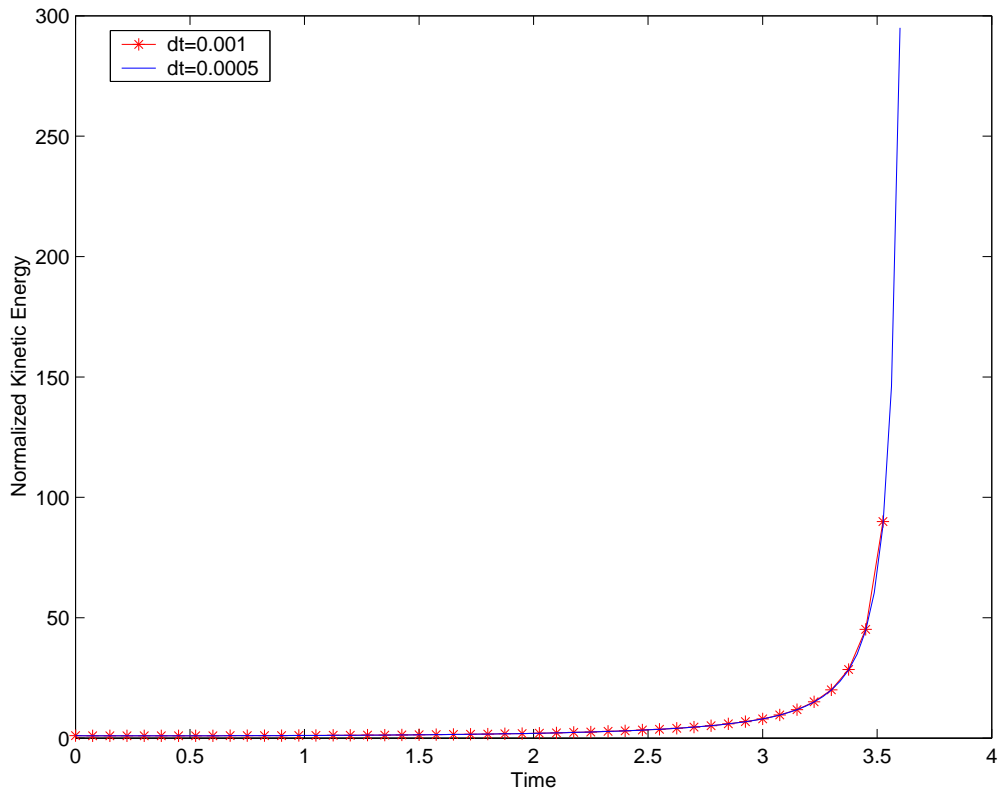
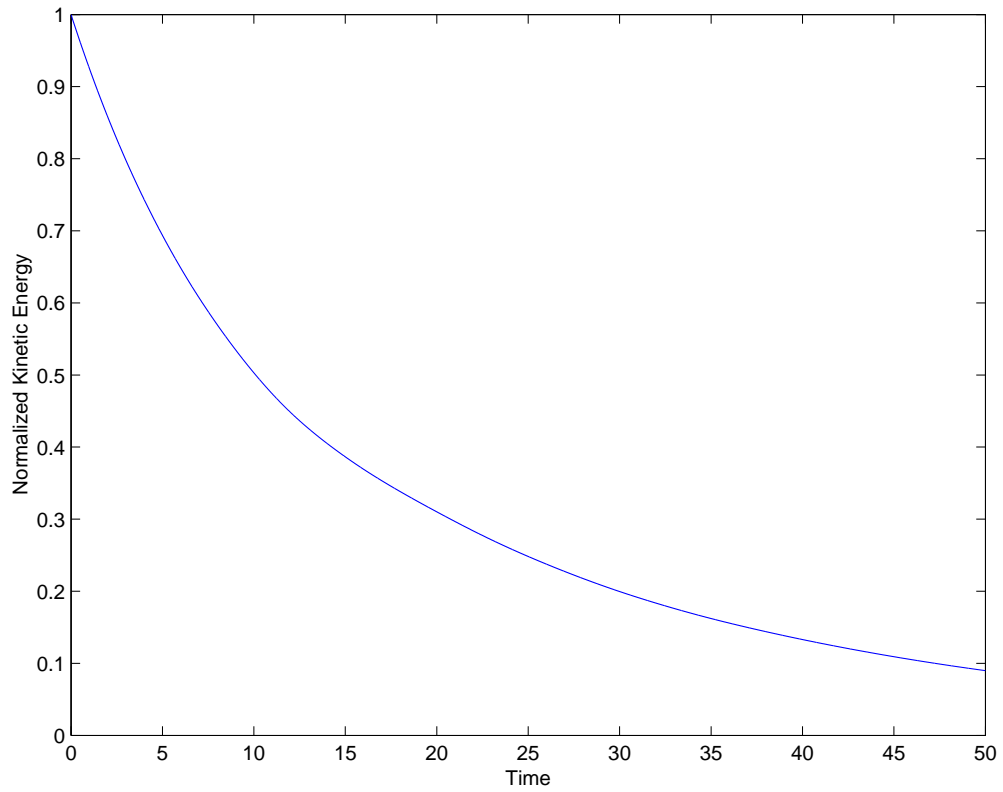Figure 3: Time vs. $E_E/E_E^{initial}$, $n_F = 16$, $n_Z = 8$, $Re = 100000$

Figure 4: Time vs. $E_D/E_D^{initial}$, $n_F = 8, n_Z = 8, Re = 100000, dt = 0.001$

7.1.1 Influence of the Nonlinear Term

It was very hard to find an example that shows that the solution with the exact filter can actually be unstable. For more insight into the problem, we analyzed the nonlinear term more closely, since this is the main source of the difference between the two filters in the analysis.

Let h denote the mesh size used to filter ($h = 1/n_F$) and let H denote the coarse mesh size ($h = 1/n_Z$), used to compute the solution itself. We wrote a small program to compute $E := B^h(\varsigma^H, \varsigma^H, A^H \varsigma^H)$ for a given quantity ς^H defined in the finite element space, according to the algorithm below.

Algorithm 7.1.1.

Construct ς^H.

Solve for $\boldsymbol{\Psi}^h := T^h(\varsigma^H \cdot \nabla \varsigma^H + \frac{1}{2}(\nabla \cdot \varsigma^H)\varsigma^H)$ in a mesh with $n_F \times n_F$ points in space.

Calculate

$$E := (\boldsymbol{\Psi}^h, \varsigma^H) + \delta^2(\nabla \boldsymbol{\Psi}^h, \nabla \varsigma^H),$$

which comes from

$$
\begin{aligned}
B^h(\varsigma^H, \varsigma^H, A^H \varsigma^H) &= (T^h(\varsigma^H \cdot \nabla \varsigma^H + (\nabla \cdot \varsigma^H)\varsigma^H), A^H \varsigma^H) \\
&= (\boldsymbol{\Psi}^h, -\delta^2 \Delta^H \varsigma^H + \varsigma^H) = (\delta^2 \nabla \boldsymbol{\Psi}^h, \nabla \varsigma^H) + (\boldsymbol{\Psi}^h, \varsigma^H).
\end{aligned}
$$

We have proven that if $H = h$ (discrete filter), $E = 0$. Otherwise (exact filter), this term could artificially input energy into the numerical scheme. This experiment was designed to give us an estimate on how big E can actually be when $H \neq h$. We choose two distinct ς^H and compute E for various combinations of H and h, according to the following.

We first take $\varsigma^h = \mathbf{w}_0$ (as constructed from (7.1.1)) and then take $\varsigma^h = \frac{1}{1000}\mathbf{w}_0$, both with $\delta = 2H$. The results are displayed in Tables 1 and 2, respectively.

78

H \ h	1/4	1/8	1/16	1/32	1/64	1/128
1/4	$2.2\,10^{-15}$	$1.00\,10^{-1}$	$1.39\,10^{-1}$	$3.14\,10^{-2}$	$6.28\,10^{-3}$	$1.19\,10^{-2}$
1/8	–	$8.31\,10^{-16}$	$1.60\,10^{-1}$	$2.13\,10^{-2}$	$1.14\,10^{-2}$	$2.42\,10^{-3}$
1/16	–	–	$2.46\,10^{-16}$	$2.82\,10^{-3}$	$5.76\,10^{-3}$	$3.58\,10^{-3}$
1/32	–	–	–	$1.32\,10^{-16}$	$5.60\,10^{-4}$	$9.86\,10^{-4}$
1/64	–	–	–	–	$3.33\,10^{-17}$	$7.46\,10^{-8}$
1/128	–	–	–	–	–	$3.13\,10^{-16}$

Table 1: Magnitude of the nonlinear term when $\boldsymbol{\varsigma}^h = \mathbf{w}_0$.

H \ h	1/4	1/8	1/16	1/32	1/64	1/128
1/4	$2.17\,10^{-24}$	$1.00\,10^{-10}$	$1.39\,10^{-10}$	$3.14\,10^{-11}$	$6.28\,10^{-12}$	$1.19\,10^{-11}$
1/8	–	$8.49\,10^{-25}$	$1.60\,10^{-10}$	$2.13\,10^{-11}$	$1.14\,10^{-11}$	$2.42\,10^{-12}$
1/16	–	–	$6.92\,10^{-27}$	$2.82\,10^{-12}$	$5.76\,10^{-12}$	$3.58\,10^{-12}$
1/32	–	–	–	$2.61\,10^{-26}$	$5.60\,10^{-13}$	$9.86\,10^{-13}$
1/64	–	–	–	–	$1.08\,10^{-25}$	$7.46\,10^{-17}$
1/128	–	–	–	–	–	$1.23\,10^{-25}$

Table 2: Magnitude of the nonlinear term when $\boldsymbol{\varsigma}^h = \frac{1}{1000}\mathbf{w}_0$.

Table 1 shows that when $\boldsymbol{\varsigma}^H$ is relatively large, E can be considerably big, while Table 2 shows that for a smaller $\boldsymbol{\varsigma}^H$, that is not the case. These computations show clearly that the choice of $\boldsymbol{\varsigma}^H$ does not affect the case $H = h$ (discrete filter), but they say a lot about the case $h \neq H$ (exact filter). Hence, the magnitude of ς^H plays a major role in the magnitude of E.

These results confirm instability of the exact filter. We believe that this discretization produces some initial noise that gets amplified as the time evolves and this seems to be due to a combination of factors. A large oscillatory initial condition on a coarse mesh and high Reynolds number play a major role. It appears that for fixed initial condition and Reynolds number, mesh refinement should eventually dissipate the initial noise.

We thus concentrate on the discrete filter (cheaper), since the exact filter proved to be unreliable (and more expensive).

7.2   TESTS WITH THE DISCRETE FILTER

The main idea of the examples in this section is to show how reliable the discrete filter is in tests that involve more than homogeneous boundary conditions and zero forcing term. In this section, since all filters are discrete, we denote filtering simply by *overbar*. We present three test problems. The first is one for which the true solution is known and the other two are conventional test problems.

Finding good test problems with known solutions for the model turns out to be nontrivial (a partial differential equation must be solved!). This is so because whenever $(\mathbf{w}, p)$ is prescribed, $\overline{\nabla \cdot (\mathbf{w}\,\mathbf{w})}$ and $\overline{\nabla p}$ must be computed in order to find $\overline{\mathbf{f}}$. Most of the cases where $\overline{\mathbf{f}}$ can be found exactly are when $\mathbf{w}$ is such that $\nabla \cdot (\mathbf{w}\,\mathbf{w})$ is linear or constant (in the space variable), because then $\overline{\nabla \cdot (\mathbf{w}\,\mathbf{w})} = \nabla \cdot (\mathbf{w}\,\mathbf{w})$. The same is true for $\overline{\nabla p}$. However, there is at least one interesting case where $\nabla \cdot (\mathbf{w}\,\mathbf{w})$ and ∇p can be computed exactly. It is known as the Chorin vortex decay problem, detailed below.

7.2.1 Chorin Vortex Decay Problem

This problem can be found in Chorin [14] and it was also used by Tafti [83] and John and Layton [45]. The prescribed solution in $\Omega = (0,1) \times (0,1)$ has the form

$$
\begin{aligned}
w_1(x,y,t) &= -\cos(n\pi x)\sin(n\pi y)e^{-2n^2\pi^2 t/\tau} \\
w_2(x,y,t) &= \sin(n\pi x)\cos(n\pi y)e^{-2n^2\pi^2 t/\tau} \\
p(x,y,t) &= -\frac{1}{4}(\cos(2n\pi x)+\cos(2n\pi x))e^{-2n^2\pi^2 t/\tau}
\end{aligned}
\tag{7.2.1}
$$

When the relaxation time $\tau = Re$, this is a solution of the model with $\bar{\mathbf{f}} = \mathbf{0}$, consisting of a $n \times n$ array of oppositely signed vortices that decay as $t \to \infty$, as shown in Figure 5.
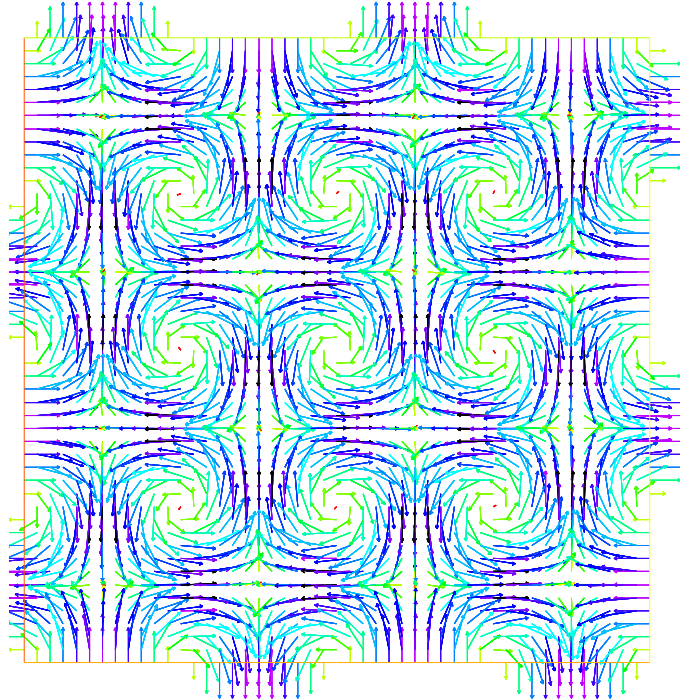

Figure 5: True solution of Chorin problem, $n = 4$, $Re = \tau$.

The right-hand side $\bar{\mathbf{f}}$ can be computed and the initial/boundary data can be chosen so that (w_1, w_2, p) is a closed solution of (6.1.3). It is possible to compute $\bar{\mathbf{f}}$ because $\nabla \cdot (\mathbf{w}\,\mathbf{w})$

and ∇p are of the form

$$\boldsymbol{\psi} = g(t) \begin{bmatrix} \sin(2n\pi x) \\ \sin(2n\pi y) \end{bmatrix}.$$

In that case, it is easy to check that the solution of

$$-\delta^2 \Delta \overline{\boldsymbol{\psi}} + \overline{\boldsymbol{\psi}} = \boldsymbol{\psi} \quad \text{in} \quad \Omega$$

$$\overline{\boldsymbol{\psi}} = \boldsymbol{\psi} \quad \text{on} \quad \partial\Omega.$$

is

$$\overline{\boldsymbol{\psi}} = \frac{f(t)}{4n^2\delta^2 + 1} \boldsymbol{\psi}.$$

This implies that

$$\overline{\nabla \cdot (\mathbf{w}\,\mathbf{w})} = \frac{-\frac{n\pi}{2} e^{-4n^2\pi^2 t/\tau}}{4n^2\delta^2 + 1} \begin{bmatrix} \sin(2n\pi x) \\ \sin(2n\pi y) \end{bmatrix}$$

and

$$\overline{\nabla p} = \frac{\frac{n\pi}{2} e^{-4n^2\pi^2 t/\tau}}{4n^2\delta^2 + 1} \begin{bmatrix} \sin(2n\pi x) \\ \sin(2n\pi y) \end{bmatrix}.$$

Therefore, when computing $\overline{\mathbf{f}}$, $\overline{\nabla \cdot (\mathbf{w}\,\mathbf{w})}$ and $\overline{\nabla p}$ cancel each other out and

$$\overline{\mathbf{f}} = \mathbf{w}_t - \nu \Delta \mathbf{w},$$

i. e.,

$$\overline{\mathbf{f}} = 2n^2\pi^2 (\frac{1}{\tau} - \nu) e^{-2n^2\pi^2 t/\tau} \begin{bmatrix} \cos(n\pi x)\sin(n\pi y) \\ -\sin(n\pi x)\cos(n\pi y) \end{bmatrix}.$$

From this expression, it is obvious that when $\tau = Re \ (\equiv 1/\nu)$, $\overline{\mathbf{f}} = \mathbf{0}$.

Figure 6 shows the model's true and computed kinetic energy, compared with the kinetic energy from the Navier-Stokes and Smagorinsky's equations. The parameters are $n = 4$, $Re = 10^4$ and $\tau = Re$. The mesh width is $h = 1/16$, the filter radius is $\delta = 2h$ and the time step, $dt = 0.01$.

Note that (7.2.1) is also a true solution of the Navier-Stokes equations. Figure 6 shows that (7.2.1) being a true solution to both the model and the Navier-Stokes equations, the model's computed kinetic energy is much closer to the true kinetic energy than the Navier-Stokes computed kinetic energy. Furthermore, the Smagorinsky model proves to be more dissipative, as expected.
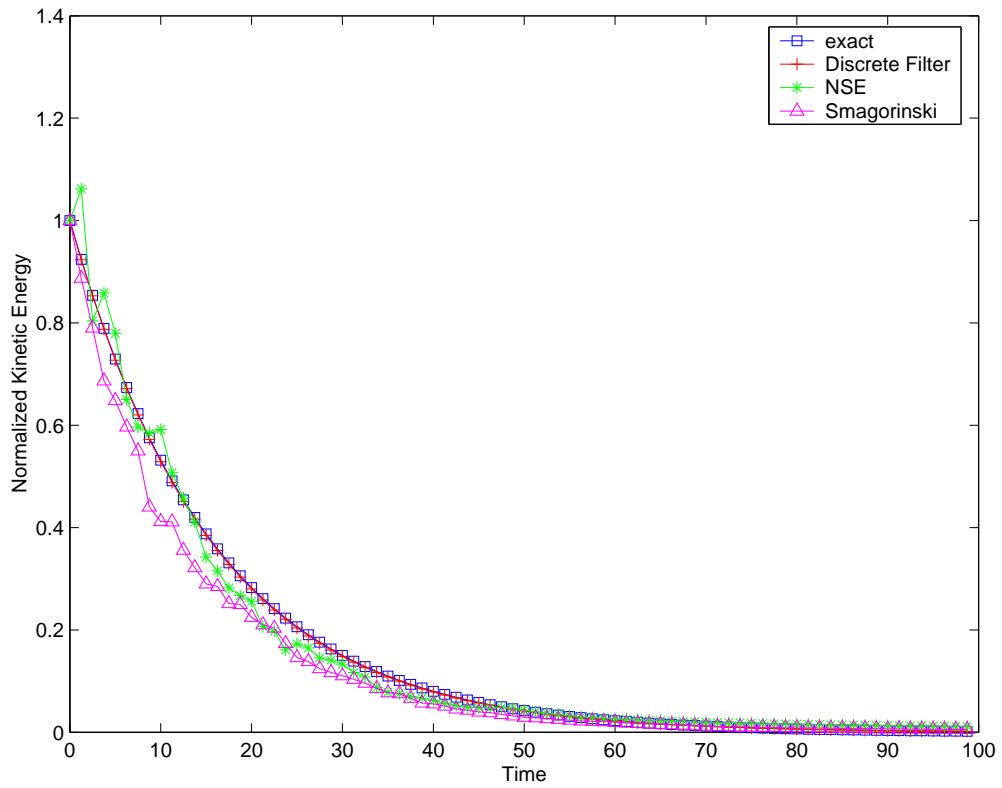
Figure 6: Comparison of kinetic energy for different models.

7.2.2 Flow around a Cylinder

The domain Ω for this problem is depicted in Figure 7. It is a well known benchmark problem, well explained in Schäfer and Turek [75]. The time dependent inflow and outflow profile are

$$w_1(0, y, t) = w_1(2.2, y, t) = \frac{6}{0.41^2} \sin(\pi\, t/8) y(0.41 - y)$$
$$w_2(0, y, t) = w_2(2.2, y, t) = 0$$

no slip boundary conditions are prescribed along the top and bottom walls and the initial condition is $\mathbf{w}(x, y, 0) = \mathbf{0}$. The viscosity is $\nu = 10^{-3}$ and the external force $\overline{\mathbf{f}} = \mathbf{0}$. The Reynolds number of the flow, based on the diameter of the cylinder and on the mean velocity inflow is $0 \le Re \le 100$. The filter radius is chosen as the length of the cylinder divided by n_C, the number of mesh points around the cylinder: $\delta = 2\pi(0.05)/n_C$ (here, $n_C = 40$).
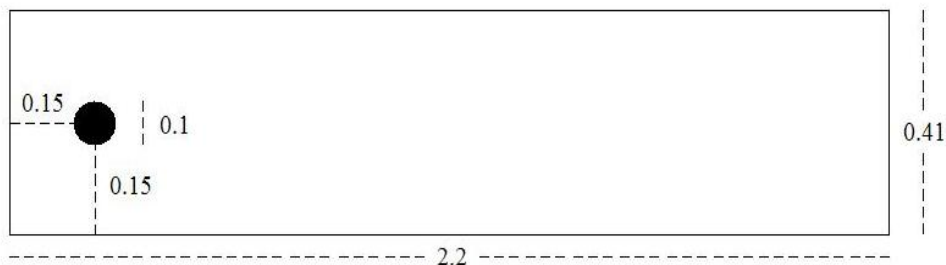
Figure 7: Cylinder Domain

For this setting, it is expected that, as the flow increases, from time $t = 2$ to $t = 4$, two vortices start to develop behind the cylinder. Between $t = 4$ and $t = 5$, the vortices should separate from the cylinder, so that a vortex street develops, and they continue to be visible until the final time $t = 8$. In general, turbulence models do not perform well for this value of Reynolds number, but the Zeroth Order Model surprisingly does.
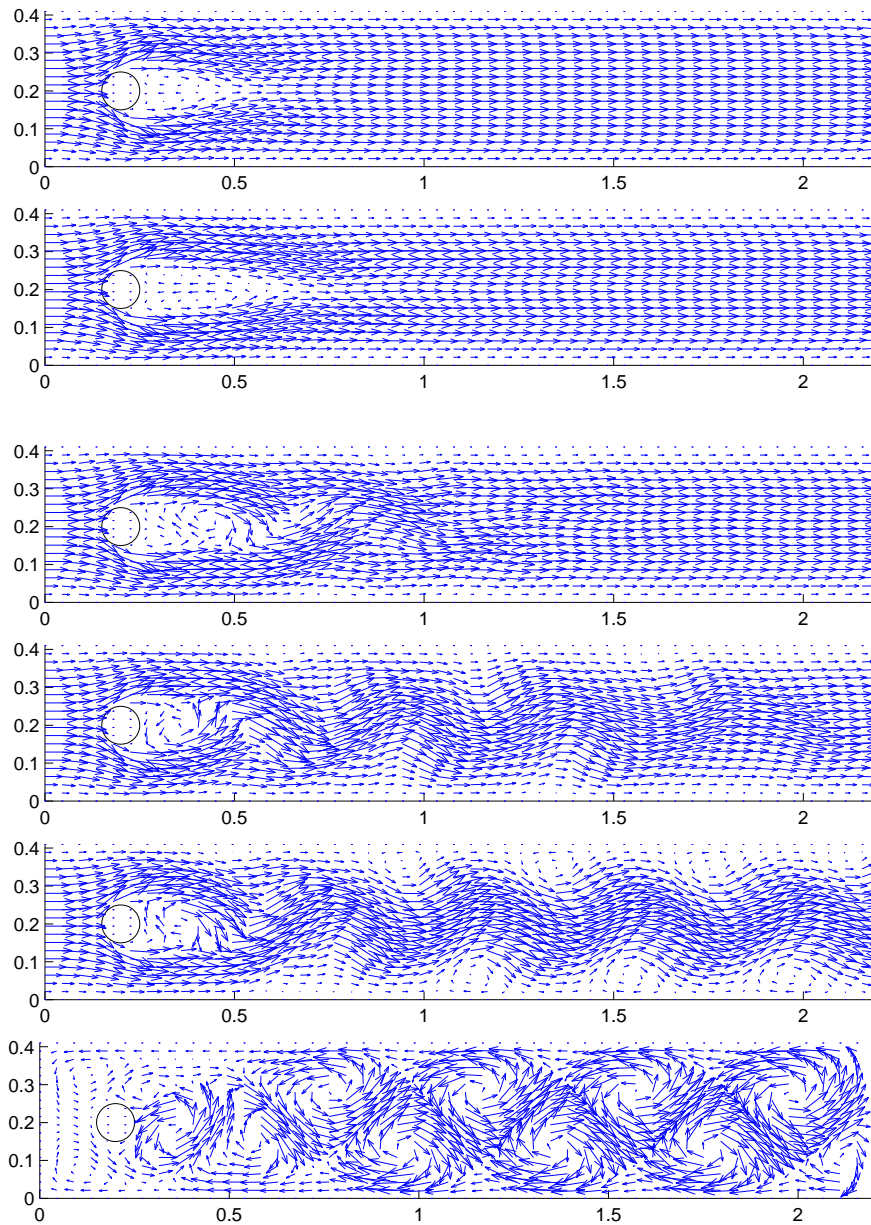
Figure 8: Formation of a vortex street, flow field at T = 2, 4, 5, 6, 7, 8.

7.2.3 Step Problem

The domain Ω is sketched in Figure 9. The inflow boundary conditions (and initial conditions) are

$$w_1(0, y, t) = y(1 - y)/25$$
$$w_2(0, y, t) = 0$$

and the fluid leaves the domain by outflow boundary conditions. At the top and bottom walls (including the step), homogeneous Dirichlet boundary conditions are imposed.
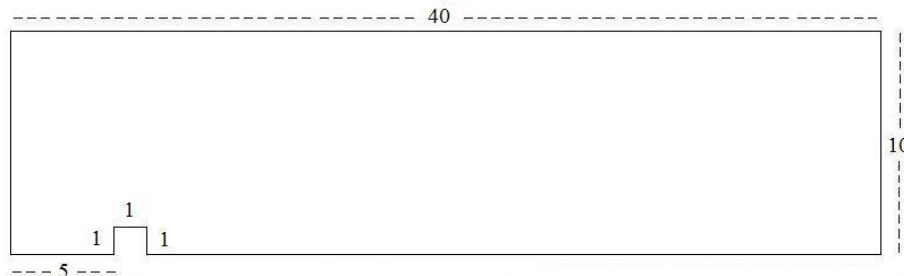
Figure 9: Step Domain

Perhaps the most commonly known form of this problem is the backward facing step, but the configuration we adopt here is more challenging, because the solution does not scale with the Reynolds number, see Gunzburger [33]. At a critical Reynolds number, for which the flow should be time dependent, some models are not able to capture the correct (non stationary) physical properties of the flow, e.g. John, Layton and Sahin [47].

The results shown here are for viscosity $\nu = 1/600$ and time step $dt = 0.005$. The filter width is chosen as $\delta = 2\frac{1}{n_S}$, where n_S is the number of mesh points on the back of the step (which has length 1).

We show the solution for two meshes at four instants of time, $T = 10, 20, 30, 40$. Figure 10 displays the streamlines for the solution computed in the coarser mesh, with 5827 total degrees of freedom and $\delta = 1/8$. It does not show vortex shedding behind the step after time T=40. On the other hand, refining the mesh (24562 total degrees of freedom and $\delta = 1/16$), we can see the expected behavior in Figure 11: vortices start shedding behind the step at around $T = 30$.
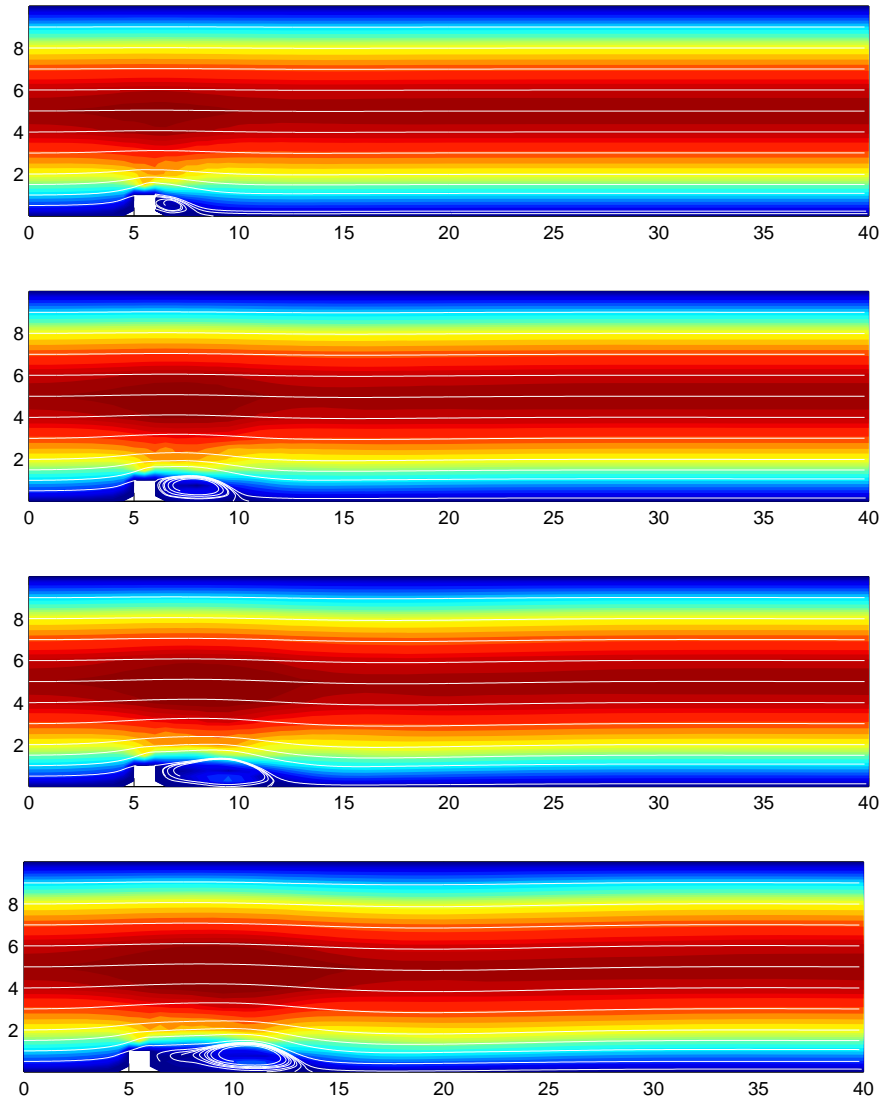
Figure 10: Coarse mesh: no vortices shed after T=40
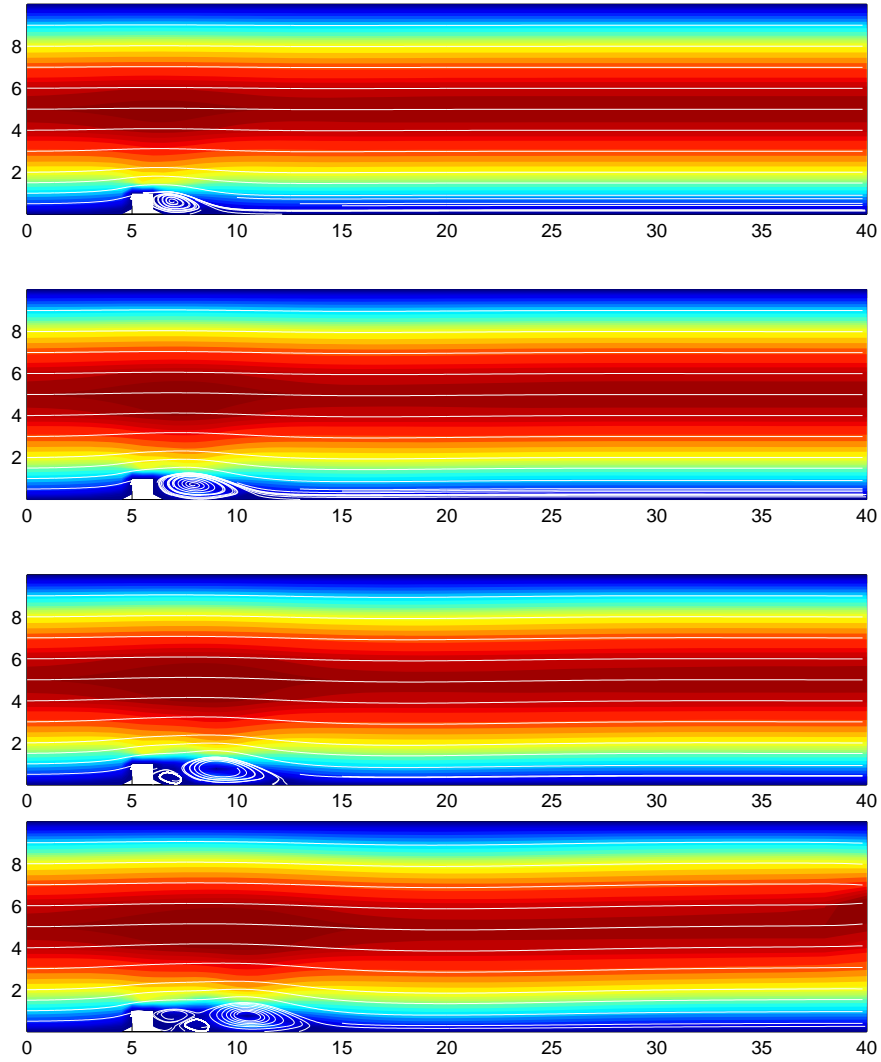
Figure 11: Fine mesh: correct, expected physical behavior.

7.3 NOTES ON IMPLEMENTATION

Let us now discuss briefly some implementation issues. It is not clear what is the best way of implementing these time-stepping schemes, since the filtered terms are a solution of a Poisson problem, which should ideally be computed at the same time as the velocity and pressure are computed.

The simplest idea, especially if one has a code for solving the time dependent Navier-Stokes equations, is to lag the filtered terms and add and subtract appropriate terms to make the discretization similar to the known Navier-Stokes discretization. This is the approach we adopted to compute the results in this chapter. We outline the algorithm we used below. Note that we drop the superscript h for convenience.

Algorithm 7.3.1 (Backward Euler).

> *For n=1 to number of time steps*
>
>> *For i=1 to number of fixed point iterations*
>>
>>> *Filter* $\nabla \cdot (\mathbf{w}\,\mathbf{w}) + \frac{1}{2}(\nabla \cdot \mathbf{w})\mathbf{w}$.
>>>
>>> *Filter* ∇p.
>>>
>>> *Solve*

$$\frac{1}{dt}(\mathbf{w}^{n+1}, \mathbf{v}) \quad + \quad \nu(\nabla \mathbf{w}^{n+1}, \nabla \mathbf{v}) + b(\mathbf{w}^i, \mathbf{w}^{n+1}, \mathbf{v}) - (p^{n+1}, \nabla \cdot \mathbf{v})$$
$$= (\overline{\mathbf{f}^{n+1}}, \mathbf{v}) + \frac{1}{dt}(\mathbf{w}^n, \mathbf{v}) - B^h(\mathbf{w}^i, \mathbf{w}^i, v) - (\overline{\nabla p^i}, \mathbf{v})$$
$$+ b(\mathbf{w}^i, \mathbf{w}^i, \mathbf{v}) - (p^i, \nabla \cdot \mathbf{v})$$

>>> *Stop if* $\max_{\mathbf{x} \in \Omega} |\mathbf{w}^{n+1} - \mathbf{w}^i| < TOL_{\mathbf{w}}$ *and* $\max_{\mathbf{x} \in \Omega} |p^{n+1} - p^i| < TOL_p$.
>>>
>>> $\mathbf{w}^i = \mathbf{w}^{n+1}$ *and* $p^i = p^{n+1}$.

In our opinion, the biggest issue seems to be related to the correct prescription of boundary conditions for the differential filters. We remarked earlier that if, given ϕ, one wants to compute $\overline{\phi}$, then it must be specified that $\overline{\phi} = \phi$ on $\partial\Omega$. The question is what to do when ϕ is not known on the boundary!

Filtering the nonlinear term does not seem to be so critical as filtering the pressure term. Boundary conditions for the Poisson problem related to the nonlinear term can be

prescribed, once the velocity is known on the boundary. However, p is not usually known on the boundary, much less ∇p. In the case of zero boundary conditions, we have shown in Chapter 6 that $\overline{\nabla p}$ must vanish on $\partial\Omega$. For the test problems with non homogeneous Dirichlet boundary conditions, we have found that the best results were obtained when we assign no boundary conditions to $\overline{\nabla p}$.

Another delicate issue is the stopping criteria for the nonlinear solver. We tried to set $TOL_p = TOL_{\mathbf{w}}$, but the computations are not practical at all, because the pressure converges extremely slowly. Thus, it could take hundreds or thousands of iterations per time step until the fixed point iteration converges. We found that what works better is not to set any conditions on the pressure, because whenever the velocity converges, the pressure converges too, eventually. In this case, even if, in the first time steps, the nonlinear solver needs a large number of iterations to converge, this number will decrease as time progresses.

We also tried to write the filter and model equations as a coupled system and solve for $\mathbf{w}, \overline{\nabla p}$ and $\overline{\mathbf{w} \cdot \nabla \mathbf{w} + \frac{1}{2}(\nabla \cdot \mathbf{w})\mathbf{w}}$, but this approach requires much larger matrices and therefore, computations take much longer.

8.0 ON AN ALTERNATIVE DISCRETIZATION OF THE ZEROTH ORDER MODEL

In this chapter, we consider a new discretization of the Approximate Deconvolution Models in Large Eddy Simulation (LES), focusing once more on the pivotal Zeroth Order Model. The usual finite element approach was already considered in the previous chapter and in [63] and its stability was proven to be dependent on the exact way the filtering operation is performed. The discretization we propose here grows out of the natural formulation for the continuous model, i.e. it comes directly from a formulation that gives the correct energy balance for the large scales. It is inspired by the technique used by Layton and Lewandowski [54] to prove existence and uniqueness of strong solutions in the continuous case. In contrast to the approach of Chapter 6, it is less sensitive to the details of the filter, but its implementation introduces more degrees of freedom. After all, Ferziger [26], "...there is a close connection between the numerical methods and the modeling approach used in simulation; this connection has not been sufficiently appreciated ...." We prove that the new discretization is stable and give optimal convergence rates, including an analysis of time averaged errors.

Recall the Zeroth Order Model, derived in Section 6.1,

$$
\begin{aligned}
\mathbf{w}_t - \nu \Delta \mathbf{w} + \overline{\nabla \cdot (\mathbf{w}\mathbf{w})} + \overline{\nabla p} &= \overline{\mathbf{f}} && \text{in } (0, T] \times \Omega, \\
\nabla \cdot \mathbf{w} &= 0 && \text{in } [0, T] \times \Omega, \\
\mathbf{w} &= \mathbf{0} && \text{in } [0, T] \times \partial\Omega. \\
\mathbf{w}(0, \mathbf{x}) &= \overline{\mathbf{u}}_0(\mathbf{x}) && \text{in } \Omega
\end{aligned}
\tag{8.0.1}
$$

Here, we were inspired by the idea in Layton and Lewandowski [54], in which the variational formulation is in $H^2(\Omega)$ (see Section 8.1). This would be computationally expensive,

requiring the use of C^1 elements. Instead, we study a mixed formulation that requires less regularity of the true solution $\mathbf{w}$. The error analysis is performed and optimal convergence rates are derived. We also include a section on time averaged errors, since this method is designed for simulation of turbulent flows. In such cases, the usual procedure is to compute time averages of the physical quantities of interest, e.g Moser, Kim and Mansour [68] and Berselli, Iliescu and Layton [6].

The derivation of the discretization and its stability properties are explained in Section 8.1. Optimal convergence rates are derived in Section 8.2, with the help of a modified Stokes projection. In Section 8.3, time averaged errors are analyzed.

8.1   DERIVATION OF THE NEW DISCRETIZATION

This section develops a mixed variational formulation for (8.0.1) and its finite element discretization. We recall that the operations of differentiation and filtering do not commute and use a strategy that gives the correct balance of energy for the model. The stability of the discrete solution is also investigated.

By choosing a differential filter as an averaging operator, following the discussion in Layton and Lewandowski [54], we define $A\mathbf{v} = -\delta^2 \Delta \mathbf{v} + \mathbf{v}$, for all $\mathbf{v} \in \mathbf{X} \cap (H^2(\Omega))^d$, so that $A\overline{\mathbf{v}} = \mathbf{v}$. Note that since the Laplace operator Δ is self-adjoint, so is A.

Let $\mathbf{w}$ be a smooth strong solution of (8.0.1). The development of the model starts with multiplying (8.0.1) by $A\mathbf{v}$ and integrating over the domain. One has

$$(\mathbf{w}_t, A\mathbf{v}) - \nu(\Delta \mathbf{w}, A\mathbf{v}) + (\overline{\nabla \cdot (\mathbf{w}\,\mathbf{w})}, A\mathbf{v}) + (\overline{\nabla p}, A\mathbf{v}) = (\overline{\mathbf{f}}, A\mathbf{v}), \quad \forall \mathbf{v} \in \mathbf{X} \cap (H^2(\Omega))^d.$$

By using the self-adjointness of the operator A, together with the property that $A\overline{\mathbf{v}} = \mathbf{v}$, followed by integration by parts, we derive the following variational formulation: Find $\mathbf{w}$: $[0, T] \to \mathbf{X} \cap (H^2(\Omega))^d$, $p : (0, T] \to Q$ satisfying $\mathbf{w}(0, \mathbf{x}) = \overline{\mathbf{u}}_0(\mathbf{x})$ and

$$
\begin{aligned}
(\mathbf{w}_t, \mathbf{v}) + \delta^2(\nabla \mathbf{w}_t, \nabla \mathbf{v}) \;\; + \;\; & \nu[(\nabla \mathbf{w}, \nabla \mathbf{v}) + \delta^2(\Delta \mathbf{w}, \Delta \mathbf{v})] \\
& + (\nabla \cdot (\mathbf{w}\,\mathbf{w}), \mathbf{v}) - (p, \nabla \cdot \mathbf{v}) = (\mathbf{f}, \mathbf{v}), \\
& (\nabla \cdot \mathbf{w}, q) = 0,
\end{aligned}
\tag{8.1.1}
$$

for all $(\mathbf{v}, q) \in (\mathbf{X} \cap (H^2(\Omega))^d, Q)$.

No similar formulation follows by the usual approach of multiplying by $\mathbf{v}$ and integrating by parts. The formulation (8.1.1) contains the term $(\Delta\mathbf{w}, \Delta\mathbf{v})$ which is a fourth order term. This suggests using C^1 elements. Instead, we consider a mixed formulation of (8.1.1): Find $\mathbf{w} : [0, T] \to \mathbf{X}, \boldsymbol{\phi} : [0, T] \to \mathbf{X}$ and $p : (0, T] \to Q$ satisfying $\mathbf{w}(0, \mathbf{x}) = \bar{\mathbf{u}}_0(\mathbf{x})$ and:

$$(\mathbf{w}_t, \mathbf{v}) + \delta^2(\nabla\mathbf{w}_t, \nabla\mathbf{v}) + b(\mathbf{w}, \mathbf{w}, \mathbf{v})$$

$$+\nu(\nabla\mathbf{w}, \nabla\mathbf{v}) + \nu\delta^2(\nabla\boldsymbol{\phi}, \nabla\mathbf{v}) - (p, \nabla \cdot \mathbf{v}) = (\mathbf{f}, \mathbf{v}), \tag{8.1.2}$$

$$(\nabla\mathbf{w}, \nabla\boldsymbol{\xi}) = (\boldsymbol{\phi}, \boldsymbol{\xi}), \tag{8.1.3}$$

$$(\nabla \cdot \mathbf{w}, q) = 0, \tag{8.1.4}$$

for all $(\mathbf{v}, \boldsymbol{\xi}, q) \in (\mathbf{X}, \mathbf{X}, Q)$.

In $\mathbf{V}$, this formulation becomes: Find $(\mathbf{w}, \boldsymbol{\phi}) : [0, T] \to (\mathbf{V}, \mathbf{X})$ such that

$$(\mathbf{w}_t, \mathbf{v}) + \delta^2(\nabla\mathbf{w}_t, \nabla\mathbf{v}) + b(\mathbf{w}, \mathbf{w}, \mathbf{v})$$

$$+\nu(\nabla\mathbf{w}, \nabla\mathbf{v}) + \nu\delta^2(\nabla\boldsymbol{\phi}, \nabla\mathbf{v}) = (\mathbf{f}, \mathbf{v}), \tag{8.1.5}$$

$$(\nabla\mathbf{w}, \nabla\boldsymbol{\xi}) = (\boldsymbol{\phi}, \boldsymbol{\xi}). \tag{8.1.6}$$

for all $(\mathbf{v}, \boldsymbol{\xi}) \in (\mathbf{V}, \mathbf{X})$.

The kinetic energy and the energy dissipation rate at time t associated with this model are defined as

$$\kappa(\mathbf{w}) = \frac{1}{2}\left(|| \mathbf{w}(t) ||^2 + \delta^2 || \nabla\mathbf{w}(t) ||^2\right) \quad \text{and} \quad \varepsilon(\mathbf{w}, \boldsymbol{\phi}) = \frac{\nu}{|\Omega|}\left(|| \nabla\mathbf{w}(t) ||^2 + \delta^2 || \boldsymbol{\phi}(t) ||^2\right),$$

where $|\Omega|$ is the measure of Ω.

We first establish uniformly boundness of the kinetic energy of $\mathbf{w}$ at time T.

Lemma 8.1.1. *Let* $\mathbf{f} \in L^\infty(0, \infty, H^{-1}(\Omega))$. *Then the kinetic energy* $\kappa(\mathbf{w})$ *at time* T *is uniformly bounded as*

$$\kappa(\mathbf{w}) \leq \left(|| \mathbf{w}(0) ||^2 + \delta^2 || \nabla\mathbf{w}(0) ||^2\right) e^{-\nu C_{PF}^{-2} T}$$

$$+\nu^{-2}C_{PF}^2 || \mathbf{f} ||^2_{L^\infty(0,\infty;H^{-1}(\Omega))}.$$

In particular,

$$\lim_{T\to\infty} \frac{1}{T}\kappa(\mathbf{w}) = 0.$$

93

Proof. Set $\mathbf{v} = \mathbf{w}$ in (8.1.5) and $\boldsymbol{\xi} = \boldsymbol{\phi}$ in (8.1.6). Then, since $b(\mathbf{w}, \mathbf{w}, \mathbf{w}) = 0$, we get

$$\frac{1}{2}\frac{d}{dt}\left(||\mathbf{w}||^2 + \delta^2||\nabla\mathbf{w}||^2\right) + \frac{\nu}{2}(||\nabla\mathbf{w}||^2 + 2\,\delta^2||\boldsymbol{\phi}||^2) \leq \frac{1}{2\,\nu}||\mathbf{f}||^2_{-1}. \tag{8.1.7}$$

Letting $\boldsymbol{\xi} = \mathbf{w}$ in equation (8.1.6) and using Poincaré-Friedrich's inequality, we have that $||\nabla\mathbf{w}|| \leq C_{PF}||\boldsymbol{\phi}||$. Then (8.1.7) becomes

$$\frac{d}{dt}\left(||\mathbf{w}||^2 + \delta^2||\nabla\mathbf{w}||^2\right) + \nu\,C_{PF}^{-2}(||\mathbf{w}||^2 + \delta^2||\nabla\mathbf{w}||^2) \leq \nu^{-1}||\mathbf{f}||^2_{-1}. \tag{8.1.8}$$

Setting $y = ||\mathbf{w}||^2 + \delta^2||\nabla\mathbf{w}||^2$ and using an integrating factor, equation (8.1.8) gives

$$y(T) \leq y(0)\,e^{-\nu\,C_{PF}^{-2}T} + \nu^{-2}C_{PF}^2\,||\mathbf{f}||^2_{L^\infty(0,T;H^{-1}(\Omega))}.$$

This proves the uniform boundedness. Now, dividing by T and taking the limit as $T \to \infty$ gives the second claim. $\qquad\square$

Remark 8.1.1. *One can also show that the total energy is bounded. We only present the proof for the discrete case (Lemma 8.1.3), since the idea is the same in both cases.*

Our goal is to understand the behavior of numerical methods based on (8.1.2)-(8.1.4). Therefore, we consider a continuous in time finite element discretization of the problem (8.1.2)-(8.1.4). Let $\mathbf{X}^h \subset \mathbf{X}$ and $Q^h \subset Q$ satisfy (2.2.1). The finite element approximation to $(\mathbf{w}, \boldsymbol{\phi}, p)$ are maps $\mathbf{w}^h : [0,T] \to \mathbf{X}^h$, $\boldsymbol{\phi}^h : [0,T] \to \mathbf{X}^h$ and $p^h : (0,T] \to Q^h$ such that

$$(\mathbf{w}_t^h, \mathbf{v}^h) + \delta^2(\nabla\mathbf{w}_t^h, \nabla\mathbf{v}^h) + b(\mathbf{w}^h, \mathbf{w}^h, \mathbf{v}^h)$$
$$+\nu(\nabla\mathbf{w}^h, \nabla\mathbf{v}^h) + \nu\delta^2(\nabla\boldsymbol{\phi}^h, \nabla\mathbf{v}^h) - (p^h, \nabla\cdot\mathbf{v}^h) = (\mathbf{f}, \mathbf{v}^h), \tag{8.1.9}$$
$$(\nabla\mathbf{w}^h, \nabla\boldsymbol{\xi}^h) = (\boldsymbol{\phi}^h, \boldsymbol{\xi}^h), \tag{8.1.10}$$
$$(q^h, \nabla\cdot\mathbf{w}^h) = 0, \tag{8.1.11}$$

for all $(\mathbf{v}^h, \boldsymbol{\xi}^h, q^h) \in (\mathbf{X}^h, \mathbf{X}^h, Q^h)$.

In $\mathbf{V}^h$, the semi-discrete approximation of (8.1.9)-(8.1.11) is: Find $(\mathbf{w}^h, \boldsymbol{\phi}^h) \in (\mathbf{V}^h, \mathbf{X}^h)$ such that

$$(\mathbf{w}_t^h, \mathbf{v}^h) + \delta^2(\nabla\mathbf{w}_t^h, \nabla\mathbf{v}^h) + b(\mathbf{w}^h, \mathbf{w}^h, \mathbf{v}^h)$$
$$+\nu(\nabla\mathbf{w}^h, \nabla\mathbf{v}^h) + \nu\delta^2(\nabla\boldsymbol{\phi}^h, \nabla\mathbf{v}^h) = (\mathbf{f}, \mathbf{v}^h), \tag{8.1.12}$$
$$(\nabla\mathbf{w}^h, \nabla\boldsymbol{\xi}^h) = (\boldsymbol{\phi}^h, \boldsymbol{\xi}^h), \tag{8.1.13}$$

for all $(\mathbf{v}^h, \boldsymbol{\xi}^h) \in (\mathbf{V}^h, \mathbf{X}^h)$.

A discrete version of Lemma 8.1.1 shows that the kinetic energy of the discrete solution is also uniformly bounded.

Lemma 8.1.2. *Let* $\mathbf{f} \in L^\infty(0, \infty, H^{-1}(\Omega))$. *Then the kinetic energy* $\kappa(\mathbf{w}^h)$ *is uniformly bounded as*

$$\kappa(\mathbf{w}^h) \leq (||\mathbf{w}^h(0)||^2 + \delta^2 ||\nabla \mathbf{w}^h(0)||^2) e^{-\nu C_{PF}^{-2} T}$$
$$+ \nu^{-2} C_{PF}^2 ||\mathbf{f}||^2_{L^\infty(0,\infty;H^{-1}(\Omega))}.$$

As a consequence,

$$\lim_{T \to \infty} \frac{1}{T} \kappa(\mathbf{w}^h) = 0.$$

Proof. The claim exactly follows as in the continuous case of Lemma 8.1.1. $\square$

In addition, the next result shows that the total energy of the approximate solution $\mathbf{w}^h$ is bounded.

Lemma 8.1.3. *(Stability of $\mathbf{w}^h$) Let* $\mathbf{f} \in L^2(0, T, H^{-1}(\Omega))$. *Then any solution* $(\mathbf{w}^h, \boldsymbol{\phi}^h)$ *of (8.1.12)-(8.1.13) satisfies the following stability bound:*

$$\frac{1}{2}\|\mathbf{w}^h(t)\|^2 + \frac{\delta^2}{2}\|\nabla \mathbf{w}^h(t)\|^2 + \int_0^t [\frac{\nu}{2}\|\nabla \mathbf{w}^h\|^2 + \nu\delta^2\|\boldsymbol{\phi}^h\|^2]dt'$$
$$\leq \frac{1}{2}\|\mathbf{w}^h(0)\|^2 + \frac{\delta^2}{2}\|\nabla \mathbf{w}^h(0)\|^2 + \frac{1}{2\nu}\int_0^t \|\mathbf{f}\|^2_{-1}dt'.$$

Proof. Set $\mathbf{v}^h = \mathbf{w}^h$ in (8.1.12), $\boldsymbol{\xi}^h = \boldsymbol{\phi}^h$ in (8.1.13) and use $b(\mathbf{w}^h, \mathbf{w}^h, \mathbf{w}^h) = 0$ to get:

$$\frac{1}{2}\frac{d}{dt}\left(\|\mathbf{w}^h\|^2 + \delta^2\|\nabla \mathbf{w}^h\|^2\right) + \nu\|\nabla \mathbf{w}^h\|^2 + \nu\delta^2(\nabla\boldsymbol{\phi}^h, \nabla \mathbf{w}^h) = (\mathbf{f}, \mathbf{w}^h) \quad (8.1.14)$$

$$(\nabla \mathbf{w}^h, \nabla\boldsymbol{\phi}^h) = (\boldsymbol{\phi}^h, \boldsymbol{\phi}^h). \quad (8.1.15)$$

Multiplying (8.1.15) by $-\nu\delta^2$, adding it to (8.1.14), and then using the Cauchy Schwarz inequality, one has

$$\frac{1}{2}\frac{d}{dt}\left(\|\mathbf{w}^h\|^2 + \delta^2\|\nabla \mathbf{w}^h\|^2\right) + \frac{\nu}{2}\|\nabla \mathbf{w}^h\|^2 + \nu\delta^2\|\boldsymbol{\phi}^h\|^2 \leq \frac{1}{2\nu}\|\mathbf{f}\|^2_{-1}.$$

Integrating the last equation over $(0, t)$ with $t \leq T$ gives the required result. $\square$

8.2 CONVERGENCE ANALYSIS

It is useful to define the following modified Stokes projection aiming at simplifying the error analysis.

Definition 8.2.1. *(Modified Stokes Projection) The modified Stokes projection operator P_S : $(\mathbf{X}, \mathbf{X}, Q) \to (\mathbf{X}^h, \mathbf{X}^h, Q^h)$ is defined as follows: Let $P_S(\mathbf{w}, \boldsymbol{\phi}, p) = (\tilde{\mathbf{w}}, \tilde{\boldsymbol{\phi}}, \tilde{p})$ where $(\tilde{\mathbf{w}}, \tilde{\boldsymbol{\phi}}, \tilde{p})$ satisfies*

$$
\begin{aligned}
\nu(\nabla(\mathbf{w} - \tilde{\mathbf{w}}), \nabla\mathbf{v}^h) + \nu\delta^2(\nabla(\boldsymbol{\phi} - \tilde{\boldsymbol{\phi}}), \nabla\mathbf{v}^h) - (p - \tilde{p}, \nabla \cdot \mathbf{v}^h) &= 0, \\
(\nabla(\mathbf{w} - \tilde{\mathbf{w}}), \nabla\boldsymbol{\xi}^h) &= (\boldsymbol{\phi} - \tilde{\boldsymbol{\phi}}, \boldsymbol{\xi}^h), \\
(q^h, \nabla \cdot (\mathbf{w} - \tilde{\mathbf{w}})) &= 0, \qquad (8.2.1)
\end{aligned}
$$

for all $(\mathbf{v}^h, \boldsymbol{\xi}^h, q^h) \in (\mathbf{X}^h, \mathbf{X}^h, Q^h)$.

In $(\mathbf{V}^h, \mathbf{X}^h)$, this formulation reads: Given $(\mathbf{w}, \boldsymbol{\phi})$, find $(\tilde{\mathbf{w}}, \tilde{\boldsymbol{\phi}}) \in (\mathbf{V}^h, \mathbf{X}^h)$ satisfying

$$
\nu(\nabla(\mathbf{w} - \tilde{\mathbf{w}}), \nabla\mathbf{v}^h) + \nu\delta^2(\nabla(\boldsymbol{\phi} - \tilde{\boldsymbol{\phi}}), \nabla\mathbf{v}^h) - (p - q^h, \nabla \cdot \mathbf{v}^h) = 0, \qquad (8.2.2)
$$

$$
(\nabla(\mathbf{w} - \tilde{\mathbf{w}}), \nabla\boldsymbol{\xi}^h) = (\boldsymbol{\phi} - \tilde{\boldsymbol{\phi}}, \boldsymbol{\xi}^h), (8.2.3)
$$

for all $(\mathbf{v}^h, \boldsymbol{\xi}^h) \in (\mathbf{V}^h, \mathbf{X}^h)$ and any $q^h \in Q^h$.

Under the discrete inf-sup condition (2.2.1), $(\tilde{\mathbf{w}}, \tilde{\boldsymbol{\phi}}, \tilde{p})$ is a quasi optimal approximation of $(\mathbf{w}, \boldsymbol{\phi}, p)$. Since the stability and error estimation of the projection operator will be used to approximate the error between $\mathbf{w}$ and $\mathbf{w}^h$, we now give two related results.

Proposition 8.2.1. *(Stability of the modified Stokes projection) Let $(\mathbf{w}, \boldsymbol{\phi}, p)$ be given. Then, any solution $(\tilde{\mathbf{w}}, \tilde{\boldsymbol{\phi}}, \tilde{p})$ of (8.2.1) satisfies*

$$
\nu\|\nabla\tilde{\mathbf{w}}\|^2 + \nu\delta^2\|\tilde{\boldsymbol{\phi}}\|^2 \le C\{(\nu + \nu\delta^2 h^{-2})\|\nabla\mathbf{w}\|^2 + \nu\delta^4\|\nabla\boldsymbol{\phi}\|^2 + \nu\delta^2\|\boldsymbol{\phi}\|^2 + \nu^{-1}\|p\|^2\}
$$

and

$$
\|\tilde{p}\| \le C\left\{\|p\| + \nu\|\nabla\mathbf{w}\| + \nu\delta^2\|\nabla\boldsymbol{\phi}\| + \nu\|\nabla\tilde{\mathbf{w}}\| + \nu\delta^2\|\tilde{\boldsymbol{\phi}}\|\right\},
$$

where C is independent of ν, δ and h.

Proof. We first set $\mathbf{v}^h = \tilde{\mathbf{w}}$ in (8.2.2) and $\boldsymbol{\xi}^h = \tilde{\boldsymbol{\phi}}$ in (8.2.3). Then, we obtain

$$\nu\|\nabla\tilde{\mathbf{w}}\|^2 \;=\; \nu(\nabla\mathbf{w},\nabla\tilde{\mathbf{w}}) + \nu\delta^2(\nabla(\boldsymbol{\phi}-\tilde{\boldsymbol{\phi}}),\nabla\tilde{\mathbf{w}}) - (p,\nabla\cdot\tilde{\mathbf{w}}), \qquad (8.2.4)$$

$$(\nabla\tilde{\mathbf{w}},\nabla\tilde{\boldsymbol{\phi}}) \;=\; (\nabla\mathbf{w},\nabla\tilde{\boldsymbol{\phi}}) + (\tilde{\boldsymbol{\phi}}-\boldsymbol{\phi},\tilde{\boldsymbol{\phi}}). \qquad (8.2.5)$$

Multiplying (8.2.5) by $\nu\delta^2$, substituting in (8.2.4) and applying the Cauchy-Schwarz inequality yields

$$\begin{aligned}
\nu\|\nabla\tilde{\mathbf{w}}\|^2 + \nu\delta^2\|\tilde{\boldsymbol{\phi}}\|^2 \;\leq\; & \nu\|\nabla\mathbf{w}\|\|\nabla\tilde{\mathbf{w}}\| + \nu\delta^2\|\nabla\boldsymbol{\phi}\|\|\nabla\tilde{\mathbf{w}}\| \\
& + \nu\delta^2\|\nabla\mathbf{w}\|\|\nabla\tilde{\boldsymbol{\phi}}\| + \nu\delta^2\|\boldsymbol{\phi}\|\|\tilde{\boldsymbol{\phi}}\| + \|p\|\|\nabla\cdot\tilde{\mathbf{w}}\|.
\end{aligned}$$

Lastly, we apply the inverse inequality

$$\|\nabla\tilde{\boldsymbol{\phi}}\| \leq C\,h^{-1}\|\tilde{\boldsymbol{\phi}}\|,$$

and Young's inequality to obtain the first claimed inequality.

The second claimed inequality comes from rewriting the first equation in (8.2.1) in terms of the pressure, and then using the Cauchy-Schwarz inequality to write

$$\frac{(\tilde{p},\nabla\cdot\mathbf{v}^h)}{\|\nabla\mathbf{v}^h\|} \leq C\left\{\|p\| + \nu\|\nabla\mathbf{w}\| + \nu\delta^2\|\nabla\boldsymbol{\phi}\| + \nu\|\nabla\tilde{\mathbf{w}}\| + \nu\delta^2\|\tilde{\boldsymbol{\phi}}\|\right\}.$$

The inf-sup condition (2.2.1) gives the result. $\qquad\qquad\square$

Proposition 8.2.2. *(Error in the modified Stokes projection) Suppose the discrete inf-sup condition (2.2.1) holds. Then, $(\tilde{\mathbf{w}},\tilde{\boldsymbol{\phi}},\tilde{p})$ exists uniquely in $(\mathbf{X}^h,\mathbf{X}^h,Q^h)$ and satisfies*

$$\begin{aligned}
\nu\|\nabla(\mathbf{w}-\tilde{\mathbf{w}})\|^2 + \nu\delta^2\|\boldsymbol{\phi}-\tilde{\boldsymbol{\phi}}\|^2 \leq C\left[\inf_{\widehat{\mathbf{w}}\in\mathbf{X}^h}(\nu+\nu\delta^2 h^{-2})\|\nabla(\mathbf{w}-\widehat{\mathbf{w}})\|^2 + \inf_{q^h\in Q^h}\nu^{-1}\|p-q^h\|^2\right. \\
\left. + \inf_{\widehat{\boldsymbol{\phi}}\in\mathbf{X}^h}\nu\delta^2\|\boldsymbol{\phi}-\widehat{\boldsymbol{\phi}}\|^2 + \nu\delta^4\|\nabla(\boldsymbol{\phi}-\widehat{\boldsymbol{\phi}})\|^2\right],
\end{aligned}$$

and

$$\|p-\tilde{p}\| \leq C\left[\nu\|\nabla(\mathbf{w}-\tilde{\mathbf{w}})\| + \nu\delta^2\|\boldsymbol{\phi}-\tilde{\boldsymbol{\phi}}\| + \inf_{q^h\in Q^h}\|p-q^h\|\right],$$

where C is a constant independent of ν,δ and h.

Proof. The *à priori* bounds in Proposition 8.2.1 (and the discrete inf-sup condition (2.2.1)) are enough to guarantee existence and uniqueness, since $(\tilde{\mathbf{w}}, \tilde{\boldsymbol{\phi}}, \tilde{p})$ is the solution of a linear system.

For the error bound, set $\mathbf{e}_{\mathbf{w}} = \mathbf{w} - \tilde{\mathbf{w}}$ and $\mathbf{e}_{\boldsymbol{\phi}} = \boldsymbol{\phi} - \tilde{\boldsymbol{\phi}}$ and let $\widehat{\mathbf{w}}$ and $\widehat{\boldsymbol{\phi}}$ be approximations of $\mathbf{w} \in \mathbf{V}^h$ and $\boldsymbol{\phi} \in \mathbf{X}^h$, respectively. Then decompose $\mathbf{e}_{\mathbf{w}}$ and $\mathbf{e}_{\boldsymbol{\phi}}$ in two parts as $\mathbf{e}_{\mathbf{w}} = \boldsymbol{\eta}_{\mathbf{w}} - \boldsymbol{\psi}_{\mathbf{w}}^h = (\mathbf{w} - \widehat{\mathbf{w}}) - (\tilde{\mathbf{w}} - \widehat{\mathbf{w}})$, and $\mathbf{e}_{\boldsymbol{\phi}} = \boldsymbol{\eta}_{\boldsymbol{\phi}} - \boldsymbol{\psi}_{\boldsymbol{\phi}}^h = (\boldsymbol{\phi} - \widehat{\boldsymbol{\phi}}) - (\tilde{\boldsymbol{\phi}} - \widehat{\boldsymbol{\phi}})$, so that equations (8.2.2) and (8.2.3) become

$$\nu(\nabla\boldsymbol{\psi}_{\mathbf{w}}^h, \nabla\mathbf{v}^h) + \nu\delta^2(\nabla\boldsymbol{\psi}_{\boldsymbol{\phi}}^h, \nabla\mathbf{v}^h) = \nu(\nabla\boldsymbol{\eta}_{\mathbf{w}}, \nabla\mathbf{v}^h) + \nu\delta^2(\nabla\boldsymbol{\eta}_{\boldsymbol{\phi}}, \nabla\mathbf{v}^h)$$
$$-(p - q^h, \nabla \cdot \mathbf{v}^h) \tag{8.2.6}$$

$$(\nabla(\boldsymbol{\eta}_{\mathbf{w}} - \boldsymbol{\psi}_{\mathbf{w}}^h), \nabla\boldsymbol{\xi}^h) = (\boldsymbol{\eta}_{\boldsymbol{\phi}} - \boldsymbol{\psi}_{\boldsymbol{\phi}}^h, \boldsymbol{\xi}^h). \tag{8.2.7}$$

Choose $\mathbf{v}^h = \boldsymbol{\psi}_{\mathbf{w}}^h$ in (8.2.6) and $\boldsymbol{\xi}^h = \boldsymbol{\psi}_{\boldsymbol{\phi}}^h$ in (8.2.7), which gives

$$\nu\|\nabla\boldsymbol{\psi}_{\mathbf{w}}^h\|^2 + \nu\delta^2(\nabla\boldsymbol{\psi}_{\boldsymbol{\phi}}^h, \nabla\boldsymbol{\psi}_{\mathbf{w}}^h) = \nu(\nabla\boldsymbol{\eta}_{\mathbf{w}}, \nabla\boldsymbol{\psi}_{\mathbf{w}}^h) + \nu\delta^2(\nabla\boldsymbol{\eta}_{\boldsymbol{\phi}}, \nabla\boldsymbol{\psi}_{\mathbf{w}}^h)$$
$$-(p - q^h, \nabla \cdot \boldsymbol{\psi}_{\mathbf{w}}^h), \tag{8.2.8}$$

$$(\nabla\boldsymbol{\eta}_{\mathbf{w}}, \nabla\boldsymbol{\psi}_{\boldsymbol{\phi}}^h) + \|\boldsymbol{\psi}_{\boldsymbol{\phi}}^h\|^2 = (\nabla\boldsymbol{\psi}_{\mathbf{w}}^h, \nabla\boldsymbol{\psi}_{\boldsymbol{\phi}}^h) + (\boldsymbol{\eta}_{\boldsymbol{\phi}}, \boldsymbol{\psi}_{\boldsymbol{\phi}}^h). \tag{8.2.9}$$

Multiply (8.2.9) by $\nu\delta^2$ and substitute the resulting expression in the left hand side of (8.2.8). With the application of the Cauchy-Schwarz inequality, we obtain

$$\nu\|\nabla\boldsymbol{\psi}^h\|^2 + \nu\delta^2\|\boldsymbol{\psi}_{\boldsymbol{\phi}}^h\|^2 \leq \nu\|\nabla\boldsymbol{\eta}_{\mathbf{w}}\|\|\nabla\boldsymbol{\psi}_{\mathbf{w}}^h\| + \nu\delta^2\|\nabla\boldsymbol{\eta}_{\mathbf{w}}\|\|\nabla\boldsymbol{\psi}_{\boldsymbol{\phi}}^h\| + \nu\delta^2\|\boldsymbol{\eta}_{\boldsymbol{\phi}}\|\|\boldsymbol{\psi}_{\boldsymbol{\phi}}^h\|$$
$$+\nu\delta^2\|\nabla\boldsymbol{\eta}_{\boldsymbol{\phi}}\|\|\nabla\boldsymbol{\psi}_{\mathbf{w}}^h\| + \|p - q^h\|\|\nabla \cdot \boldsymbol{\psi}_{\mathbf{w}}^h\|. \tag{8.2.10}$$

By using the following inverse inequality,

$$\|\nabla\boldsymbol{\psi}_{\boldsymbol{\phi}}^h\| \leq Ch^{-1}\|\boldsymbol{\psi}_{\boldsymbol{\phi}}^h\|,$$

and using Young's inequality for the terms on the right hand side of (8.2.10), we get

$$\nu\|\nabla\boldsymbol{\psi}_{\mathbf{w}}^h\|^2 + \nu\delta^2\|\boldsymbol{\psi}_{\boldsymbol{\phi}}^h\|^2 \leq C\Big\{(\nu + \nu\delta^2 h^{-2})\|\nabla\boldsymbol{\eta}_{\mathbf{w}}\|^2 + \nu\delta^2\|\boldsymbol{\eta}_{\boldsymbol{\phi}}\|$$
$$+\nu\delta^4\|\nabla\boldsymbol{\eta}_{\boldsymbol{\phi}}\|^2 + \nu^{-1}\|p - q^h\|^2\Big\}$$

The first result follows from applying the triangle inequality and taking the infimum over $\widehat{\mathbf{w}} \in \mathbf{V}^h$ and $\widehat{\boldsymbol{\phi}} \in \mathbf{X}^h$. Note that, under the inf-sup condition and the condition $\nabla \cdot \mathbf{w} = 0$, the infimum over $\mathbf{V}^h$ can be replaced by infimum over $\mathbf{X}^h$ (see e.g. Girault and Raviart [30], p.60).

The second claim follows from adding and subtracting $(q^h, \nabla \cdot \mathbf{v}^h)$ to (8.2.1) and then using the Cauchy-Schwarz inequality, followed by the inf-sup condition (2.2.1), to get

$$\|\tilde{p} - q^h\| \leq C \left[\nu \|\nabla(\mathbf{w} - \tilde{\mathbf{w}})\| + \nu\delta^2 \|\boldsymbol{\phi} - \tilde{\boldsymbol{\phi}}\| + \|p - q^h\| \right].$$

The proof concludes by using the triangle inequality and taking infimum over q^h in Q^h. $\quad\square$

Remark 8.2.1. *The statements of Proposition 8.2.1 and Proposition 8.2.2 suggest that to get an optimal bound, one has to choose $\delta = \mathcal{O}(h)$.*

Remark 8.2.2. *The error in the modified Stokes projection $(\tilde{\mathbf{w}}, \tilde{\boldsymbol{\phi}}, \tilde{p})$ is bounded by approximation theoretic terms, according to Proposition 8.2.2.*

The semi-discrete convergence analysis of the new discretization uses properties of the modified Stokes projection defined above. It follows the usual finite element technique and calls for the use of Gronwall's inequality. A term similar to the nonlinear one that arises in the analysis of the Navier-Stokes equations appears here, making it necessary to make *á priori* assumptions on $\mathbf{w}$.

Theorem 8.2.1. *Let $(\mathbf{w}, p)$ solve (8.1.2)-(8.1.4). Assuming that $\nabla\mathbf{w} \in L^4(0, T; L^2(\Omega))$, $\mathbf{w}_t \in L^2(0, T; H^{-1}(\Omega))$, $\nabla\mathbf{w}_t \in L^2(0, T; L^2(\Omega))$, and $p \in L^2(0, T; L_0^2(\Omega))$, the error $\mathbf{e} = \mathbf{w} - \mathbf{w}^h$ satisfies*

$$\|\mathbf{e}\|_{L^\infty(0,T;L^2)}^2 + \delta^2 \|\nabla\mathbf{e}\|_{L^\infty(0,T;L^2)}^2 + \nu \|\nabla\mathbf{e}\|_{L^2(0,T;L^2)}^2 + \nu\delta^2 \|\boldsymbol{\phi} - \boldsymbol{\phi}^h\|_{L^2(0,T;L^2)}^2$$

$$\leq CC^*(\|\mathbf{w}(0) - \mathbf{w}^h(0)\|^2 + \|\nabla(\mathbf{w}(0) - \mathbf{w}^h(0))\|^2) + C\,\mathcal{F}(\mathbf{w} - \tilde{\mathbf{w}}, \boldsymbol{\phi} - \tilde{\boldsymbol{\phi}})$$

where $(\tilde{\mathbf{w}}, \tilde{\phi})$ *is the modified Stokes projection,* $C^* = \exp(\frac{C}{\nu^3} \int_0^T \|\nabla \mathbf{w}\|^4 dt')$ *and*

$$
\begin{aligned}
\mathcal{F}(\mathbf{w} - \tilde{\mathbf{w}}, \phi - \tilde{\phi}) \quad = \quad & \|\mathbf{w} - \tilde{\mathbf{w}}\|^2 + \delta^2 \|\nabla(\mathbf{w} - \tilde{\mathbf{w}})\|^2_{L^2(0;T;L^2)} \\
& + \nu\delta^2 \|\phi - \tilde{\phi}\|^2_{L^2(0;T;L^2)} + C^*(T) \Big[\|\mathbf{w}(0) - \tilde{\mathbf{w}}(0)\|^2 \\
& + \|\nabla(\mathbf{w}(0) - \tilde{\mathbf{w}}(0))\|^2 + \nu^{-1} \|(\mathbf{w} - \tilde{\mathbf{w}})_t\|^2_{L^2(0;T;H^{-1})} \\
& + \nu^{-1}\delta^4 \|\nabla(\mathbf{w} - \tilde{\mathbf{w}})_t\|^2_{L^2(0;T;L^2)} \\
& + (\|\nabla\mathbf{w}^h\|_{L^2(0;T;L^2)} + \|\nabla\mathbf{w}\|^2_{L^4(0;T;L^2)}) \|\nabla(\mathbf{w} - \tilde{\mathbf{w}})\|^2_{L^4(0;T;L^2)} \Big].
\end{aligned}
$$

Proof. We first set $\mathbf{v} = \mathbf{v}^h$ in (8.1.2) and $\boldsymbol{\xi} = \boldsymbol{\xi}^h$ in (8.1.3). Then, subtracting (8.1.2) from (8.1.12) and (8.1.3) from (8.1.13) and letting $\mathbf{e} = \mathbf{w} - \mathbf{w}^h$ give the following error equations:

$$
\begin{aligned}
& (\mathbf{e}_t, \mathbf{v}^h) + \delta^2 (\nabla\mathbf{e}_t, \nabla\mathbf{v}^h) + \nu(\nabla\mathbf{e}, \nabla\mathbf{v}^h) + b(\mathbf{w}, \mathbf{w}, \mathbf{v}^h) - b(\mathbf{w}^h, \mathbf{w}^h, \mathbf{v}^h) \\
& + \nu\delta^2 (\nabla(\phi - \phi^h), \nabla\mathbf{v}^h) - (p - q^h, \nabla \cdot \mathbf{v}^h) = 0 \quad \forall \mathbf{v}^h \in \mathbf{V}^h \quad (8.2.11)
\end{aligned}
$$

$$
(\nabla\mathbf{e}, \nabla\boldsymbol{\xi}^h) = (\phi - \phi^h, \boldsymbol{\xi}^h) \quad \forall \boldsymbol{\xi}^h \in \mathbf{X}^h. \quad (8.2.12)
$$

Decompose the error in two parts: $\mathbf{e} = \boldsymbol{\eta} - \boldsymbol{\psi}^h$ where $\boldsymbol{\eta} = \mathbf{w} - \tilde{\mathbf{w}}$, $\boldsymbol{\psi}^h = \mathbf{w}^h - \tilde{\mathbf{w}}$, and add and subtract $\nu\delta^2 (\nabla\tilde{\phi}, \nabla\mathbf{v}^h)$ in (8.2.11), where $\tilde{\mathbf{w}} \in \mathbf{V}^h, \tilde{\phi} \in \mathbf{X}^h$ are chosen as the Stokes projection, defined via (8.2.2)-(8.2.3). Putting all these together and setting $\mathbf{v}^h = \boldsymbol{\psi}^h$ in (8.2.11), and $\boldsymbol{\xi} = \phi^h - \tilde{\phi}$ in (8.2.12) yields

$$
\begin{aligned}
& (\boldsymbol{\psi}^h_t, \boldsymbol{\psi}^h) + \delta^2 (\nabla\boldsymbol{\psi}^h_t, \nabla\boldsymbol{\psi}^h) + \nu(\nabla\boldsymbol{\psi}^h, \nabla\boldsymbol{\psi}^h) + \nu\delta^2 (\nabla(\phi^h - \tilde{\phi}), \nabla\boldsymbol{\psi}^h) \\
& = (\boldsymbol{\eta}_t, \boldsymbol{\psi}^h) + \delta^2 (\nabla\boldsymbol{\eta}_t, \nabla\boldsymbol{\psi}^h) + b(\mathbf{w}, \mathbf{w}, \boldsymbol{\psi}^h) - b(\mathbf{w}^h, \mathbf{w}^h, \boldsymbol{\psi}^h) \quad (8.2.13)
\end{aligned}
$$

$$
(\nabla\boldsymbol{\psi}^h, \nabla(\phi^h - \tilde{\phi})) = (\phi^h - \tilde{\phi}, \phi^h - \tilde{\phi}). \quad (8.2.14)
$$

Note that since $(\tilde{\mathbf{w}}, \tilde{\phi})$ is taken to be the modified Stokes projection of $(\mathbf{w}, \phi)$ in $(\mathbf{V}^h, \mathbf{X}^h)$, some of the terms in the error equation (8.2.13) vanish.

We then multiply both sides of (8.2.14) by $\nu\delta^2$, substitute in (8.2.13), and apply Cauchy-Schwarz inequality. This gives

$$
\begin{aligned}
& \frac{1}{2}\frac{d}{dt}\|\boldsymbol{\psi}^h\|^2 + \frac{\delta^2}{2}\frac{d}{dt}\|\nabla\boldsymbol{\psi}^h\|^2 + \nu\|\nabla\boldsymbol{\psi}^h\|^2 + \nu\delta^2\|\phi^h - \tilde{\phi}\|^2 \\
& \leq \|\boldsymbol{\eta}_t\|_{-1}\|\nabla\boldsymbol{\psi}^h\| + \delta^2\|\nabla\boldsymbol{\eta}_t\|\|\nabla\boldsymbol{\psi}^h\| + |b(\mathbf{w}, \mathbf{w}, \boldsymbol{\psi}^h) - b(\mathbf{w}^h, \mathbf{w}^h, \boldsymbol{\psi}^h)|. \quad (8.2.15)
\end{aligned}
$$

The nonlinear term on the right hand side of (8.2.15) is decomposed into three parts:

$$b(\mathbf{w}, \mathbf{w}, \boldsymbol{\psi}^h) - b(\mathbf{w}^h, \mathbf{w}^h, \boldsymbol{\psi}^h) = b(\boldsymbol{\eta}, \mathbf{w}, \boldsymbol{\psi}^h) - b(\boldsymbol{\psi}^h, \mathbf{w}, \boldsymbol{\psi}^h) + b(\mathbf{w}^h, \boldsymbol{\eta}, \boldsymbol{\psi}^h).$$

By applying the improved estimate (2.1.4), Poincaré-Friedrich's and Young's inequalities, the nonlinear terms are bounded as:

$$
\begin{aligned}
b(\boldsymbol{\eta}, \mathbf{w}, \boldsymbol{\psi}^h) &\leq C\|\boldsymbol{\eta}\|^{1/2}\|\nabla\boldsymbol{\eta}\|^{1/2}\|\nabla\mathbf{w}\|\|\nabla\boldsymbol{\psi}^h\| \\
&\leq \frac{\epsilon}{4}\|\nabla\boldsymbol{\psi}^h\|^2 + \frac{C}{\epsilon}\|\nabla\boldsymbol{\eta}\|^2\|\nabla\mathbf{w}\|^2 \\
b(\boldsymbol{\psi}^h, \mathbf{w}, \boldsymbol{\psi}^h) &\leq \|\nabla\boldsymbol{\psi}^h\|^{3/2}\|\boldsymbol{\psi}^h\|^{1/2}\|\nabla\mathbf{w}\| \\
&\leq \frac{\epsilon}{2}\|\nabla\boldsymbol{\psi}^h\|^2 + \frac{C}{\epsilon^3}\|\nabla\mathbf{w}\|^4\|\boldsymbol{\psi}^h\|^2 \\
b(\mathbf{w}^h, \boldsymbol{\eta}, \boldsymbol{\psi}^h) &\leq C\|\mathbf{w}^h\|^{1/2}\|\nabla\mathbf{w}^h\|^{1/2}\|\nabla\boldsymbol{\eta}\|\|\nabla\boldsymbol{\psi}^h\| \\
&\leq \frac{\epsilon}{4}\|\nabla\boldsymbol{\psi}^h\|^2 + \frac{C}{\epsilon}\|\mathbf{w}^h\|\|\nabla\mathbf{w}^h\|\|\nabla\boldsymbol{\eta}\|^2
\end{aligned}
$$

On the right hand side of (8.2.15), we apply Young's inequality and choose $\epsilon = \nu/4$,

$$
\begin{aligned}
&\frac{1}{2}\frac{d}{dt}\|\boldsymbol{\psi}^h\|^2 + \frac{\delta^2}{2}\frac{d}{dt}\|\nabla\boldsymbol{\psi}^h\|^2 + \frac{\nu}{2}\|\nabla\boldsymbol{\psi}^h\|^2 + \nu\delta^2\|\boldsymbol{\phi}^h - \tilde{\boldsymbol{\phi}}\|^2 \\
&\leq 2\nu^{-1}\|\boldsymbol{\eta}_t\|_{-1}^2 + \nu^{-1}\delta^4\|\nabla\boldsymbol{\eta}_t\|^2 + \frac{C}{\nu}(\|\nabla\mathbf{w}\|^2 + \|\mathbf{w}^h\|\|\nabla\mathbf{w}^h\|)\|\nabla\boldsymbol{\eta}\|^2 + \frac{C}{\nu^3}\|\nabla\mathbf{w}\|^4\|\boldsymbol{\psi}^h\|^2.
\end{aligned}
$$

Since by assumption $\|\nabla\mathbf{w}\|^4 \in L^1(0,T)$, Gronwall inequality implies that

$$
\begin{aligned}
&\|\boldsymbol{\psi}^h\|^2 + \delta^2\|\nabla\boldsymbol{\psi}^h\|^2 + \int_0^t [\nu\|\nabla\boldsymbol{\psi}^h\|^2 + 2\nu\delta^2\|\boldsymbol{\phi}^h - \tilde{\boldsymbol{\phi}}\|^2]dt' \\
&\leq C^*(\|\boldsymbol{\psi}^h(0)\|^2 + \|\nabla\boldsymbol{\psi}^h(0)\|^2) + CC^* \int_0^t \Big[\nu^{-1}\|\boldsymbol{\eta}_t\|_{-1}^2 + \nu^{-1}\delta^4\|\nabla\boldsymbol{\eta}_t\|^2 \\
&\quad + \frac{1}{\nu}(\|\nabla\mathbf{w}\|^2 + \|\mathbf{w}^h\|\|\nabla\mathbf{w}^h\|)\|\nabla\boldsymbol{\eta}\|^2\Big]dt',
\end{aligned}
$$

where $C^* = \exp(\frac{C}{\nu^3}\int_0^t\|\nabla\mathbf{w}\|^4 dt')$. In order to complete proof, one has to study the $L^1(0,T)$ regularity of terms in the last inequality. Note that using the Cauchy-Schwarz inequality

$$\int_0^t \|\nabla\mathbf{w}\|^2\|\nabla\boldsymbol{\eta}\|^2 dt' \leq \|\nabla\mathbf{w}\|_{L^4(0,t;L^2)}^2\|\nabla\boldsymbol{\eta}\|_{L^4(0,t;L^2)}^2 < \infty.$$

Similarly, using Hölder's inequality and Lemma 8.1.3 imply that

$$
\begin{aligned}
\int_0^t \|\mathbf{w}^h\| \|\nabla\mathbf{w}^h\| \|\nabla\boldsymbol{\eta}\|^2 dt' &\leq \|\mathbf{w}^h\|_{L^\infty(0,t;L^2)} \|\nabla\mathbf{w}^h\|_{L^2(0,t;L^2)} \|\nabla\boldsymbol{\eta}\|^2_{L^4(0,t;L^2)} \\
&\leq C\big(\frac{1}{\nu^{1/2}}\|\mathbf{w}^h(0)\|^2 + \frac{\delta^2}{\nu^{1/2}}\|\nabla\mathbf{w}^h(0)\|^2 \\
&\quad + \frac{1}{\nu^{3/2}}\|\mathbf{f}\|^2_{L^2(0,t;H^{-1})}\big)\|\nabla\boldsymbol{\eta}\|^2_{L^4(0,t;L^2)} < \infty.
\end{aligned}
$$

The stated error estimate now follows by applying the triangle inequality. $\square$

8.3 TIME AVERAGED ERRORS

In this section, we analyze time averaged errors. In practical flow computations, pointwise flow quantities may not make sense, whereas statistics of flow quantities may be relevant. The analysis we employ here follows the same approach as in Chapter 4, where statistics of weak solutions of the Navier-Stokes are investigated. Accordingly, we consider the case where the solution to the time dependent problem converges to a stationary solution, provided the steady-state body force is small enough. In this context, statistics are optimally computable. In the general case, it is not known if a closed estimate is feasible (see Chapter 4).

We must point out once more that weak solutions of the Zeroth Order Model are indeed strong solutions and satisfy an energy equality. This has been proven for the periodic case, but it is reasonable to assume that the same also holds true in the non periodic case (operationally, this will allow us to choose e.g. $\mathbf{w}$ as a test function in the estimates below).

We will need properties of the steady-state solution, denoted with superscript $*$, so we first consider the equilibrium variational formulation of problem (8.1.2)-(8.1.4) when $\mathbf{f}(x,t) \to \mathbf{f}^*(x)$ as $t \to \infty$: Find $(\mathbf{w}^*, \boldsymbol{\phi}^*, p^*) \in (\mathbf{X}, \mathbf{X}, Q)$ such that

$$
\nu(\nabla\mathbf{w}^*, \nabla\mathbf{v}) + \nu\delta^2(\nabla\boldsymbol{\phi}^*, \nabla\mathbf{v}) + b(\mathbf{w}^*, \mathbf{w}^*, \mathbf{v}) - (p^*, \nabla\cdot\mathbf{v}) = (\mathbf{f}^*, \mathbf{v}), \ \forall\,\mathbf{v} \in \mathbf{X} \tag{8.3.1}
$$

$$
(\nabla\mathbf{w}^*, \nabla\boldsymbol{\xi}) = (\boldsymbol{\phi}^*, \boldsymbol{\xi}), \quad \forall\,\boldsymbol{\xi} \in \mathbf{X} \tag{8.3.2}
$$

$$
(q, \nabla\cdot\mathbf{w}^*) = 0, \quad \forall\,q \in Q \tag{8.3.3}
$$

In $\mathbf{V}$, the variational formulation becomes: Find $(\mathbf{w}^*, \boldsymbol{\phi}^*) \in (\mathbf{V}, \mathbf{X})$ satisfying

$$\nu(\nabla \mathbf{w}^*, \nabla \mathbf{v}) + \nu\delta^2(\nabla\boldsymbol{\phi}^*, \nabla \mathbf{v}) + b(\mathbf{w}^*, \mathbf{w}^*, \mathbf{v}) = (\mathbf{f}^*, \mathbf{v}), \quad \forall\, \mathbf{v} \in \mathbf{V} \qquad (8.3.4)$$

$$(\nabla \mathbf{w}^*, \nabla \boldsymbol{\xi}) = (\boldsymbol{\phi}^*, \boldsymbol{\xi}), \quad \forall\, \boldsymbol{\xi} \in \mathbf{X} \qquad (8.3.5)$$

Our first result in this section gives an *á priori* bound on $(\mathbf{w}^*, \boldsymbol{\phi}^*)$.

Lemma 8.3.1. *A pair $(\mathbf{w}^*, \boldsymbol{\phi}^*)$ satisfying (8.3.4)-(8.3.5) is bounded such that*

$$|| \nabla \mathbf{w}^* ||^2 + 2\delta^2 || \boldsymbol{\phi}^* ||^2 \leq \nu^{-2} || \mathbf{f}^* ||^2_{-1}.$$

Proof. Setting $\mathbf{v} = \mathbf{w}^*$ in (8.3.4) and $\boldsymbol{\xi} = \boldsymbol{\phi}^*$ in (8.3.5) gives the claimed result. $\qquad\square$

This result, together with assumptions on the steady state body force $\mathbf{f}^*$ and on its relationship with the time dependent body force $\mathbf{f}$ give, in turn, a relationship between the solutions $\mathbf{w}$ and $\mathbf{w}^*$.

Proposition 8.3.1. *Let $\mathbf{f} \in L^\infty(0, \infty, H^{-1}(\Omega))$. Suppose that for all T sufficiently large, $|| \mathbf{f} - \mathbf{f}^* ||_{-1}$ is bounded for $0 \leq t \leq T/2$ and $\int_{T/2}^T || \mathbf{f}(\cdot, t) - \mathbf{f}^*(\cdot) ||^2_{-1}\, dt \to 0$ as $T \to \infty$, then $\mathbf{w}(x,t) \to \mathbf{w}^*(x)$ in $H^1(\Omega)$, whenever $M\, \nu^{-2} || \mathbf{f}^* ||_{-1} := \alpha < 1$.*

Proof. The idea behind this proof is to divide the time axis in two parts. The first, where the difference between $\mathbf{f}$ and $\mathbf{f}^*$ is bounded (and the exponentials involved tend to zero), and the second part, which becomes small when $\mathbf{f}$ and $\mathbf{f}^*$ are sufficiently close.

We first subtract (8.3.4) from (8.1.5) and (8.3.5) from (8.1.6) and set $\mathbf{W} = \mathbf{w} - \mathbf{w}^*$ and $\boldsymbol{\Phi} = \boldsymbol{\phi} - \boldsymbol{\phi}^*$. Then, we have an equation of the form

$$(\mathbf{W}_t, \mathbf{v}) + \delta^2(\nabla \mathbf{W}_t, \nabla \mathbf{v}) + \nu(\nabla \mathbf{W}, \nabla \mathbf{v})$$
$$+\nu\delta^2(\nabla \boldsymbol{\Phi}, \nabla \mathbf{v}) + b(\mathbf{w}, \mathbf{w}, \mathbf{v}) - b(\mathbf{w}^*, \mathbf{w}^*, \mathbf{v}) = (\mathbf{f} - \mathbf{f}^*, \mathbf{v}), \qquad (8.3.6)$$
$$(\nabla \mathbf{W}, \nabla \boldsymbol{\xi}) = (\boldsymbol{\Phi}, \boldsymbol{\xi}), \qquad (8.3.7)$$

for all $(\mathbf{v}, \boldsymbol{\xi}) \in (\mathbf{V}, \mathbf{X})$.

Setting $\mathbf{v} = \mathbf{W}$ in (8.3.6) and $\boldsymbol{\xi} = \boldsymbol{\Phi}$ in (8.3.7), adding the two resulting equations together and adding and subtracting the term $b(\mathbf{w}, \mathbf{w}^*, \mathbf{W})$, we have

$$\frac{1}{2}\frac{d}{dt}\left(|| \mathbf{W} ||^2 + \delta^2 || \nabla \mathbf{W} ||^2\right) + \nu\left(|| \nabla \mathbf{W} ||^2 + \delta^2 || \boldsymbol{\Phi} ||^2\right) = -b(\mathbf{W}, \mathbf{w}^*, \mathbf{W}) + (\mathbf{f} - \mathbf{f}^*, \mathbf{W}) \quad (8.3.8)$$

Using the bound on nonlinear term, $b(\mathbf{W}, \mathbf{w}^*, \mathbf{W}) \le M \|\nabla \mathbf{w}^*\| \|\nabla \mathbf{W}\|^2$, together with the *á priori* bound $\|\nabla \mathbf{w}^*\| \le \nu^{-1} \|\mathbf{f}^*\|_{-1}$ (from Lemma 8.3.1), followed by $(\mathbf{f} - \mathbf{f}^*, \mathbf{W}) \le \|\mathbf{f} - \mathbf{f}^*\|_{-1} \|\nabla \mathbf{W}\|$ and Young's inequality, we get, for fixed $\epsilon > 0$,

$$\frac{1}{2}\frac{d}{dt}\left(\|\mathbf{W}\|^2 + \delta^2 \|\nabla \mathbf{W}\|^2\right) + \nu(1 - \alpha - \epsilon)\|\nabla \mathbf{W}\|^2 + \nu\delta^2 \|\mathbf{\Phi}\|^2 \le \frac{1}{4\epsilon\nu}\|\mathbf{f} - \mathbf{f}^*\|^2_{-1}. \quad (8.3.9)$$

Letting $\boldsymbol{\xi} = \mathbf{W}$ in equation (8.3.7) and using Poincaré-Friedrich's inequality, we find that $\|\nabla \mathbf{W}\| \le C_{PF} \|\mathbf{\Phi}\|$. Application of Poincaré-Friedrich's inequality to (8.3.9) yields

$$\frac{d}{dt}\left(\|\mathbf{W}\|^2 + \delta^2 \|\nabla \mathbf{W}\|^2\right) + 2\,C_{PF}^{-2}\,\nu\left((1 - \alpha - \epsilon)\|\mathbf{W}\|^2 + \delta^2\|\nabla \mathbf{W}\|^2\right) \le \frac{1}{2\epsilon\nu}\|\mathbf{f} - \mathbf{f}^*\|^2_{-1}.$$

Set $y = \|\mathbf{W}\|^2 + \delta^2 \|\nabla \mathbf{W}\|^2$. Then, for ϵ small enough, $K := 2\,\nu\,C_{PF}^{-2}(1 - \alpha - \epsilon) > 0$ and this inequality becomes

$$\frac{dy}{dt} + K\,y < \frac{1}{2\epsilon\nu}\|\mathbf{f} - \mathbf{f}^*\|^2_{-1}. \quad (8.3.10)$$

Choosing an integrating factor, equation (8.3.10) gives

$$\begin{aligned}
y(T) &\le y(0)\,e^{-KT} + \frac{1}{2\epsilon\nu}\int_0^{\frac{T}{2}} e^{K(t-T)}\|\mathbf{f} - \mathbf{f}^*\|^2_{-1}\,dt \\
&\quad + \frac{1}{2\epsilon\nu}\int_{\frac{T}{2}}^T e^{K(t-T)}\|\mathbf{f} - \mathbf{f}^*\|^2_{-1}\,dt.
\end{aligned} \quad (8.3.11)$$

The integrals on the right hand side of (8.3.11) can be estimated, respectively, as:

$$\int_0^{\frac{T}{2}} e^{K(t-T)}\|\mathbf{f} - \mathbf{f}^*\|^2_{-1}\,dt \le K^{-1}\left(e^{-K\frac{T}{2}} - e^{-KT}\right)\|\mathbf{f} - \mathbf{f}^*\|^2_{L^\infty(0,T/2;H^{-1}(\Omega))},$$

and

$$\int_{\frac{T}{2}}^T e^{K(t-T)}\|\mathbf{f} - \mathbf{f}^*\|^2_{-1}\,dt \le \int_{\frac{T}{2}}^T \|\mathbf{f} - \mathbf{f}^*\|^2_{-1}\,dt,$$

since $e^{K(t-T)} \le 1$ for $\frac{T}{2} \le t \le T$.

Combining everything together, (8.3.11) becomes

$$\begin{aligned}
y(T) &\le y(0)\,e^{-KT} + \frac{1}{2\epsilon\nu K}\left(e^{-K\frac{T}{2}} - e^{-KT}\right)\|\mathbf{f} - \mathbf{f}^*\|^2_{L^\infty(0,T/2;H^{-1}(\Omega))} \\
&\quad + \frac{1}{2\epsilon\nu}\|\mathbf{f} - \mathbf{f}^*\|^2_{L^2(T/2,T;H^{-1}(\Omega))}.
\end{aligned}$$

Letting $T \to \infty$ concludes the proof. $\qquad\square$

The first result involving time averages shows that the time averaged energy dissipation rate of the non stationary solution converges, as $T \to \infty$, to the steady state energy dissipation rate.

Proposition 8.3.2. *Under the same assumptions as Proposition 8.3.1, we have that*

$$< \varepsilon(\mathbf{w} - \mathbf{w}^*, \boldsymbol{\phi} - \boldsymbol{\phi}^*) >= 0.$$

Proof. The proof is similar to the proof of Proposition 8.3.1, so we start directly from equation (8.3.9), with $\mathbf{W} = \mathbf{w} - \mathbf{w}^*$ and $\boldsymbol{\Phi} = \boldsymbol{\phi} - \boldsymbol{\phi}^*$. We multiply it by 2, use the fact that $\min\{1 - \alpha - \epsilon, 1\} = 1 - \alpha - \epsilon$ and integrate from 0 to T to obtain

$$|| \mathbf{W}(T) ||^2 + \delta^2 || \nabla \mathbf{W}(T) ||^2 \quad + \quad (1 - \alpha - \epsilon) \nu \int_0^T \left(|| \nabla \mathbf{W} ||^2 + \delta^2 || \boldsymbol{\Phi} ||^2 \right) \, dt$$

$$\leq || \mathbf{W}(0) ||^2 + \delta^2 || \nabla \mathbf{W}(0) ||^2 + \frac{1}{2\epsilon\nu} \int_0^T || \mathbf{f} - \mathbf{f}^* ||_{-1}^2 \, dt \quad (8.3.12)$$

Dividing everything by T and taking limit supremum on both sides, we see that the first and second terms on the left hand side vanish (as a consequence of Lemma 8.1.1 and of the fact that $\mathbf{w}^*$ does not depend on time). Observing that $|| \mathbf{W}(0) ||^2 + \delta^2 || \nabla \mathbf{W}(0) ||^2$ is a constant and using the hypothesis on $\mathbf{f}$ and $\mathbf{f}^*$, the right hand side also vanishes and we are left with

$$(1 - \alpha - \epsilon) \nu < || \nabla \mathbf{W} ||^2 + \delta^2 || \boldsymbol{\Phi} ||^2 >\leq 0.$$

The fact that $(1 - \alpha - \epsilon) > 0$ gives the desired result. $\qquad \square$

Properties of the approximate solution $\mathbf{w}^{*h}$ are also needed. Thus, we also consider finite element approximation of (8.3.1)-(8.3.3). Finite element approximation of the equilibrium solution is to: Find $(\mathbf{w}^{*h}, \boldsymbol{\phi}^{*h}, p^{*h}) \in (\mathbf{X}^h, \mathbf{X}^h, Q^h)$ satisfying

$$\nu(\nabla \mathbf{w}^{*h}, \nabla \mathbf{v}^h) + \nu\delta^2(\nabla \boldsymbol{\phi}^{*h}, \nabla \mathbf{v}) + b(\mathbf{w}^{*h}, \mathbf{w}^{*h}, \mathbf{v}^h) - (p^{*h}, \nabla \cdot \mathbf{v}^h) = (\mathbf{f}^*, \mathbf{v}^h), \quad (8.3.13)$$

$$(\nabla \mathbf{w}^{*h}, \nabla \boldsymbol{\xi}^h) = (\boldsymbol{\phi}^{*h}, \boldsymbol{\xi}^h), \quad (8.3.14)$$

$$(q^h, \nabla \cdot \mathbf{w}^{*h}) = 0, \quad (8.3.15)$$

for all $(\mathbf{v}^h, \boldsymbol{\xi}^h, q^h) \in (\mathbf{X}^h, \mathbf{X}^h, Q^h)$, with the usual extension to the formulation in $(\mathbf{V}^h, \mathbf{X}^h)$.

Lemma 8.3.2. *The pair* $(\mathbf{w}^{*h}, \boldsymbol{\phi}^{*h})$ *satisfying (8.3.13)-(8.3.15) has the following bound:*

$$|| \nabla \mathbf{w}^{*h} ||^2 + 2\delta^2 || \boldsymbol{\phi}^{*h} ||^2 \leq \nu^{-2} || \mathbf{f}^* ||^2_{-1}.$$

Proof. The claim exactly follows the proof of Lemma 8.3.1. □

We now derive error estimates. The following result uses the modified Stokes projection defined via (8.2.2)-(8.2.3). Recall that according to Proposition 8.2.2, the error in the modified Stokes projection $(\tilde{\mathbf{w}}, \tilde{\boldsymbol{\phi}})$ is bounded.

Proposition 8.3.3. *Assume that* $(\mathbf{X}^h, Q^h)$ *satisfy an inf-sup condition. Under the small data condition,* $M\nu^{-2}|| \mathbf{f} ||_{-1} := \alpha < 1$, *the following error estimate holds:*

$$\nu || \nabla(\mathbf{w}^* - \mathbf{w}^{*h}) ||^2 + \nu\delta^2 || \boldsymbol{\phi}^* - \boldsymbol{\phi}^{*h} ||^2 \leq C \left\{ (\nu + \nu^{-3}|| \mathbf{f}^* ||^2_{-1}) || \nabla(\mathbf{w}^* - \tilde{\mathbf{w}}) ||^2 \right.$$
$$\left. + \nu\delta^2 || \boldsymbol{\phi}^* - \tilde{\boldsymbol{\phi}} ||^2 \right\},$$

where $(\tilde{\mathbf{w}}, \tilde{\boldsymbol{\phi}})$ *is the modified Stokes projection.*

Proof. Subtracting (8.3.13) from (8.3.1), for $\mathbf{v}^h \in \mathbf{V}^h$, and subtracting (8.3.14) from (8.3.2), for $\boldsymbol{\xi}^h \in \mathbf{X}^h$, we find the error equations:

$$\nu(\nabla(\mathbf{w}^* - \mathbf{w}^{*h}), \nabla\mathbf{v}^h) \quad + \quad \nu\delta^2(\nabla(\boldsymbol{\phi}^* - \boldsymbol{\phi}^{*h}), \nabla\mathbf{v}^h)$$
$$+ b(\mathbf{w}^*, \mathbf{w}^*, \mathbf{v}^h) - b(\mathbf{w}^{*h}, \mathbf{w}^{*h}, \mathbf{v}^h) - (p^* - q^h, \nabla \cdot \mathbf{v}^h) = 0$$
$$(\nabla(\mathbf{w}^* - \mathbf{w}^{*h}), \nabla\boldsymbol{\xi}^h) \quad = \quad (\boldsymbol{\phi}^* - \boldsymbol{\phi}^{*h}, \boldsymbol{\xi}^h)$$

Decompose the error as $\mathbf{e} = \boldsymbol{\eta} - \boldsymbol{\psi}^h$, where $\boldsymbol{\eta} = \mathbf{w}^* - \tilde{\mathbf{w}}$, $\boldsymbol{\psi}^h = \mathbf{w}^{*h} - \tilde{\mathbf{w}}$, and add and subtract $\tilde{\boldsymbol{\phi}}$, where $\tilde{\mathbf{w}} \in \mathbf{V}^h, \tilde{\boldsymbol{\phi}} \in \mathbf{X}^h$ are chosen as the modified Stokes projection. Putting all these together and setting $\mathbf{v}^h = \boldsymbol{\psi}^h$ and $\boldsymbol{\xi}^h = \boldsymbol{\phi}^{*h} - \tilde{\boldsymbol{\phi}}$ yields

$$\nu || \nabla\boldsymbol{\psi}^h ||^2 \quad + \quad \nu\delta^2 || \boldsymbol{\phi}^{*h} - \tilde{\boldsymbol{\phi}} ||^2 = b(\boldsymbol{\eta}, \mathbf{w}^*, \boldsymbol{\psi}^h) - b(\boldsymbol{\psi}^h, \mathbf{w}^*, \boldsymbol{\psi}^h) + b(\mathbf{w}^{*h}, \boldsymbol{\eta}, \boldsymbol{\psi}^h) \quad (8.3.16)$$

where the nonlinear term was decomposed into three parts (by adding and subtracting appropriate terms).

Using the bounds on the trilinear form followed by Young's inequality and the Cauchy-Schwarz inequality, together with the a priori estimates for $\mathbf{w}^*$ and $\mathbf{w}^{*h}$, we write

$$
\begin{aligned}
b(\boldsymbol{\eta}, \mathbf{w}^*, \boldsymbol{\psi}^h) \ &\le \ M|| \nabla \boldsymbol{\eta} || \, || \nabla \mathbf{w}^* || \, || \nabla \boldsymbol{\psi}^h || \\
&\le \ \frac{\nu}{4} || \nabla \boldsymbol{\psi}^h ||^2 + C\nu^{-1} || \nabla \mathbf{w}^* ||^2 \, || \nabla \boldsymbol{\eta} ||^2 \\
&\le \ \frac{\nu}{4} || \nabla \boldsymbol{\psi}^h ||^2 + C\nu^{-3} || \mathbf{f}^* ||^2_{-1} \, || \nabla \boldsymbol{\eta} ||^2
\end{aligned}
$$

$$
\begin{aligned}
b(\boldsymbol{\psi}^h, \mathbf{w}^*, \boldsymbol{\psi}^h) \ &\le \ M|| \nabla \mathbf{w}^* || \, || \nabla \boldsymbol{\psi}^h ||^2 \\
&\le \ M\nu^{-1} || \mathbf{f}^* ||_{-1} \, || \nabla \boldsymbol{\psi}^h ||^2
\end{aligned}
$$

$$
\begin{aligned}
b(\mathbf{w}^{*h}, \boldsymbol{\eta}, \boldsymbol{\psi}^h) \ &\le \ M|| \nabla \boldsymbol{\eta} || \, || \nabla \mathbf{w}^{*h} || \, || \nabla \boldsymbol{\psi}^h || \\
&\le \ \frac{\nu}{4} || \nabla \boldsymbol{\psi}^h ||^2 + C\nu^{-3} || \mathbf{f}^* ||^2_{-1} \, || \nabla \boldsymbol{\eta} ||^2
\end{aligned}
$$

With the help of the estimates above and the fact that $1 - \alpha > 0$, equation (8.3.16) becomes

$$
\nu || \nabla \boldsymbol{\psi}^h ||^2 \ + \ \nu\delta^2 || \boldsymbol{\phi}^{*h} - \tilde{\boldsymbol{\phi}} ||^2 \le C\nu^{-3} || \mathbf{f}^* ||^2_{-1} \, || \nabla \boldsymbol{\eta} ||^2.
$$

The triangle inequality gives the stated result. $\qquad \square$

The discrete counterpart of Proposition 8.3.2 is given in the following statement.

Proposition 8.3.4. *With the same assumptions as in Proposition 8.3.2, we have that*

$$
< \varepsilon(\mathbf{w}^h - \mathbf{w}^{*h}, \boldsymbol{\phi}^h - \boldsymbol{\phi}^{*h}) >= 0.
$$

Proof. The argument is the same as in the proof of Proposition 8.3.2 for the continuous case. $\qquad \square$

The next theorem is the major result in this section. It shows that under the condition that the body force driving the flow, when it has reached steady state, is small enough statistics can be accurately computed.

Theorem 8.3.1. *Assuming the hypotheses of Proposition 8.3.1 hold, then*

$$
< \varepsilon(\mathbf{w} - \mathbf{w}^h, \boldsymbol{\phi} - \boldsymbol{\phi}^h) > \le C\,\nu \left(|| \nabla(\mathbf{w}^* - \mathbf{w}^{*h}) ||^2 + \delta^2 || \boldsymbol{\phi}^* - \boldsymbol{\phi}^{*h} ||^2 \right). \qquad (8.3.17)
$$

Proof. Add and subtract $\mathbf{w}^*$, $\mathbf{w}^{*h}$, $\boldsymbol{\phi}^*$, $\boldsymbol{\phi}^{*h}$ appropriately to the formula of $< \varepsilon(\mathbf{w} - \mathbf{w}^h, \boldsymbol{\phi} - \boldsymbol{\phi}^h) >$. Then, the proof follows by the application of triangle inequality and from Propositions 8.3.2 and 8.3.4. $\qquad\square$

Corollary 8.3.1. *Suppose that the small data condition holds and $(\mathbf{X}^h, Q^h)$ satisfy an inf-sup condition. Then,*

$$< \varepsilon(\mathbf{w} - \mathbf{w}^h, \boldsymbol{\phi} - \boldsymbol{\phi}^h) > \le C \left\{ (\nu + \nu^{-3} ||\, \mathbf{f}^* \,||_{-1}^2) ||\, \nabla(\mathbf{w}^* - \tilde{\mathbf{w}}) \,||^2 + \nu\delta^2 ||\, \boldsymbol{\phi}^* - \tilde{\boldsymbol{\phi}} \,||^2 \right\},$$

where $(\tilde{\mathbf{w}}, \tilde{\boldsymbol{\phi}})$ is the modified Stokes projection.

Proof. Use the estimates of Proposition 8.3.3 on the right-hand side of (8.3.17). $\qquad\square$

9.0 THE JOINT ENERGY-HELICITY CASCADE FOR HOMOGENEOUS, ISOTROPIC TURBULENCE GENERATED BY ADM

We consider herein aspects of flow statistics and the physical fidelity related to the coherent rotational structures and integral invariants (helicity and helicity statistics) predicted by the Stolz-Adams ADM described in Chapter 5. Notation and properties are used as introduced there. We take $\Omega = (0, L)^3$ and impose periodic boundary conditions on all variables (with the usual normalization condition of the periodic case $\int_\Omega \phi = 0$, $\phi = \mathbf{w}, \mathbf{w}_0, \mathbf{f}$ and q). We study the joint energy-helicity cascade for homogeneous, isotropic turbulence generated by these models. Our goal is to give a comparison of the energy and helicity statistics of ADM to the true flow statistics and a comparison of their respective energy and helicity cascades.

Both energy,

$$E(t) := \frac{1}{2L^3} \int_\Omega |\mathbf{u}(\mathbf{x}, t)|^2 \, d\mathbf{x}, \tag{9.0.1}$$

and helicity,

$$H(t) := \frac{1}{L^3} \int_\Omega \mathbf{u}(\mathbf{x}, t) \cdot (\nabla \times \mathbf{u}(\mathbf{x}, t)) d\mathbf{x}, \tag{9.0.2}$$

are conserved by the Euler equations and dissipated (primarily at the small scales) by viscosity. Energy and helicity dissipation rates are defined, respectively, as

$$\varepsilon(t) \quad := \quad \frac{\nu}{L^3} \| \nabla \mathbf{w}(t) \|^2, \tag{9.0.3}$$

$$\gamma(t) \quad := \quad \frac{\nu}{L^3} (\nabla \times \mathbf{w}(t), (\nabla \times)^2 \mathbf{w}(t)). \tag{9.0.4}$$

It is widely believed that both cascades, e.g. André and Lesieur [4], and the details of their respective cascades are intertwined. Recent studies, confirmed by Bourne and Orszag [8]

109

have suggested that for homogeneous, isotropic turbulence averaged fluid velocities exhibit a joint energy and helicity cascade through the inertial range (where viscous effects are considered to be negligible) of wave numbers given by

$$E(k) = C_E \varepsilon^{2/3} k^{-5/3}, \qquad H(k) = C_H \gamma \varepsilon^{-1/3} k^{-5/3}, \tag{9.0.5}$$

where k is wave number, ε the mean energy dissipation, and γ the mean helicity dissipation, see also Chen, Chen and Eyink [11], Chen, Chen, Eyink and Holm [12], Ditlevsen and Giuliani [19]. The cascades are referred to as "joint" because they travel with the same speed through wave space (i.e. the exponents of k are equal). The energy cascade given in (9.0.5) is the famous Kolmogorov cascade, and the work of Chen, Chen and Eyink [11] showed that the helicity cascade in (9.0.5) is consistent for wave numbers up to the standard Kolmogorov wave number, $k_E = \nu^{-3/4} \varepsilon^{1/4}$. Herein, we explore the existence and details of a comparable joint cascade in the ADM (5.2.1), to examine if this qualitative feature of the NSE is matched in the ADM. The ADM conserve helicity, e.g. Rebholz [73], which is a first and necessary step for correct helicity cascade statistics, implying that the existence of a helicity cascade is possible.

Other authors have compared LES model energy cascades to energy cascades of the NSE. This was pioneered by Muschinsky [69] for the Smagorinsky model. In [13] by Cheskidov, Holm, Olson and Titi the energy cascade of the Leray-α model was explored, as was the energy cascade of the ADM (5.2.1) and associated regularization in Layton and Neda [56, 57]. The work in [56] found that, with some key assumptions, the energy cascade in the ADM is identical to that of the NSE up to the cut-off length scale of δ, and begins to truncate scales like $k^{-11/3}$ for length scales $< \delta$, until viscosity takes over at a length scale larger than $\eta_{Kolmogorov}$. The effects of time relaxation on scale truncation was explored using similar tools in [57]. There are many other applications of $K41$ phenomenology to understanding LES models, Sagaut [74].

The study of helicity in fluid flow and turbulence has only recently begun. It was not until 1961 that helicity's inviscid invariance was discovered by Moreau [67], and two decades later Moffatt gave the topological interpretation of helicity [65]: that helicity is nonzero if and only if the flow is not rotationally symmetric. This topological interpretation leads to

the commonly accepted interpretation of helicity: it is the degree to which the vortex lines are knotted and intertwined. Another interesting and important feature of helicity is that it is a *rotationally* meaningful quantity that can be checked for accuracy in a simulation. Moffat and Tsoniber gave a good summary of the early results on helicity in [66].

We show that solutions of the ADM possess a joint energy/helicity cascade that is asymptotically (in the filter width δ) equivalent to that of the NSE. In Layton and Neda [56], it is shown that there exists a piecewise cascade for energy in the ADM; that is, up to wave number $\frac{1}{\delta}$, i.e., over the resolved scales, the ADM cascades energy in the same manner as in the NSE ($k^{-5/3}$). However, after this wave number and up to the model's microscale, the ADM cascades energy at a faster rate ($k^{-11/3}$). Interestingly, the results for helicity in the ADM are analogous; helicity is cascaded at the correct rate of $k^{-5/3}$ for wave numbers less than $\frac{1}{\delta}$, and for higher wave numbers up to the model's microscale, helicity is cascaded at a rate of $k^{-11/3}$. This $k^{-11/3}$ rate of enhanced decay is filter dependent, see Remark 9.3.2. We deduce the microscale helicity in the ADM and we also show that the helicity cascade is consistent (in the sense introduced by Chen, Chen and Eyink [11]) up to the model's energy microscale.

The following proposition recalls, from Rebholz [73], the helicity balance of the ADM (5.2.1) (function spaces as in (5.2.2) and (5.2.3)).

Proposition 9.0.5 (Model's helicity balance). *For* $\mathbf{w}_0 \in \overline{H}^2(\mathcal{C}) \cap H(\mathcal{C})$ *and* $\mathbf{f} \in L^2(0, T; \mathbf{V}')$, *the unique strong solution* $\mathbf{w}$ *of (5.2.1) satisfies*

$$
(\mathbf{w}(t), \nabla \times \mathbf{w}(t))_N + \delta^2 (\nabla \times \mathbf{w}(t), (\nabla \times)^2 \mathbf{w}(t))_N
$$
$$
+ 2\nu \int_0^t (\nabla \times \mathbf{w}(t'), (\nabla \times)^2 \mathbf{w}(t'))_N + \delta^2 ((\nabla \times)^2 \mathbf{w}(t'), (\nabla \times)^3 \mathbf{w}(t'))_N \ dt'
$$
$$
= (\mathbf{w}_0, \nabla \times \mathbf{w}_0)_N + \delta^2 (\nabla \times \mathbf{w}_0, (\nabla \times)^2 \mathbf{w}_0)_N + \int_0^t (\mathbf{f}(t'), \nabla \times \mathbf{w}(t'))_N \ dt' \quad (9.0.6)
$$

Proof. See Rebholz [73]. □

Remark 9.0.1. *Recall that the ADM renorms energy. See Section 5.1 for the definition and properties of the new norm* $|| \cdot ||_N$ *and inner product* $(\cdot, \cdot)_N$.

Remark 9.0.2. *From this proposition, we can clearly identify the analogs in the ADM (5.2.1) of the physical quantities of helicity (H_{model}) and helicity dissipation rate (γ_{model}).*

Definition 9.0.1. *The model's helicity, and the model's helicity dissipation rate, are*

$$H_{model}(t) \quad := \quad \frac{1}{L^3}\{\mathbf{w}(t), \nabla \times \mathbf{w}(t))_N + \delta^2(\nabla \times \mathbf{w}(t), (\nabla\times)^2\mathbf{w}(t))_N\} \tag{9.0.7}$$

$$\gamma_{model}(t) \quad := \quad \frac{2\nu}{L^3}\{(\nabla \times \mathbf{w}(t), (\nabla\times)^2\mathbf{w}(t))_N + \delta^2((\nabla\times)^2\mathbf{w}(t), (\nabla\times)^3\mathbf{w}(t))_N\} \tag{9.0.8}$$

Proposition 9.0.6. *For smooth* $\mathbf{w}$,

$$H_{model}(t) = H(t) + O(\delta^2), \qquad \gamma_{model}(t) = \gamma(t) + O(\delta^2).$$

Proof. Follows from Definition 9.0.1, Proposition 5.1.1 and Lemma 5.1.4. $\square$

In this chapter, if two real quantities A, B (such as energy and helicity), satisfy $C_1(N)A \leq B \leq C_2(N)A$, where C_1, C_2 are positive constants depending only on N (which is fixed), we write

$$A \simeq B.$$

We start by giving the decomposition of energy and helicity in spectral modes in Section 9.1. Section 9.2 derives the joint cascade of energy and helicity in the ADM and Section 9.3 shows how the ADM truncates scales for helicity.

9.1   SPECTRAL REPRESENTATION OF ENERGY AND HELICITY

In order to represent the true kinetic energy and the model's kinetic energy spectrally, we expand the velocity field $\mathbf{w}(\mathbf{x}, t)$ in Fourier series[1] as follows:

$$\mathbf{w}(\mathbf{x}, t) = \sum_k \sum_{|\mathbf{k}|=k} \widehat{\mathbf{w}}(\mathbf{k}, t)e^{i\mathbf{k}\cdot\mathbf{x}}, \tag{9.1.1}$$

---

[1]In fact, under the Kolmogorov theory of homogeneous and isotropic turbulence, these sums are finite, because the scales larger than the cut-off length scale are negligible.

where the wave numbers $\mathbf{k}$ are given by $\mathbf{k} = \frac{2\pi}{L}\mathbf{n}$, $\mathbf{n} \in \mathbb{Z}^3$, $k = \frac{2\pi}{L}n$, $n \in \mathbb{N}$, and

$$\widehat{\mathbf{w}}(\mathbf{k}, t) = \frac{1}{L^3} \int_\Omega \mathbf{w}(\mathbf{x}, t) e^{-i\mathbf{k}\cdot\mathbf{x}} \, d\mathbf{x} \tag{9.1.2}$$

are the Fourier coefficients.

Using Parseval's equality, the kinetic energy $E(t)$ in (5.2.9) can be expressed as

$$\frac{1}{2\,L^3} \|\mathbf{w}(t)\|^2 = \sum_k \sum_{|\mathbf{k}|=k} \frac{1}{2} |\widehat{\mathbf{w}}(\mathbf{k}, t)|^2. \tag{9.1.3}$$

The above formula is equivalent to writing

$$E(t) = \frac{2\pi}{L} \sum_k E(k, t), \tag{9.1.4}$$

where

$$E(k, t) := \frac{L}{2\pi} \sum_{|\mathbf{k}|=k} \frac{1}{2} |\widehat{\mathbf{w}}(\mathbf{k}, t)|^2. \tag{9.1.5}$$

Then, the time averaged kinetic energy[2] is

$$E =< E(t) >, \quad \text{or} \quad E = \frac{2\pi}{L} \sum_k E(k), \tag{9.1.7}$$

where $E(k) =< E(k, t) >$.

---

[2]In full generality, since $\limsup a_n + b_n \leq \limsup a_n + \limsup b_n$, we only have

$$E \leq \frac{2\pi}{L} \sum_k E(k). \tag{9.1.6}$$

This is a mathematical technicality, and equality holds if we use limits or generalized Banach limits (see e.g. Foias et al. [27]) in the appropriate definitions. Furthermore, in the Kolmogorov theory, it is believed that the limits involved exist. The same observation is true in Remark 9.1.1

Remark 9.1.1. *Equations similar to (9.1.4) and (9.1.7) hold with E replaced by E_{model}, ε, ε_{model}, H, H_{model}, γ, or γ_{model}. In other words, if $X \in \{E_{model}, \varepsilon, \varepsilon_{model}, H, H_{model}, \gamma, \gamma_{model}\}$, then*

$$X(t) = \frac{2\pi}{L} \sum_k X(k,t), \tag{9.1.8}$$

and

$$X = < X(t) >, \quad or \quad X = \frac{2\pi}{L} \sum_k X(k), \tag{9.1.9}$$

where $X(k) = < X(k,t) >$. Obviously, $\{E_{model}, \varepsilon, \varepsilon_{model}, H, H_{model}, \gamma, \gamma_{model}\}$ are not identical; what distinguishes between them in (9.1.8) and (9.1.9) is the fact that (9.1.5) has a particular decomposition in each case, as illustrated by (9.1.3).

The model's kinetic energy (5.2.5) and energy dissipation rate (5.2.6) can also be decomposed in Fourier modes.

Proposition 9.1.1. *In Fourier space, (5.2.5) corresponds to*

$$E_{model}(t) = \sum_k \widehat{D}_N(k)\,(1 + \delta^2 k^2) E(k,t), \tag{9.1.10}$$

or equivalently,

$$E_{model}(t) = \sum_k E_{model}(k,t), \tag{9.1.11}$$

where

$$E_{model}(k,t) := \widehat{D}_N(k)\,(1 + \delta^2 k^2) E(k,t). \tag{9.1.12}$$

Proof. Using Parseval's equality again, we get

$$\frac{1}{2\,L^3}\,\|\mathbf{w}(t)\|_N^2 = \sum_k \sum_{|\mathbf{k}|=k} \frac{1}{2}\widehat{D}_N(k)\,|\widehat{\mathbf{w}}(\mathbf{k},t)|^2 \tag{9.1.13}$$

and

$$\frac{1}{2\,L^3}\,\|\nabla\mathbf{w}(t)\|_N^2 = \sum_k \sum_{|\mathbf{k}|=k} \frac{1}{2}\,k^2\,\widehat{D}_N(k)\,|\widehat{\mathbf{w}}(\mathbf{k},t)|^2 . \tag{9.1.14}$$

Recall from formula (5.2.5) that

$$E_{model}(t) = \frac{1}{2L^3}\{\|\mathbf{w}(t)\|_N^2 + \delta^2\|\nabla\mathbf{w}(t)\|_N^2\},$$

so combining (9.1.13) and (9.1.14) proves the claim. $\qquad\square$

Lemma 9.1.1. *In wave number space, we can rewrite (5.2.6), the model's energy dissipation:*

$$\varepsilon_{model}(t) = \nu\frac{4\pi}{L}\sum_k \widehat{D}_N(k)\,k^2(1+\delta^2 k^2)E(k,t). \tag{9.1.15}$$

Using (9.1.12), equation (9.1.15) can be further simplified to

$$\varepsilon_{model}(t) = \nu\frac{4\pi}{L}\sum_k k^2 E_{model}(k,t). \tag{9.1.16}$$

Proof. Start with equation (5.2.6) and proceed as in the proof of Proposition 9.1.1. $\qquad\square$

We now turn to the spectral representation of helicity. We need to start by defining helical modes, e.g. Waleffe [87].

Definition 9.1.1. *In a periodic box, the helical modes $\mathbf{h}_\pm$ are orthonormal eigenvectors of the curl operator, i.e. $i\mathbf{k}\times\mathbf{h}_\pm = \pm k\mathbf{h}_\pm$. They satisfy $\mathbf{k}\cdot\mathbf{h}_s = 0$ and $\mathbf{h}_s^*\cdot\mathbf{h}_{-s} = 0$, for $s = \pm$ (here, * denotes complex conjugate).*

Remark 9.1.2. *This is a particular case of the more general Yosida-Giga Theorem, stated in Wu, Ma and Zhou [89]. In a singly-connected domain D, the solutions of the eigenvalue problem* ($\lambda = \pm 1$)

$$\nabla \times \boldsymbol{\phi}_\lambda = \lambda \, k \, \boldsymbol{\phi}_\lambda \quad in \quad D$$
$$\mathbf{n} \cdot \boldsymbol{\phi}_\lambda = 0 \quad on \quad \partial D$$

exist and form a complete orthogonal set $\{\boldsymbol{\phi}_\lambda\} \in L_0^2(\Omega)$.

Since $\mathbf{w}$ is incompressible, $\mathbf{k} \cdot \widehat{\mathbf{w}}(\mathbf{k}, t) = 0$, i.e. $\widehat{\mathbf{w}}$ is orthogonal to $\mathbf{k}$ and we can expand $\widehat{\mathbf{w}}(\mathbf{k}, t)$ in terms of its projection on an orthogonal basis, chosen as $\{\mathbf{k}, \mathbf{h}_+, \mathbf{h}_-\}$. Thus, we can write $\widehat{\mathbf{w}}(\mathbf{k}, t) = a_+(\mathbf{k}, t)\mathbf{h}_+ + a_-(\mathbf{k}, t)\mathbf{h}_-$, where $a_+(\mathbf{k}, t)$ and $a_-(\mathbf{k}, t)$ are the projections of $\widehat{\mathbf{w}}$ on $\mathbf{h}_+$ and $\mathbf{h}_-$, respectively. For the spectral decomposition of helicity, we follow Chen, Chen and Eyink [11] and Waleffe [87] and expand $\widehat{\mathbf{w}}(\mathbf{k}, t)$ in a basis of helical modes. Therefore, velocity and vorticity can be expanded as

$$\mathbf{w}(\mathbf{x}, t) \;=\; \sum_k \sum_{|\mathbf{k}|=k} \sum_{s=\pm} a_s(\mathbf{k}, t)\mathbf{h}_s(\mathbf{k})e^{i\mathbf{k}\cdot\mathbf{x}}, \tag{9.1.17}$$

$$\nabla \times \mathbf{w}(\mathbf{x}, t) \;=\; \sum_k \sum_{|\mathbf{k}|=k} \sum_{s=\pm} s\,k\,a_s(\mathbf{k}, t)\mathbf{h}_s(\mathbf{k})e^{i\mathbf{k}\cdot\mathbf{x}} \tag{9.1.18}$$

Similarly,

$$(\nabla\times)^n\mathbf{w}(\mathbf{x}, t) = \sum_k \sum_{|\mathbf{k}|=k} \sum_{s=\pm} s^n k^n a_s(\mathbf{k}, t)\mathbf{h}_s(\mathbf{k})e^{i\mathbf{k}\cdot\mathbf{x}}. \tag{9.1.19}$$

Recall first the definition of helicity, equation (9.0.2), for the model's velocity $\mathbf{w}$. Expanding $\mathbf{w}$ in helical modes, we get

$$H(t) = \frac{2\pi}{L} \sum_k H(k, t),$$

where

$$H(k, t) := k\frac{L}{2\pi} \sum_{|\mathbf{k}|=k} \sum_{s=\pm} s\,|a_s(\mathbf{k}, t)|^2.$$

116

Proposition 9.1.2. *The model's helicity spectrum, $H_{model}(k,t)$ is related to the true helicity spectrum, $H(k,t)$, as*

$$H_{model}(k,t) = \widehat{D}_N(k)(1 + \delta^2 k^2)H(k,t). \tag{9.1.20}$$

Proof. Using (9.1.17)-(9.1.19), we have

$$\frac{1}{L^3}(\mathbf{w}(t), \nabla \times \mathbf{w}(t))_N = \sum_k \sum_{|\mathbf{k}|=k} \sum_{s=\pm} s\widehat{D}_N(k)k\,|a(\mathbf{k},t)|^2$$

and

$$\frac{1}{L^3}(\nabla \times \mathbf{w}(t), (\nabla\times)^2\mathbf{w}(t))_N = \sum_k \sum_{|\mathbf{k}|=k} \sum_{s=\pm} s\widehat{D}_N(k)k^3\,|a(\mathbf{k},t)|^2$$

so that, from (9.1.8) with $X = H_{model}$, and from (9.0.7),

$$H_{model}(t) = \frac{2\pi}{L}\sum_k H_{model}(k,t) = \frac{2\pi}{L}\sum_k \widehat{D}_N(k)(1 + \delta^2 k^2)H(k,t). \tag{9.1.21}$$

$\square$

Corollary 9.1.1. *$H_{model}(k,t)$ and $H(k,t)$ satisfy $H_{model}(k,t) \simeq (1 + \delta^2 k^2)H(k,t)$:*

$$(1 + \delta^2 k^2)H(k,t) \le H_{model}(k,t) \le (N+1)(1 + \delta^2 k^2)H(k,t). \tag{9.1.22}$$

Proof. By Lemma 5.1.2, $1 \le \widehat{D}_N(k) \le N+1$ is bounded. $\square$

Lemma 9.1.2. *In wave number space, we can rewrite (9.0.8), the model's helicity dissipation in the form*

$$\gamma_{model}(t) = \nu \sum_k \sum_{|\mathbf{k}|=k} \sum_{s=\pm} \widehat{D}_N(k)\,sk^3(1 + \delta^2 k^2)\,|a_s(\mathbf{k},t)|^2. \tag{9.1.23}$$

Using (9.1.21), (9.1.23) can be further simplified to

$$\gamma_{model}(t) = \nu\frac{2\pi}{L}\sum_k k^2 H_{model}(k,t). \tag{9.1.24}$$

Proof. Use (9.1.17)-(9.1.19) to write (9.0.8) in helical modes. $\square$

117

9.2 PHENOMENOLOGY OF THE JOINT ADM ENERGY AND HELICITY CASCADE

Since helicity plays a key role in organizing three dimensional flows, it is important to understand the extent to which statistics of helicity predicted by an LES model are correct. We answer that question in this section by extending the similarity theory of approximate deconvolution models (begun in Layton and Neda [56]) to elucidate the details of the model's helicity cascade and its connection to the model's energy. Inspired by the earlier work on helicity cascades in the Navier-Stokes equations done by Brissaud, Frisch, Leorat, Lesieur and Mazure [10], Ditlevsen and Giuliani [19, 20], Chen, Chen and Eyink [11], we investigate the existence and details of the joint cascade of energy and helicity for the family of ADM, adapting a dynamic argument of Kraichnan, [50].

Let $\Pi_{model}(k)$ and $\Sigma_{model}(k)$ denote the total energy and helicity transfer from all wave numbers $< k$ to all wave numbers $> k$.

Definition 9.2.1. *We say that the model exhibits a joint cascade of energy and helicity if in some inertial range $\Pi_{model}(k)$ and $\Sigma_{model}(k)$ are independent of the wave number, i.e., $\Pi_{model}(k) = \varepsilon_{model}$ and $\Sigma_{model}(k) = \gamma_{model}$.*

Following Kraichnan's formulation of Kolmogorov's ideas of localness of interaction in k space, we assume the following.

Assumption 9.2.1. *$\Pi_{model}(k)$ ($\Sigma_{model}(k)$) is proportional to the ratio of the total energy $\sim kE_{model}(k)$ (total helicity $\sim kH_{model}(k)$) available in wave numbers of order k and to some effective rate of shear $\sigma(k)$ which acts to distort flow structures of scale $1/k$.*

The distortion time $\tau(k)$ of flow structures of scale $1/k$ due to the shearing action $\sigma(k)$ of all wave numbers $\leq k$ is given by:

$$\tau(k) \sim \frac{1}{\sigma(k)} \qquad \text{with} \qquad \sigma(k)^2 \sim \int_0^k p^2 E_{model}(p)dp. \tag{9.2.1}$$

The conjecture of joint linear cascades of energy and helicity is based on the idea (supported by numerical experiments of Bourne and Orszag [8]) that since energy and helicity

118

are both dissipated by the same mechanism (viscosity), they relax over comparable time scales.

Assumption 9.2.2. $\tau(k)$ *and* $\sigma(k)$ *are the same for energy and helicity of the model.*

We therefore write

$$\Pi_{model}(k) \sim kE_{model}(k)/\tau(k) \qquad \text{and} \qquad \Sigma_{model}(k) \sim kH_{model}(k)/\tau(k). \qquad (9.2.2)$$

In the definition of mean-square shear (9.2.1) the major contribution is from $p \sim k$, in accord with Kolmogorov's localness assumption. This gives

$$\tau(k) \sim k^{-3/2}E_{model}^{-1/2}(k). \qquad (9.2.3)$$

The energy spectrum $E_{model}(k)$ was derived in Layton and Neda [56], using similar tools:

$$E_{model}(k) \quad \sim \quad \varepsilon_{model}^{2/3}k^{-5/3}. \qquad (9.2.4)$$

Putting (9.2.2) and (9.2.3) together with the fact that $\Sigma_{model}(k) = \gamma_{model}$, it follows that the ADM model helicity spectrum is given by:

$$H_{model}(k) \sim \gamma_{model}k^{-5/2}E_{model}^{-1/2}(k)$$

i.e.,

$$H_{model}(k) \sim \gamma_{model}\varepsilon_{model}^{-1/3}k^{-5/3}. \qquad (9.2.5)$$

Using relation (9.1.22), we write

$$H(k) \simeq \frac{\gamma_{model}\varepsilon_{model}^{-1/3}k^{-5/3}}{1 + \delta^2 k^2},$$

which shows that the true helicity spectrum is cut by this family of models as

$$H(k) \quad \sim \quad \gamma_{model}\varepsilon_{model}^{-1/3}k^{-5/3}, \text{ for } k \leq \frac{1}{\delta}, \qquad (9.2.6)$$

$$H(k) \quad \sim \quad \gamma_{model}\varepsilon_{model}^{-1/3}\delta^{-2}k^{-11/3} , \text{ for } k \geq \frac{1}{\delta} . \qquad (9.2.7)$$

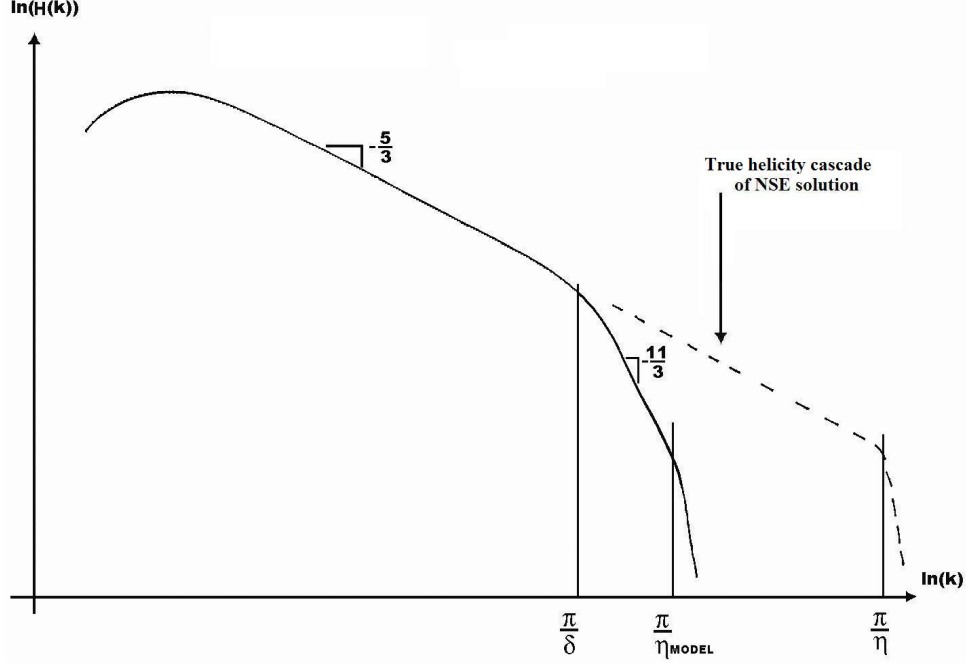The above result is depicted in Figure 12.

Figure 12: The helicity spectrum of Approximate Deconvolution Models

The true energy spectrum is influenced by the ADM in a similar fashion, as proven in Layton and Neda [56]

$$E(k) \sim \varepsilon_{model}^{2/3} k^{-5/3}, \text{ for } k \leq \frac{1}{\delta}, \quad (9.2.8)$$

$$E(k) \sim \varepsilon_{model}^{2/3} \delta^{-2} k^{-11/3}, \text{ for } k \geq \frac{1}{\delta}. \quad (9.2.9)$$

Thus, down to the cut-off length scale (or up to the cut-off wave number) the ADM predicts the correct energy and helicity cascades.

9.3 MODEL'S HELICITY MICROSCALE AND CONSISTENCY OF THE CASCADE

On a small enough scale, viscosity grinds down all the flow's organized structures (including helicity) and ends all cascades (including the helicity cascade). The length scale, η_H, at

120

which helical structures do not persist and begin to decay exponentially fast is called the helicity microscale (in analogy with the Kolmogorov microscale for kinetic energy). The correct estimate of the helicity microscale for the NSE is unclear: two estimates with strong arguments in favor of each appear in the literature. The microscale has been estimated for isotropic turbulence by Ditlevsen and Giuliani in [19] to be different (larger) than the Kolmogorov scale $\eta_{Kolmogorov}$: $\eta_H \sim \nu^{-3/7}\gamma^{3/7}\varepsilon^{-2/7}$ based on the decomposition of helicity flux in $\pm$ helical modes. On the other hand, Chen, Chen and Eyink in [11] show that the net helicity flux is constant up to $\eta_{Kolmogorov}(= k_E^{-1})$, so there is no shorter inertial range for helicity cascade.

In this section, we find that the same occurs when one computes the model's helicity microscale. Based on the equilibrium of the helicity flux, we derive a model's helicity microscale, η_{model}^H, whereas we show that the model's helicity cascade derived in Section 9.2 is consistent up to $k_{E_{model}}(= (\eta_{model}^E)^{-1})$, in the sense introduced by and Chen, Chen and Eyink in [11]. These two results do not contradict each other.

9.3.1 Model's helicity microscale

Using ideas in [56] from the derivation of the energy microscale, η_{model}^E, we estimate the ADM's helicity microscale to be:

$$\eta_{model}^H \sim Re^{-3/11}\delta^{6/11}L^{5/11}, \qquad \text{if } \delta < \eta_{model}^H$$

$$\eta_{model}^H \sim Re^{-3/5}L, \qquad \text{if } \delta > \eta_{model}^H$$

Let the reference velocity and length scale for the large scales be U, L, and $w_{small}, \eta_{model}^H$, for the small scales. From Layton and Neda [56] the analog of the small scales and large scales Reynolds number of the model are given by

$$Re_{large} \sim \left.\frac{|\text{nonlinearity}|}{|\text{viscous terms}|}\right|_{\text{large scales}}, \qquad Re_{small} \sim \left.\frac{|\text{nonlinearity}|}{|\text{viscous terms}|}\right|_{\text{small scales}}.$$

Definition 9.3.1.

$$Re_{model-Large} = \frac{UL}{\nu(1 + (\frac{\delta}{L})^2)} \qquad and \qquad Re_{model-Small} = \frac{w_{small}\eta_{model}^H}{\nu(1 + (\frac{\delta}{\eta_{model}^H})^2)} \qquad (9.3.1)$$

The ADM' energy and helicity cascade are halted by viscosity grinding down eddies exponentially fast. This occurs when $Re_{model-Small} \sim O(1)$, that is, when

$$\frac{w_{small}\eta_{model}^H}{\nu(1 + (\frac{\delta}{\eta_{model}^H})^2)} \sim 1. \tag{9.3.2}$$

Equation (9.3.2) determines w_{small}

$$w_{small} \sim \frac{\nu(1 + (\frac{\delta}{\eta_{model}^H})^2)}{\eta_{model}^H}. \tag{9.3.3}$$

The next important equation to determine the helicity microscale comes from statistical equilibrium of the helicity flux: the helicity input at the large scales must match helicity dissipation at the microscale. The rate of helicity input to the largest scales is the total helicity (from (9.0.7)) over the associated time scales

$$\frac{H_{model}}{(\frac{L}{U})} = \frac{\frac{U^2}{L}(1 + (\frac{\delta}{L})^2)}{(\frac{L}{U})} = \frac{U^3}{L^2}\left(1 + \left(\frac{\delta}{L}\right)^2\right). \tag{9.3.4}$$

From (9.0.8), we see that helicity dissipation at the model's microscale scales as

$$\gamma_{small} \sim \nu\left(\frac{w_{small}^2}{(\eta_{model}^H)^3}\left(1 + \left(\frac{\delta}{\eta_{model}^H}\right)^2\right)\right). \tag{9.3.5}$$

This must match the helicity input. There are three cases with the third being the only important one: $\delta = O(\eta_{Kolmogorov})$, $\delta = O(L)$ and the typical case of δ in the inertial range: $\eta_{Kolmogorov} << \delta << L$. If $\delta \sim O(\eta_{Kolmogorov})$, then the simulation reduces to a direct numerical simulation of the NSE. If $\delta \sim O(L)$, then we do not have LES, but VLES (Very Large Eddy Simulation). In the case of VLES, results follow similarly to those below, but are omitted here.

In the case $\delta = O(\eta_{Kolmogorov})$, we have

$$(1 + \left(\frac{\delta}{L}\right)^2) \sim 1 \text{ and } (1 + \left(\frac{\delta}{\eta_{model}^H}\right)^2) \sim 1. \tag{9.3.6}$$

Thus, under (9.3.6), at statistical equilibrium (9.3.4) and (9.3.5) imply that

$$\frac{U^3}{L^2} \sim \nu\frac{w_{small}^2}{(\eta_{model}^H)^3}. \tag{9.3.7}$$

122

Since w_{small} simplifies to ν/η_{model}^H, we get

$$\eta_{model}^H \sim Re^{-3/5}L,$$

using that $Re = LU/\nu$.

In the most important case,

$$\eta_{model}^H << \delta << L$$

we have

$$(1 + \left(\frac{\delta}{L}\right)^2) \sim 1 \text{ and } (1 + \left(\frac{\delta}{\eta_{model}^H}\right)^2) \sim \left(\frac{\delta}{\eta_{model}^H}\right)^2.$$

Matching helicity microscale dissipation to large scale input thus simplifies in this case to

$$\frac{U^3}{L^2} \sim \nu \frac{w_{small}^2 \delta^2}{(\eta_{model}^H)^3(\eta_{model}^H)^2}. \tag{9.3.8}$$

Further, when $\eta_{Kolmogorov} << \delta << L$, the small scale velocity in (9.3.3) reduces to

$$w_{small} \sim \frac{\nu\delta^2}{(\eta_{model}^H)^3}. \tag{9.3.9}$$

Substituting (9.3.9) into (9.3.8) gives

$$\frac{U^3}{L^2} \sim \frac{\nu^3\delta^6}{(\eta_{model}^H)^{11}}. \tag{9.3.10}$$

Solving (9.3.10) for η_{model}^H, and using $Re = LU/\nu$ gives the model's helicity microscale,

$$\eta_{model}^H \sim Re^{-3/11}\delta^{6/11}L^{5/11}. \tag{9.3.11}$$

The ADM helicity microscale is slightly larger than the ADM energy microscale (found in Layton and Neda [56]): $\eta_{model}^E \sim Re^{-3/10}L^{4/10}\delta^{6/10}$. Hence, capturing wave numbers up to the highest energetic wave number will also capture all wave numbers containing significant helicity.

9.3.2 Consistency of the ADM joint cascade

The model's energy and helicity dissipation rates are given by equations (9.1.16) and (9.1.24) above, which are equivalent to [3]

$$\varepsilon_{model}(t) \sim \nu \int_0^\infty k^2 E_{model}(k,t)dk. \tag{9.3.12}$$

and

$$\gamma_{model}(t) \sim \nu \int_0^\infty k^2 H_{model}(k,t)dk. \tag{9.3.13}$$

Lemma 9.3.1. *The wavenumber of the energy microscale of the ADM model (5.2.1) is given by*

$$k_{E_{model}} \sim \nu^{-3/4} \varepsilon_{model}^{1/4}.$$

Proof. Based on (9.3.12), the mean (time-averaged) energy dissipation equals to

$$< \varepsilon_{model}(t) > \sim \nu \int_0^{k_{E_{model}}} k^2 E_{model}(k)dk,$$

where the upper limit of the integral is $k_{E_{model}}$, the wave number of the smallest persistent scales in the model's solution. Using also (9.2.4) we derive the estimate for $k_{E_{model}}$ in the usual way as k_E was derived for NSE.

$$< \varepsilon_{model}(t) > \sim \nu k_{E_{model}}^3 E_{model}(k_{E_{model}}) \sim \nu k_{E_{model}}^3 (\varepsilon_{model}^{2/3} k_{E_{model}}^{-5/3}) \sim \varepsilon_{model}.$$

Solving for $k_{E_{model}}$ gives the result. □

Since γ_{model} is usually defined as $< \gamma_{model}(t) >$ and the RHS of (9.3.13) can be calculated by spectral integration through the inertial range, checking this definition is a way to test if the estimate derived for the end of the inertial range is correct (or consistent).

---

[3] Recall that $\mathbf{k} = \frac{2\pi\mathbf{n}}{L}$, and observe that (9.1.1) and (9.1.2) can be written as

$$\mathbf{w}(\mathbf{x},t) = \sum_{\mathbf{k}} \widehat{\mathbf{w}}(\mathbf{k},t)e^{i\mathbf{k}\cdot\mathbf{x}}\Delta k, \quad \text{and} \quad \widehat{\mathbf{w}}(\mathbf{k},t) = \frac{1}{(2\pi)^3} \int_\Omega \mathbf{w}(\mathbf{x},t)e^{-i\mathbf{k}\cdot\mathbf{x}} \, d\mathbf{x},$$

with $\Delta k = \Delta k_1 \Delta k_2 \Delta k_3$ and $\Delta k_i = \frac{2\pi}{L}, i = 1, 2, 3$. Then, for small enough Δk_i (or large enough L), the sum can be replaced by an integral.

Lemma 9.3.2. *Provided the largest wave number containing helicity is no larger than* k_{Emodel}:

$$< \gamma_{model}(t) > \sim \gamma_{model}.$$

Proof. Substituting the helicity cascade result (9.2.5) and evaluating the integral (9.3.13) up to k_{Emodel} gives

$$
\begin{aligned}
< \gamma_{model}(t) > \quad &\sim \quad \nu \gamma_{model} \varepsilon_{model}^{-1/3} (k_{Emodel}^{4/3}) \\
&\sim \quad \nu \gamma_{model} \varepsilon_{model}^{-1/3} \nu^{-1} \varepsilon_{model}^{1/3} \\
&\sim \quad \gamma_{model}
\end{aligned}
$$

$\square$

Remark 9.3.1. *We want to stress out that* $< \gamma_{model}(t) > \sim \gamma_{model}$ *only if we integrate up to* $k_{E_{model}}$, *i.e. only if the end of the inertial range for helicity is the same as the end of the inertial range of energy.*

Remark 9.3.2 (Other Filters)**.** *With the differential filter (5.1.1), scales begin to be truncated by the model at the lengthscale* $l = O(\delta)$ *by an enhanced decay of the energy and helicity cascade of* $k^{-11/3}$. *Examining the derivation, the exponent* $-11/3 (= -5/3 + (-2))$ *occurs because the filter decays as* k^{-2}. *With a fourth order differential filter, these results would be modified to* $k^{-14/3}$ $(-14/3 = -5/3 + (-4))$ *between the cut-off wavenumber and the microscale. Continuing, it is clear that with the Gaussian filter (which decay exponentially after* $k_C = O(1/\delta)$), *exponential decay begins at* $k_C = 1/\delta$. *In other words, with the Gaussian filter,* $k_C = O(1/\delta) = O(1/\eta_{model}^H) = O(1/\eta_{model}^E)$.

10.0 CONCLUSIONS AND OPEN PROBLEMS

The central idea and major motivation for this thesis was to understand and develop the mathematical theory related to turbulent flow problems. In Chapters 2 to 4 we have concentrated on the Navier-Stokes equations, while in Chapters 5 to 9, we have focused on LES models.

In Chapter 2, we discussed the concept of turbulence and its connection to the Navier-Stokes equations, explaining why these are a never-ending source of exciting and challenging questions. Then, in Chapter 3, we addressed the importance of accurately predicting statistics. We studied a simple yet interesting case of internal flow, with higher Reynolds number, large initial data and asymptotically small body force. These estimates were applied to the practical problems of predicting drag and lift. We also pointed out where the difficulty in the analysis lies for the case of arbitrary body force and initial condition. However, in the case of large body force (shear flow) we determined that statistics of the computed approximation do reflect statistics of the true solution.

Our long-term goal is to develop a theory paralleling and inspired by the theory of shadowing in approximation of dynamical systems,, e.g. Pilyugin [71], Ostermann and Palencia [70] and Hammel, Yorke and Grebogi [34], i.e., to understand when computed time-averaged statistics from numerical simulations of the Navier-Stokes equations reflect statistics corresponding to the exact solution of the Navier-Stokes equations with the data (which is essentially driving the flow) perturbed.

In Chapter 5 we narrowed our investigation of turbulent flow simulation to focus in LES models, in particular, ADM. In Chapter 6, we studied the finite element semi-discretization of the Zeroth Order Model, proving that the precise implementation of the filtering operation plays a major role in the stability and convergence properties of the scheme: filtering must

be implemented in the same mesh as the solution is computed. This guarantees a stable formulation, with optimal convergence rates when $\delta = O(h)$, which is consistent with the literature and simulations with other models, e.g. Iliescu, John, Layton, Matthies and Tobiska [39] and John [41]. In terms of computations, this means that solving the filter problem in a finer mesh does not improve the overall performance of the scheme and may even produce an unstable approximation.

Numerical confirmation for these results were pursued and presented in Chapter 7. We provided an example where the kinetic energy computed with the exact filter blows up in finite time and then presented more extensive tests with the discrete filter. At this time, we are not (yet) able to numerically verify the convergence rates predicted by the theory. We have preliminary convergence studies for the Chorin problem described in Section 7.2 with $n = 1$, $\tau = Re = 1$, $dt = 0.0001$ and 200 time steps (i.e. $T = 0.2$). Set $\mathbf{e} = \mathbf{u} - \mathbf{u}^h$. The results are shown in Table 3. They indicate that the time step should be even smaller, because the convergence rates for $\|\mathbf{e}\|_{L^\infty(0,T,L^2(\Omega))}$ begin to deteriorate for small h.

h	$\|\mathbf{e}\|_{L^\infty(0,T,L^2(\Omega))}$	rate	$\|\nabla\mathbf{e}\|_{L^\infty(0,T,L^2(\Omega))}$	rate	$\|\nabla\mathbf{e}\|_{L^2(0,T,L^2(\Omega))}$	rate
1/4	$5.22 \, 10^{-3}$	2.98	$2.79 \, 10^{-1}$	2.98	$2.16 \, 10^{-2}$	1.96
1/8	$6.64 \, 10^{-4}$	2.99	$3.55 \, 10^{-2}$	2.99	$5.55 \, 10^{-3}$	1.99
1/16	$8.34 \, 10^{-5}$	2.40	$4.45 \, 10^{-3}$	3.00	$1.40 \, 10^{-3}$	1.99
1/32	$1.58 \, 10^{-5}$		$5.58 \, 10^{-4}$		$3.51 \, 10^{-4}$	

Table 3: Preliminary convergence studies for the discrete filter.

In Chapter 8, we proposed a discretization of the Zeroth Order Model based on a mixed variational formulation that reflects the natural energy properties of the model. Optimal convergence rates are obtained if $\delta = O(h)$. Additionally, time averaged error estimates were presented. For the special case of asymptotically small body force, they proved to be optimally computable.

Lastly, in Chapter 9, a joint energy and helicity cascade has been shown to exist for homogeneous, isotropic turbulence generated by approximate deconvolution models. The energy and helicity both cascade at the correct $O(k^{-5/3})$ rate for inertial range wave numbers

up to the cut-off wave number of $O(\frac{1}{\delta})$, and at $O(k^{-11/3})$ afterward until the model's energy and helicity microscale. A microscale for helicity dissipation has been identified for flows predicted by ADM. As expected, it is larger than both the Kolmogorov scale (i.e. the ADM truncates scales), and the microscale for energy dissipation in the ADM (i.e. capturing all scales containing energy will also capture all scales containing helicity).

Next, we consider some open questions and future research problems.

10.1 FILTERING AS THE SOLUTION OF A STOKES PROBLEM

The natural choice of a differential filter for an incompressible fluid LES model is the Stokes filter, since incompressibility is preserved. In that case, $\overline{\boldsymbol{\phi}}$ is the solution of

$$- \delta^2 \Delta \overline{\boldsymbol{\phi}} + \overline{\boldsymbol{\phi}} + \nabla \mu = \boldsymbol{\phi} \qquad \text{and} \qquad \nabla \cdot \overline{\boldsymbol{\phi}} = \nabla \cdot \boldsymbol{\phi} \quad \text{in } \Omega \tag{10.1.1}$$

$$\overline{\boldsymbol{\phi}} = \boldsymbol{\phi} \qquad \text{on} \quad \partial \Omega$$

Using this differential filter, proceeding as in Section 6.1, the space filtered Navier-Stokes equations become

$$\begin{aligned}
\overline{\mathbf{u}}_t + \overline{\nabla \cdot (\overline{\mathbf{u}}\,\overline{\mathbf{u}} + O(\delta^2))} - \nu \Delta \overline{\mathbf{u}} + \nabla \overline{p} &= \overline{\mathbf{f}} & \text{in } (0,T] \times \Omega, \\
\nabla \cdot \overline{\mathbf{u}} &= 0 & \text{in } [0,T] \times \Omega, \\
\overline{\mathbf{u}} &= 0 & \text{on } [0,T] \times \partial\Omega, \\
\overline{\mathbf{u}}(0,\mathbf{x}) &= \overline{\mathbf{u}}_0(\mathbf{x}) & \text{in } \Omega.
\end{aligned} \tag{10.1.2}$$

Note that, comparing to (6.1.2), $\overline{\mathbf{u}}$ is exactly incompressible and the pressure p is also filtered. Letting $(\mathbf{w}, \lambda)$ denote the approximation to $(\overline{\mathbf{u}}, \overline{p})$ and dropping the $O(\delta^2)$ terms, system (10.1.2) gives that $(\mathbf{w}, \lambda)$ satisfies

$$\begin{aligned}
\mathbf{w}_t + \overline{\nabla \cdot (\mathbf{w}\mathbf{w})} - \nu \Delta \mathbf{w} + \nabla \lambda &= \overline{\mathbf{f}} & \text{in } (0,T] \times \Omega, \\
\nabla \cdot \mathbf{w} &= 0 & \text{in } [0,T] \times \Omega, \\
\mathbf{w} &= 0 & \text{on } [0,T] \times \partial\Omega, \\
\mathbf{w}(0,\mathbf{x}) &= \overline{\mathbf{u}}_0(\mathbf{x}) & \text{in } \Omega.
\end{aligned} \tag{10.1.3}$$

128

Let us look at the discretization of this model. For the moment, let T^h be the analogous of (6.2.2) for the new filter (10.1.1). The continuous in time finite element method for (10.1.3) is: find $(\mathbf{w}^h, \lambda^h)$ in $(\mathbf{X}^h, Q^h)$ such that

$$(\mathbf{w}_t^h, \mathbf{v}^h) + \nu(\nabla \mathbf{u}^h, \nabla \mathbf{v}^h) + B^h(\mathbf{w}^h, \mathbf{w}^h, \mathbf{w}^h) + (\lambda^h, \nabla \cdot \mathbf{v}^h) = (T^h(\mathbf{f}), \mathbf{v}^h), \quad \forall \mathbf{v}^h \in \mathbf{X}^h$$

$$(\nabla \cdot \mathbf{w}^h, q^h) = 0, \quad \forall q^h \in Q^h.$$

The key step for stability of this discretization is to construct $A^h : \mathbf{V}^h \to \mathbf{V}^h$, an inverse to T^h restricted to $\mathbf{V}^h$. In that case, $B^h(\mathbf{w}^h, \mathbf{w}^h, A^h \mathbf{w}^h) = 0$ and $(\lambda^h, \nabla \cdot (A^h \mathbf{w}^h)) = 0$, since $A^h \mathbf{w}^h$ is weakly divergence free.

10.2   EXTENSION OF THE DISCRETE FILTER TO THE N^{TH} ORDER MODELS

The formulation of a discretization for the Nth Order ADMs should be a straightforward extension from that of the Zeroth Order Model. Our conclusion is basically that this will be achieved as soon as the issues with the Stokes filter, pointed out in the previous section, are resolved.

The discretization proposed in Chapter 6 can be extended to the higher order models, according to

$$
\begin{aligned}
\mathbf{w}_t + \overline{\nabla \cdot (D_N \mathbf{w} D_N \mathbf{w})} - \nu \Delta \mathbf{w} + \nabla \lambda &= \overline{\mathbf{f}} && \text{in } (0, T] \times \Omega, \\
\nabla \cdot \mathbf{w} &= 0 && \text{in } [0, T] \times \Omega, \\
\mathbf{w} &= 0 && \text{on } [0, T] \times \partial \Omega, \\
\mathbf{w}(0, \mathbf{x}) &= \overline{\mathbf{u}}_0(\mathbf{x}) && \text{in } \Omega,
\end{aligned}
\tag{10.2.1}
$$

but some drawbacks must be noted:

- the $O(\delta^2)$ error introduced to guarantee incompressibility can no longer be overlooked, for it is now larger than the modeling error of $O(\delta^{2N+2})$;

- the model could be unstable: if we multiply the discrete formulation by $\mathbf{w}^h$, the pressure term vanishes, but the nonlinear term does not; if we multiply it instead by $A^h D_N \mathbf{w}^h$, then the opposite happens.

Nevertheless, we have one example, for the First Order Model, that shows that this discretization can give good results.

Consider the step problem again, flow field at T = 10, 20, 30, 40, with $\delta = 1/8$. The results in Figure 13 are comparable to the results in Figure 11, but were obtained for the same mesh used to calculate the data in Figure 10. This indicates that higher order models may be able to compute accurate approximations on coarser meshes than the meshes needed for low order models.
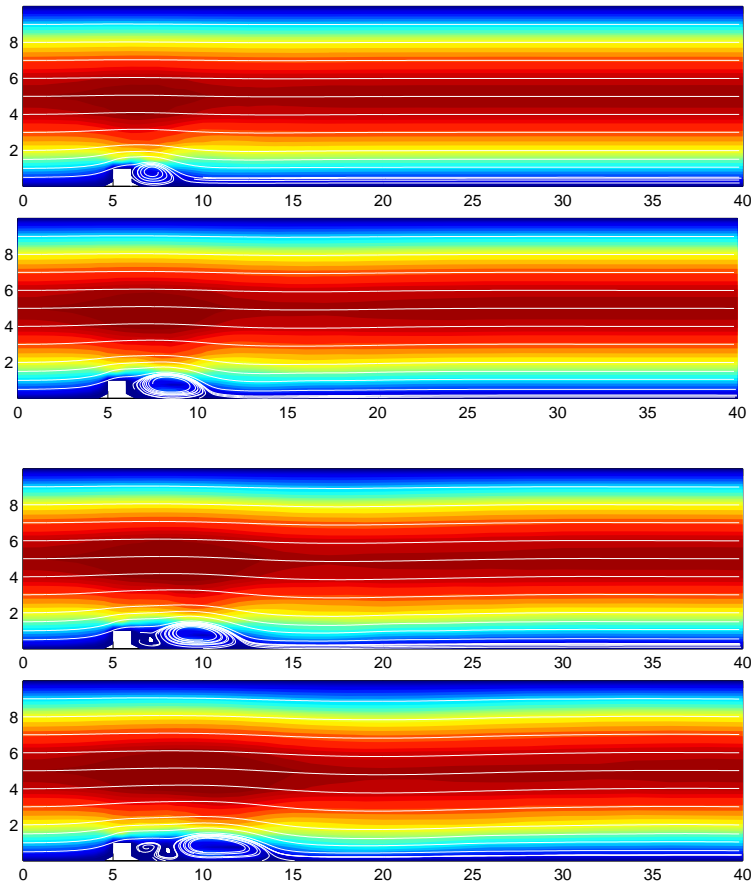

Figure 13: First Order Model comparable to Zeroth Order Model with fewer degrees of freedom.

BIBLIOGRAPHY

[1] N. A. Adams and S. Stolz. Deconvolution methods for subgrid-scale approximation in large eddy simulation. *Modern Simulation Strategies for Turbulent Flow*, 2001. R.T. Edwards.

[2] R. A. Adams. *Sobolev Spaces*. Academic Press, New York, 1975.

[3] A. A. Aldama. *Filtering Techniques for Turbulent Flow Simulation*, volume 56 of *Springer Lecture Notes in Engineering*. Springer Berlin, 1990.

[4] J. C. André and M. Lesieur. Influence of helicity on high Reynolds number isotropic turbulence. *Journal of Fluid Mechanics*, 81:187–207, 1977.

[5] L. C. Berselli. *Some Topics in Fluid Mechanics*. PhD thesis, Università degli Studi di Pisa, 2000.

[6] L.C. Berselli, T. Iliescu, and W. Layton. *Mathematics of Large Eddy Simulation of Turbulent Flows*. Scientific Computation. Springer, 2006.

[7] M. Bertero and B. Boccacci. *Introduction to Inverse Problems in Imaging*. IOP Publishing Ltd., 1998.

[8] J. Bourne and S. Orszag. Spectra in helical three-dimensional homogeneous isotropic turbulence. *Physics Review Letters E*, 55:7005–7009, 1997.

[9] F. Brezzi and M. Fortin. *Mixed and hybrid finite element methods*. Springer-Verlag, 1991.

[10] A. Brissaud, U. Frisch, J. Leorat, M. Lesieur, and A. Mazure. Helicity cascades in fully developed isotropic turbulence. *Physics of Fluids*, 16(8):1366–1367, 1973.

[11] Q. Chen, S. Chen, and G. Eyink. The joint cascade of energy and helicity in three dimensional turbulence. *Physics of Fluids*, 15(2):361–374, 2003.

[12] Q. Chen, S. Chen, G. Eyink, and D. Holm. Intermittency in the joint cascade of energy and helicity. *Phys. Rev. Lett.*, 90:214503, 2003.

[13] A. Cheskidov, D. D. Holm, E. Olson, and E. S. Titi. On a Leray-α model of turbulence. In Royal Society London, editor, *Mathematical, Physical and Engineering Sciences*, volume 461 of *A*, pages 629–649, 2005.

[14] A. Chorin. Numerical solution for the Navier-Stokes equations. *Math. Comp.*, 22:745–762, 1968.

[15] A. J. Chorin and J. E. Marsden. *A Mathematical Introduction to Fluid Mechanics*. Springer-Verlag, New-York, 1993.

[16] P. Constantin and C. Doering. Energy dissipation in shear driven turbulence. *Physical Review Letters*, 69(11):1648–1651, 1992.

[17] P. Constantin and C. Foias. *Navier-Stokes Equations*. University of Chicago Press, Chicago, IL, 1988.

[18] J. W. Deardorff. A numerical study of three-dimensional turbulent channel flow at large Reynolds numbers. *J. Fluid Mech.*, 41:453–480, 1970.

[19] P. Ditlevsen and P. Giuliani. Cascades in helical turbulence. *Physical Review E*, 63:036304, 2001.

[20] P. Ditlevsen and P. Giuliani. Dissipation in helical turbulence. *Physics of Fluids*, 13(11):3508–3509, 2001.

[21] T. Dubois, F. Jauberteau, and R. Temam. *Dynamic multilevel methods and the numerical simulation of turbulence*. Cambridge University Press, 1999.

[22] A. Dunca and Y. Epshteyn. On the Stolz-Adams deconvolution LES models. *SIAM J. Math. Anal.*, 37(6):1890–1902, 2006.

[23] A. Dunca and V. John. Finite element error analysis of space averaged flow fields defined by a differential filter. *Math. Models and Meth. in Appl. Sci.*, 14(4):603–618, 2004.

[24] A. Dunca, V. John, and W. Layton. Approximating local averages of fluid velocities: the equilibrium Navier-Stokes equations. *Appl. Numer. Math.*, 49:187–205, 2004.

[25] A. Dunca, V. John, and W. Layton. The commutation error of the space averaged Navier-Stokes equations on a bounded domain. In Birkhauser Verlag Basel, editor, *Advances in Mathematical Fluid Mechanics*, pages 53–78, Switzerland, 2004.

[26] J. H. Ferziger. Direct and Large Eddy Simulation of Turbulence. In A. Vincent, editor, *Numerical Methods in Fluid Mechanics*, volume 16 of *CRM Proceedings and Lecture Notes*, Centre de Recherches Mathematiques, Universite de Montreal, 1998. American Mathematical Society.

[27] C. Foias, O. Manley, R. Rosa, and R. Temam. *Navier-Stokes equations and turbulence*. Encyclopedia of Mathematics. Cambridge University Press, 2001.

[28] G.P. Galdi. An introduction to the Navier-Stokes initial-boundary value problem. In G.P. Galdi, J.G. Heywood, and R. Rannacher, editors, *Fundamental Directions in Mathematical Fluid Dynamics*, pages 1 – 70. Birkhäuser, 2000.

[29] M. Germano. Differential filters for the large eddy numerical simulation of turbulent flows. *Phys. Fluids*, 29:1755–1757, 1986.

[30] V. Girault and P.-A. Raviart. *Finite element approximation of the Navier-Stokes equations.* Number 749 in Lecture notes in mathematics. Springer-Verlag, 1979.

[31] V. Girault and P.-A. Raviart. *Finite element methods for Navier-Stokes equations: theory and algorithms.* Springer-Verlag, 1986.

[32] P. Grisvard. *Elliptic problems in nonsmooth domains*, volume 24 of *Monographs and studies in mathematics.* Pitman Advanced Pub. Program, 1985.

[33] M. Gunzburger. *Finite Element Methods for Viscous Incompressible Flow: A Guide to Theory, Practice, and Algorithms.* Academic Press, Boston, 1989.

[34] S. M. Hammel, J. A. Yorke, and C. Grebogi. Numerical orbits of caotic processes represent true orbits. *American Mathematical Society*, 19(2), 1988.

[35] F. Hecht, O. Pironneau, and K. Ohtsuka. Software FreeFem++. http://www.freefem.org, 2005.

[36] E. Hopf. Über die Anfangswertaufabe für die hydrodynamischen Grundgleichungen. *Math. Nachr.*, 4:213–231, 1951.

[37] T.J.R. Hughes, A. A. Oberai, and L. Mazzei. Large Eddy Simulation of Turbulent Channel Flow by the Variational Multiscale Method. *Phys. Fluids*, 13:1784–1799, 2001.

[38] T. Iliescu and P. Fischer. Backscatter in the Rational LES model. *Computers and Fluids*, 33(5-6):783–790, 2004.

[39] T. Iliescu, V. John, W. Layton, G. Matthies, and L. Tobiska. A numerical study of a class of LES models. *Int. J. Comput. Fluid Dyn.*, 17:75 – 85, 2003.

[40] V. John. *Large Eddy Simulation of Turbulent Incompressible Flows. Analytical and Numerical Results for a Class of LES Models*, volume 34 of *Lecture Notes in Computational Science and Engineering.* Springer-Verlag Berlin, Heidelberg, New York, 2003.

[41] V. John. *Large Eddy Simulation of Turbulent Incompressible Flows. Analytical and Numerical Results for a Class of LES Models*, volume 34 of *Lecture Notes in Computational Science and Engineering.* Springer-Verlag Berlin, Heidelberg, New York, 2004.

[42] V. John. Numerical solution of incompressible flows. Technical report, Lecture notes of a mini-school held at the University of Texas at El Paso, February 25, 2005.

[43] V. John and S. Kaya. A finite element variational multiscale method for the Navier-Stokes equations. *SIAM J. Sci. Comp.*, 26:1485 – 1503, 2005.

[44] V. John and W. Layton. Approximating local averages of fluid velocities: Stokes problem. *Computing*, 66:269–287, 2001.

[45] V. John and W. Layton. Analysis of numerical errors in Large Eddy Simulation. *SIAM J. Numer. Anal.*, 40(3):995–1020, 2002.

[46] V. John, W. Layton, and C. C. Manica. Convergence of time averaged statistics of finite element approximations of the Navier-Stokes equations. *Technical Report TR-MATH 06-04, University of Pittsburgh*, 2006. submitted.

[47] V. John, W. Layton, and N. Sahin. Derivation and analysis of near wall models for channel and recirculating flows. *Comput. Math. Appl.*, 48:1135 – 1151, 2004.

[48] A. A. Kiselev and O. A. Ladyzhenskaya. On the existence and uniqueness of the solution of the nonstationary problem for a viscous, incompressible fluid. *Izv. Akad. NaukSSSR. Ser. Mat.*, 21:655–680, 1957.

[49] A. V. Kolmogorov. The local structure of turbulence in incompressible viscous fluids for very large Reynolds number. *Dokl. Akad. Nauk. SSR*, 30:9–13, 1941.

[50] R. H. Kraichnan. Inertial-range transfer in two- and three- dimensional turbulence. *J. Fluid Mech.*, 47:525 – 535, 1971.

[51] O. A. Ladyzhenskaya. *The Mathematical Theory of Viscous Incompressible Flows*. Gordon and Breach Science Publishers, New York, 1969.

[52] W. Layton. Introduction to the numerical analysis of incompressible, viscous flow phenomena. Lecture Notes, 2002.

[53] W. Layton and R. Lewandowski. A simple and stable scale similarity model for large eddy simulation: energy balance and existence of weak solutions. *Applied Math. Letters*, 16:1205–1209, 2003.

[54] W. Layton and R. Lewandowski. On a well-posed turbulence model. *Discrete and Continuous Dynamical Systems - Series B*, 6:111–128, 2006.

[55] W. Layton, C. C. Manica, M. Neda, and L. Rebholz. The joint helicity-energy cascade for homogeneous, isotropic turbulence generated by approximate deconvolution models. *Technical Report TR-MATH 06-10, University of Pittsburgh*, 2006. submitted.

[56] W. Layton and M. Neda. The energy cascade for homogeneous, isotropic turbulence generated by approximate deconvolution models. Technical report, University of Pittsburgh, 2006. submitted.

[57] W. Layton and M. Neda. Truncation of scales by time relaxation. *Journal of Mathematical Analysis and Applications*, 2006. to appear.

[58] J. Leray. Étude de diverses équations intégrales non linéaires et de quélques problemes que pose l'hydrodynamique. *J. Math. Pres Appl.*, 12:1–82, 1933.

[59] J. Leray. Essay sur le mouvemennt plans d'un liquide visqueux que limitent des parois. *J. Math. Pres Appl.*, 13:331–418, 1934.

[60] J. Leray. Sur le mouvemennt d'un fluide visqueux emplissant l'espace. *Acta. Math.*, 63:193–248, 1934.

[61] R. Lewandowski and W. Layton. Residual stress in approximate deconvolution models of turbulence. *to appear, Journal of Tubulence*, 2006.

[62] D. K. Lilly. The representation of small scale turbulence in numerical simulation experiments. In H. H. Goldstine, editor, *Proc. IBM Sci. Computing Symp. On Environmental Sciences*, pages 195–210, Yorktown Heights, NY, 1967.

[63] C. C. Manica and S. Kaya Merdan. Convergence analysis of the finite element method for a fundamental model in turbulence. *Technical Report TR-MATH 06-12, University of Pittsburgh*, 2006. submitted.

[64] C. C. Manica and S. Kaya Merdan. Finite element error analysis of a zeroth order approximate deconvolution model based on a mixed formulation. *JMAA*, 2006. to appear.

[65] H. Moffatt. Simple topological aspects of turbulent vorticity dynamics. In T. Tatsumi, editor, *IUTAM Symposium on Turbulence and Chaotic Phenomena in Fluids*, pages 223–230, 1984.

[66] H. Moffatt and A. Tsoniber. Helicity in laminar and turbulent flow. *Annual Review of Fluid Mechanics*, 24:281–312, 1992.

[67] J.J. Moreau. Constantes d'unilot tourbilloinnaire en fluide parfait barotrope. *C.R. Acad.Aci. Paris*, 252:2810–2812, 1961.

[68] R. Moser, J. Kim, and N. Mansour. Direct numerical simulation of turbulent channel flow up to Re_τ=590. *Phys. Fluids*, 11:943–945, 1998.

[69] A. Muschinsky. A similarity theory of locally homogeneous and isotropic turbulence generated by a Smagorinsky-type LES. *JFM*, 325:239–260, 1996.

[70] A. Ostermann and C. Palencia. Shadowing for nonautonomous parabolic problems with applications to long-time error bounds. *SIAM J. Numer. Anal.*, 37(5):1399–1419, 2001.

[71] S. Yu Pilyugin. Shadowing in dynamical systems. *Lecture Notes in Mathematics*, 1706, 1999.

[72] S. Pope. *Turbulent Flows*. Cambridge University Press, 2000.

[73] L. Rebholz. Conservation laws of turbulence models. *Journal of Mathematical Analysis and Applications*, 2006. to appear.

[74] P. Sagaut. *Large Eddy Simulation for Incompressible Flows*. Springer-Verlag Berlin Heidelberg New York, 2001.

[75] M. Schäfer and S. Turek. The benchmark problem 'flow around a cylinder'. In Hirschel EH, editor, *Flow Simulation with high Performance Computers*, volume 52 of *Notes on Numerical Fluid Mechanics*, pages 547–566. Vieweg: Braunschweig, 1996.

[76] H. Schlichting. *Boundary-layer theory*. McGraw-Hill, 1979.

[77] J. Serrin. The initial value problem for the Navier-Stokes equations. In *Nonlinear Probl., Proc. Sympos. Madison 1962, 69-98* . 1963.

[78] J. S. Smagorisky. General circulation experiments with the primitive equations. *Mon. Weather Rev.*, 91:99–164, 1963.

[79] H. Sohr. *The Navier-Stokes Equations, An Elementary Functional Analytic Approach*. Birhäuser Advanced Texts. Birkhäuser Verlag Basel, Boston, Berlin, 2001.

[80] S. Stolz, N. A. Adams, and L. Kleiser. The approximate deconvolution model for large-eddy simulations of compressible flows and its application to the shock-turbulent-boundary-layer interaction. *Physics of Fluids*, 13(10):2985–3001, 2001.

[81] S. Stolz, N. A. Adams, and L. Kleiser. An approximate deconvolution model for large-eddy simulations with application to incompressible wall-bounded flows. *Physics of Fluids*, 13(4):997–1015, 2001.

[82] S. Stolz and N.A. Adams. On the Approximate Deconvolution procedure for LES. *Phys. Fluids*, 2:1699–1701, 1999.

[83] D. Tafti. Comparison of some upwind-biased high-order formulations with a second order central-difference scheme for time integration of the incompressible Navier-Stokes equations. *Comput. & Fluids*, 25:647–665, 1996.

[84] R. Temam. *Navier-Stokes Equations and Nonlinear Functional Analysis*. SIAM, Philadelphia, 1995.

[85] H. Tennekes and J. L. Lumley. *A First Course in Turbulence*. The MIT Press, 1972.

[86] V. Thomée. *Galerkin Finite Element Methods for Parabolic Problems*, volume 1054 of *Lecture Notes in Mathematics*. Springer-Verlag, 1984.

[87] F. Waleffe. The nature of triad interactions in homogeneous turbulence. *Phys. Fluids A*, 4:350–363, 1992.

[88] X. Wang. Time averaged energy dissipation rate for shear driven flows in R^n. *Physica D*, 99:555–563, 1997.

[89] J.-Z. Wu, H.-Y. Ma, and M.-D. Zhou. *Vorticity and Vortex Dynamics*. Springer, 2006.